ESTIMATING UNDRAINED SHEAR STRENGTH OF CLAY FROM CONE PENETRATION TESTS

By

JAMES WILLIAM GREIG

B.A.Sc., The University of British Columbia, 1981

A THESIS SUBMITTED IN PARTIAL FULFILLMENT OF

THE REQUIREMENTS FOR THE DEGREE OF

MASTER OF APPLIED SCIENCE

in

THE FACULTY OF GRADUATE STUDIES

(Department of Civil Engineering)

We accept this thesis as conforming

to the required standard

THE UNIVERSITY OF BRITISH COLUMBIA

September 1985

In presenting this thesis in partial fulfilment of the requirements for an advanced degree at the University of British Columbia, I agree that the Library shall make it freely available for reference and study. I further agree that permission for extensive copying of this thesis for scholarly purposes may be granted by the head of my department or by his or her representatives. It is understood that copying or publication of this thesis for financial gain shall not be allowed without my written permission.

Department of CIVIL ENGINEERING

The University of British Columbia
1956 Main Mall
Vancouver, Canada
V6T 1Y3

Date October 15 1985

DE-6(3/81)

ABSTRACT

This paper discusses several proposed methods for estimating undrained shear strength from cone pentration tests. This correlation has been studied in the past, however, most have focussed only on the cone bearing. In addition to discussing these traditional methods, this paper evaluates recently proposed methods of estimating Su from CPT pore pressure data.

The results of field vane and cone penetration tests from five lower mainland sites are presented in relation to the different proposed correlation techniques. The results show that there is no unique cone factor for estimating Su from CPT for all clays, however, a reasonable estimate of Su can be made by comparing the predictions from several of the proposed methods. With local correlations these techniques can be quite reliable. The results also show that the estimation of Su from CPT is influenced by various factors relating to: the choice of a reference Su, cone design, CPT test procedures and the soil characteristics. In particular, the estimation of Su from CPT is strongly influenced by such soil parameters as stress history, sensitivity and stiffness. Increases in OCR and sensitivity were reflected by increases in the traditional cone factors Nc and Nk.

The use of pore pressure data appears to be a promising means of estimating Su from CPT. Expressions have been developed that predict excess pore pressures based on cavity expansion theory and attempt to include the effects of sensitivity, stress history and stiffness.

In addition, comparisons between friction sleeve measurements and Su and a method for estimating sensitivity from friction ratios are presented.

Lastly, recommended procedures for estimating Su from CPT are given.

TABLE OF CONTENTS

LIST OF TABLES

LIST OF FIGURES

ACKNOWLEDGEMENTS

I would like to express my gratitude to my research supervisors, Dr. R.G. Campanella and Dr. P.K. Robertson, for their excellent guidance and support during the course of this study. I would also like to thank Don Gillespie for his invaluable assistance and many helpful suggestions.

Thanks are extended to Clifford Tsang, Michael Davies, Alex Sy and Karl Mokkelboost for their help in collecting data.

I am also grateful for the skillful work of Art Brookes and the many hours of assistance with the computer equipment by Glenn Jolly.

Special thanks go to my wife Karen for her patience and support during the preparation of this thesis.

Lastly, I would like to express my appreciation for the tremendous support from my parents, to whom this thesis is dedicated.

The Nilcon field vane equipment was kindly provided by Klohn Leonoff Ltd.

The financial support provided by N.S.E.R.C. is gratefully acknowledged.

CHAPTER 1

INTRODUCTION

1.1 Insitu Measurement of Undrained Shear Strength

In recent years there has been a growing tendancy towards the use of insitu testing techniques for evaluating engineering soil parameters. Wroth 1984 attributed this growth to the rapid increase in the variety and quality of insitu testing instruments in addition to our better understanding of the behaviour of real soils and the subsequent realization of some of the limitations and inadequacies of conventional laboratory testing. The high cost of offshore geotechnical investigations and the difficulties associated with the recovery of undisturbed samples make the use of insitu testing techniques particularly attractive. For routine investigations, selection of borehole locations can be more efficiently planned by employing cone penetration tests during preliminary investigations. With local experience boreholes may not even be necessary.

The soil property most often measured in the field is the undrained shear strength (Su) of clays (Schmertmann 1975, Wroth 1984). Unfortunately, Su is not a unique parameter as it depends significantly on the type of test used, the rate of strain and the orientation of the failure planes (Robertson and Campanella 1983). Based on limited test data and a speculative approach to analysis, Wroth 1984 indicated the likely variation in undrained strength ratio (Su/P') with friction angle and the hierarchy for various test methods (illustrated in figure 1.1). These ideas, he added, were supported by test results obtained by Ghionna et

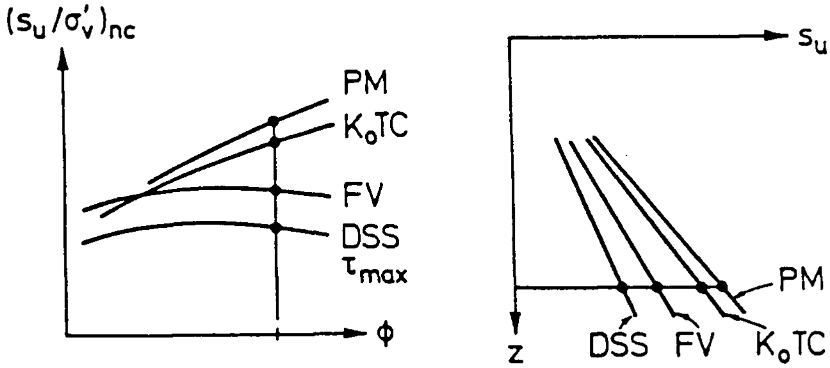

a) Likely variation in undrained strength ratio for different test methods

b) Likely hierarchy of undrained strength ratio for different test methods

TEST TYPES

PM - Pressure meter
K_oTC- K_o consolidated triaxial compression
FV - Field Vane
DSS - Direct simple shear

Figure 1.1 LIKELY VARIATION IN UNDRAINED STRENGTH RATIO AND THEIR HIERARCHY FOR VARIOUS TEST METHODS

(adapted from Wroth 1984)

METHOD	RATING
Dynamic Cone	C
Static Cone:	
Mechanical	B
Elec. Friction	B
Elec. Piezo	B
Elec. Piezo/Friction	B
Acoustic Probe	C
Dilatometer	B
Vane Shear	A
Standard Penetration Test	C
Resistivity Probe	C
Screw Plate	B
Impact Cone	C
Borehole Shear	B
Menard Pressuremeter	B
Self Boring Pressuremeter	A
Self Boring Devices:	
Lateral Penetrometer	B
Shear Vane	A
Plate Load Tests	C
A - High applicability B - Moderate applicability C - Limited applicability	

Table 1.1 PERCEIVED APPLICABILITY OF INSITU TEST METHODS

(adapted from Campanella and Robertson 1982) al. 1983. Figure 1.1 also illustrates the importance of documenting the source of undrained shear strength data.

There are several methods available for measuring the undrained shear strength of clay insitu. Campanella and Robertson 1982 presented a table listing various insitu test methods and their perceived applicability. A list of the methods relevant to the measurement of Su is reproduced in table 1.1. The suitability of each method is indicated by a rating of A, B or C indicating high, moderate and limited applicability, respectively. Campanella and Robertson based their grade on a qualitative evaluation of the confidence level assessed for each method.

Of the eighteen entries only two different methods have a rating of high applicability; the shear vane (VST) and the self boring pressuremeter (SBPMT). Their high rating is a result of their being the only tests that allow a direct evaluation of Su. The SBPMT, however, is a specific test (as described by Campanella and Robertson 1982) being relatively expensive and slow and not a likely candidate for routine soil profiling. On the other hand, the vane shear test or the field vane (FV) is currently the most common insitu method for measuring undrained shear strength. The FV has proven to be a reliable and highly repeatable test method. One of its main advantages is the great deal of experience that has been developed over its long history. However, it does suffer some serious disadvantages. The VST is incremental with tests usually being conducted at 1 meter intervals. The material type in which the test is performed must be speculated from the test results or must be confirmed by an adjacent borehole. Verticality is not ensured nor can it be measured, particularly with the Nilcon equipment. To prevent damage to the vane blades, preboring is usually required through coarse grained material.

There are nine entries having a rating of moderate applicability. Three of which would be classified as specific tests; borehole shear, Menard pressuremeter, and the lateral penetrometer. Two are incremental tests; the dilatometer and the screw plate. The remaining four methods relate to the static cone (CPT). Of these, the electric piezo/friction cone is the most promising.

Piezo/friction cone penetration tests provide a continuous profile of cone bearing, sleeve friction and dynamic pore pressure response. The test has proved to be rapid, highly repeatable and cost efficient. Robertson and Campanella 1983 report that significant advances in research, development and applications of cone penetration testing have been made in recent years. The addition of pore pressure measurements has greatly increased our understanding and potential of the CPT. The test is unequalled in its ability to define soil layer boundaries and qualitatively evaluate material types. However, because of the complex behaviour of soils and the complex changes in stress and strain around the cone tip, soil parameters are necessarily determined from empirical and semi-empirical correlations.

The estimation of undrained shear strength is one such example. The correlation has been studied by several researchers in the past, however, most have focussed only on the cone bearing as a means of estimating Su. The correlations usually employ a cone factor Nk or Nc whose values have exhibited a tremendous range (from 5 to 70) but are often relatively well defined at individual sites. The advent of the piezo cone has permitted a semi-empirical approach using cavity expansion theory and the dynamic pore pressure response to be used to estimate Su. Non-dimensional parameters based on the excess pore pressures generated during penetration have been found to provide a promising means of interpreting CPT data.

1.2 Report Organization

The research described in this report was undertaken in an attempt to better understand the effects of various soil properties on the many methods that have been proposed for estimating undrained shear strength from cone penetration tests. In addition to the traditional methods, recently proposed methods of estimating Su from pore pressure data are discussed. Test results from five lower mainland sites are presented and compared to results reported for other sites. Because the field vane is the most common method of evaluating Su, vane shear tests were used as a reference for this study. This report presents the results of this investigation and is divided into the seven following chapters:

Chapter 2 describes the equipment used for this study. Brief descriptions of the U.B.C. research vehicle, the different cone penetrometers, the data acquisition systems and the field vane equipment are presented.

A summary of the various test procedures used is presented in chapter 3. In particular, a description of the methods of calibration, saturation and actual field testing are given. In addition, details of the cone penetration and field vane data reduction are presented. Specific details of the two tests are also included in other chapters, where appropriate.

A review of the vane shear test (VST) is given in chapter 4. Various methods of analyzing vane test results and some of the factors that affect such results are discussed.

Chapter 5 presents a brief review of the cone penetration test. Such topics as soil classification, soil parameter interpretation, generation of dymanic pore pressure and factors affecting cone penetration test results are discussed.

Chapter 6 reviews traditional empirical methods of correlating cone penetration test results with the undrained shear strength of cohesive materials. In addition, recently proposed techniques using CPT pore pressure data are presented. Methods for estimating vane sensitivity and overconsolidation ratio from CPT are also discussed.

Chapter 7 describes, in detail, the field programme conducted for this study and presents the results of the field vane and cone penetration tests. A comparison is made between the correlations discussed in chapter 6 and the measured values.

Chapter 8 summarizes the investigation and presents conclusions and suggestions for further research.

CHAPTER 2
EQUIPMENT

2.1 Introduction

The design of equipment is an important aspect of any test. In order to make a proper interpretation of the test results the effects and limitations of the apparatus must be understood. Several types of equipment were used for this report: four types of cones, two data acquisition systems, and two field vane borers. This chapter briefly describes the important details of the equipment used.

2.2 Research Vehicle

The U.B.C. geotechnical research vehicle was used for all cone penetration tests performed for this report. The vehicle, described in detail by Campanella and Robertson 1981, is a self-contained insitu testing unit housing an hydraulic loading system and both analog and digital electronic data acquisition systems. The loading system consists of a pair of hydraulic pistons which are located symmetrically about the penetrometer and cone rods and are capable of applying a combined maximum load of 160 kN. Hydraulic control valves are used to manually control penetration and adjustable flow control valves regulate the rate of penetration.

2.3 Penetrometers

Four types of cone penetrometers were used:

1) U.B.C. 5 channel 10 cm^2 bearing - friction - piezometer - inclination - temperature cone (UBC#4)

2) U.B.C. 6 channel 10 cm^2 amplified bearing - friction - piezometer - seismic - inclination - temperature cone (UBC#6)

3) U.B.C. 5 channel 15 cm^2 bearing - friction - piezometer - inclination - temperature - seismic cone (UBC#5)

4) Modified Hogentogler 10 cm^2 amplified bearing - friction - piezometer - inclination - temperature cone

The four cones are illustrated in figure 2.1 and their similarities and important differences are discussed below.

All four cones have a 60° apex angle, equal end area friction sleeves, and relocatable pore pressure elements. The different porous element locations are indicated in figure 2.2. The modified Hogentogler, UBC #4, and UBC #6 cones each have a 10 cm^2 projected base area and a 150 cm^2 friction sleeve. The UBC #5 cone has a 15 cm^2 projected base area and a 225 cm^2 friction sleeve. The 10cm^2 cones use a friction reducer (an enlarged section of cone rod approximately 5 cm. in length) approximately 1 meter behind the friction sleeve. The 15 cm^2 cone is its own friction reducer.

The three U.B.C. cones are similar in mechanical design featuring independent tip and friction load cells and easily replacable pore pressure transducers which are located just behind the tip. The U.B.C. design permits load cells and transducers of different capacities to be used thereby optimizing the sensitivity of the individual measurements.

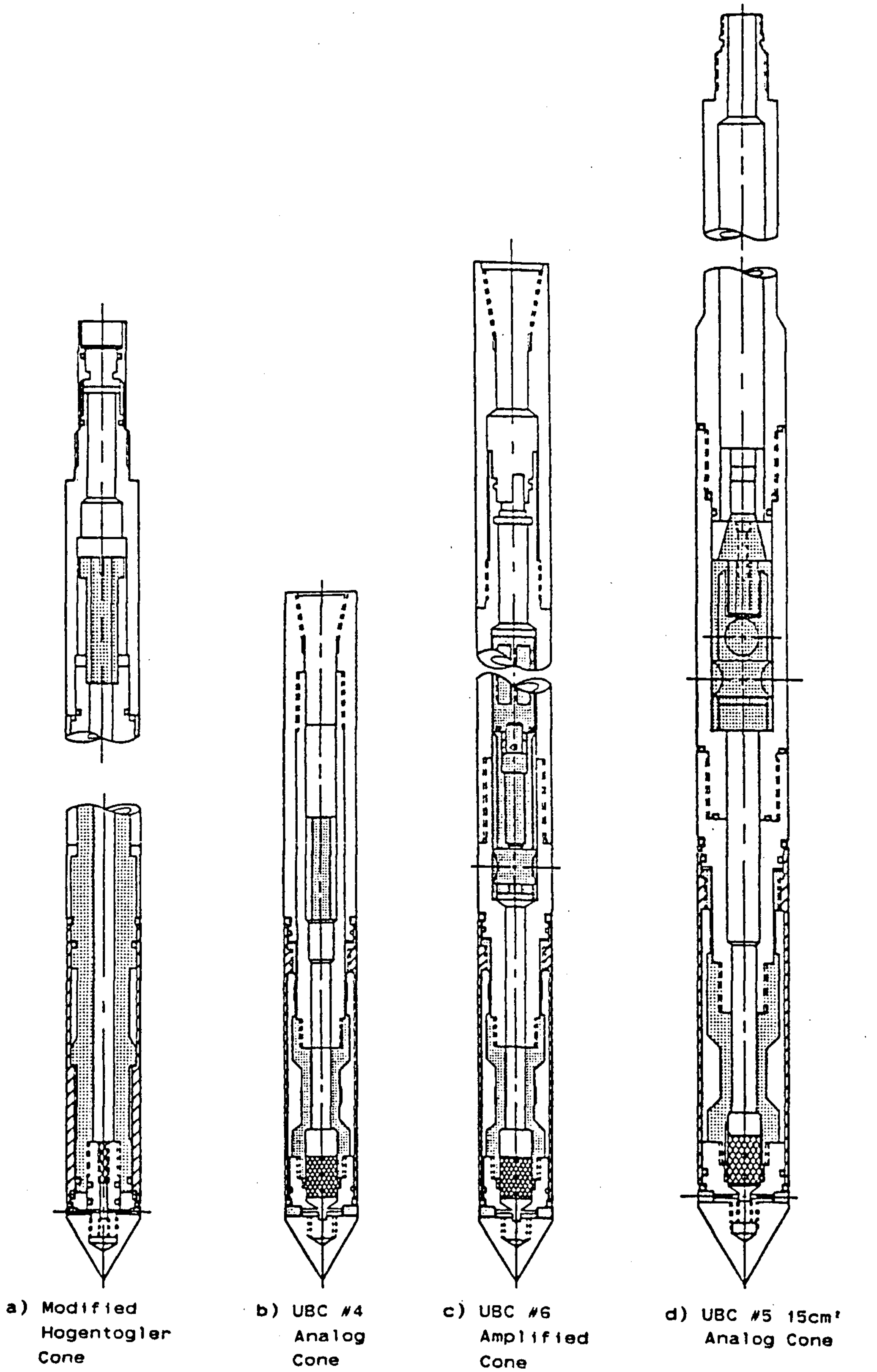

Figure 2.1 - SCHEMATIC DIAGRAM OF CONE PENETROMETERS USED FOR THIS REPORT

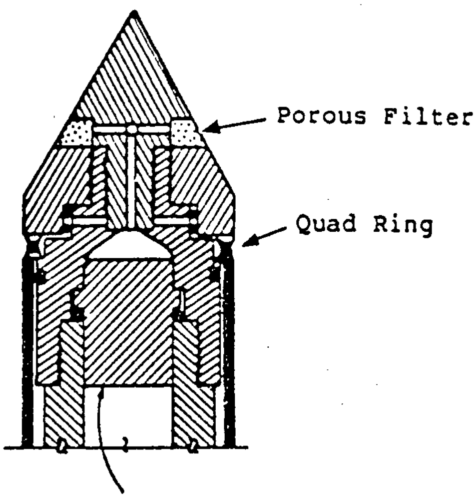

a) Tip Design

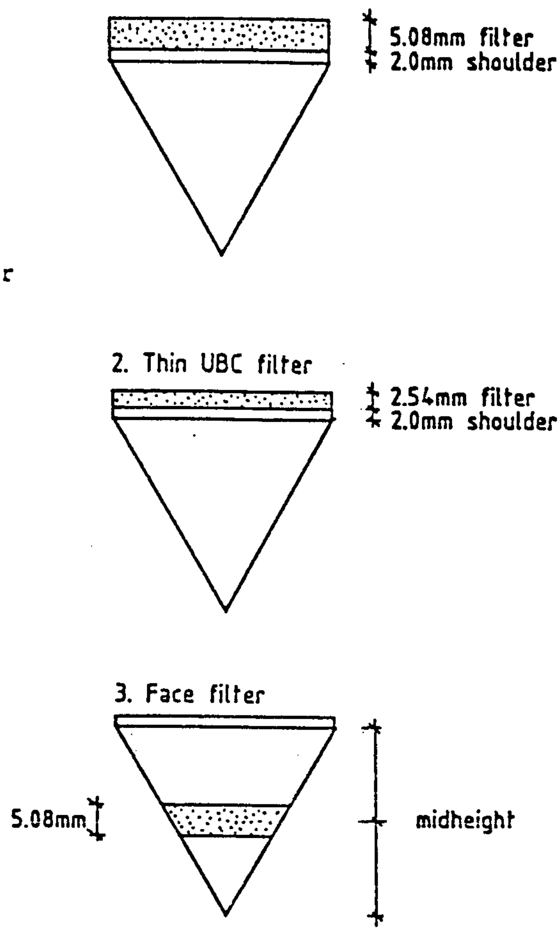

b) Porous Filter Locations

Figure 2.2 - POROUS FILTER LOCATIONS AND TIP DESIGN

The design of the UBC #4 cone has been described in greater detail by Campanella and Robertson 1981. The UBC #6 cone is a UBC #4 style cone modified to incorporate a geophone (velocity transducer) or an accelerometer and an amplifier board. The UBC #5 cone contains a triaxial geophone package and is described in greater detail by Rice 1984.

The seismic aspects of the U.B.C. cones are beyond the scope of this report. The reader is referred to Rice 1984 and Campanella and Robertson 1984 for more details.

The Hogentogler design is known as a subtraction cone. It features the bearing and friction load cells placed in series. The load cell nearest the tip records the cone bearing while the other load cell measures both the bearing and friction. To determine the friction load a differential amplifier circuit is used to electronically subtract the two measurements. A serious consequence of this design is that both load cells must be of comparable capacity which can result in poor sensitivity and resolution of the much lower (typically 0.5% to 10% of bearing) friction readings. The cone was originally designed with an unequal end area friction sleeve, however, the Hogentogler cone used for this report was modified to accommodate an equal end area friction sleeve. In addition, the front end (tip end) design was made similar to that of a U.B.C. cone to allow for relocatable pore pressure elements.

2.4 Data Acquisition Systems

Two data acquisition systems were used to collect the CPT data for this report. Data from the non-amplified cones were recorded on a six channel Watanabe strip chart recorder. Signals from the amplified cones were recorded using a Hogentogler digital data acquisition system. Both systems used a 16 conductor cable and a 10 volt excitation. The cable was connected to a junction box mounted in the truck directing the signals to the appropriate data collection system.

The non-amplified signals were routed through a signal conditioning box containing balance and attenuation resistors. In order to change ranges on the strip chart recorder without introducing an offset voltage individual balance resisitors were used to zero each transducer. Variable attenuation resistors permitted the chart recorder to plot the data directly in engineering units. A more complete description of this analog data recording system is given by Campanella and Robertson 1981.

The amplified cones were used in conjunction with a digital data acquisition system manufactured by Hogentogler & Co., Inc. of Gaithersburg, Maryland. A typical Hogentogler system consists of:

1) 5 channel amplified cone
2) 10 conductor cable
3) data collection and storage unit
4) printer
5) Hewlett Packard HP 7470A plotter

Some modifications were made to the system in order to accommodate the extra devices present in the U.B.C. cones.

Internal components of the digital data collection unit include a power supply, a microcomputer, a 12 bit analog to digital (A/D) converter, ROM (read only memory) based software, and electronic interface circuits. The external components include a 16 character LED (light emitting diode) display and alphanumeric touchpad, a digital cassette tape drive, an analog single channel thermal strip chart recorder, analog BNC connectors and serial and parallel interface ports for use with peripheral devices.

During a sounding all parameters (bearing, friction, friction ratio, pore pressure, pore pressure ratio, inclination and temperature) are listed by the printer. Since the friction sleeve is located behind the tip there is a lag between the current depth of penetration and that for which the data is listed on the printer. Because of the lag in the presentation of the data the thermal strip chart recorder is required in order to display the instantaneous bearing.

The recording system is triggered when metal event markers pass a proximity switch. The event markers are equally spaced on the circumference of a rubber wheel which is placed in contact with the cone rods. As the rods are advanced the event wheel rotates thereby triggering the system. Three sampling rates were available: 2.5 cm.; 5 cm.; and 10 cm. The digital data collected for this report were sampled every 2.5 cm.

Graphical presentation of the data is provided by a plotting routine stored in ROM and the HP 7470A plotter. The program plots each variable to fixed scales, some of which are inappropriate for the range of data collected in soft soils. To overcome this problem the author has written a flexible graphics routine (CONEPLOT) to be used on a microcomputer. In addition, CONEPLOT makes the necessary corrections (discussed in chapter 3) to the data prior to plotting.

2.5 Field Vanes

Two types of field vanes were used; the Nilcon vane borer and the Geonor field vane. They differ primarily in their method of recording and in their method of vane insertion. Both vane borers use similar vanes. The two systems are illustrated in figure 2.3.

The Nilcon borer consists of a torque loading/recording unit mounted on a jacking frame, 20 mm. vane rods, and a special slip couple. Reaction is provided by augers located in the corners of the frame base. The loading head applies the torque through a clutch assembly and a deflection arm scribes the torque-rotation curve on a wax paper disk. To determine the torque required to overcome rod friction the slip couple, placed just behind the vane, permits 15° of rod rotation before transferring the load to the vane. The friction can be determined from the test record. The slip couple is illustrated in figure 2.4.

The vane is advanced using a manual crank and a chain driven yoke. The vane rods are pushed directly in to the ground without a protective casing or sheath. The capacity of the loading system is 9900 Newtons for penetration and 113 Newton-meters for torque.

The Geonor vane is housed within a protective metal sheath during penetration. A ball screw mechanism is used to advance the sheath and the casing that follows it to a depth just above that desired for the test. An inner set of rods are then used to push the vane to the required depth. To apply and record the load a torque head is connected to the top of the casing. A

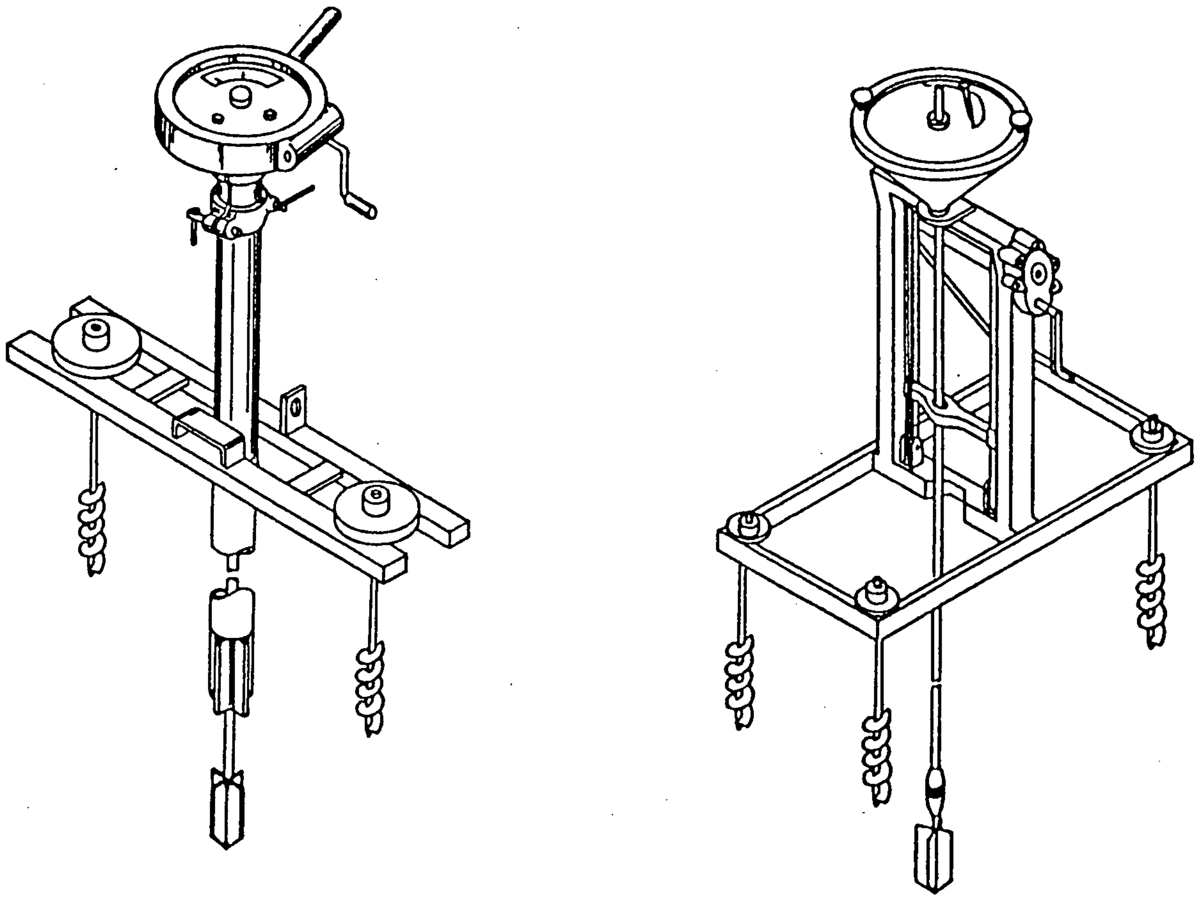

a) Geonor System

b) Nilcon System

Figure 2.3 - FIELD VANE SYSTEMS

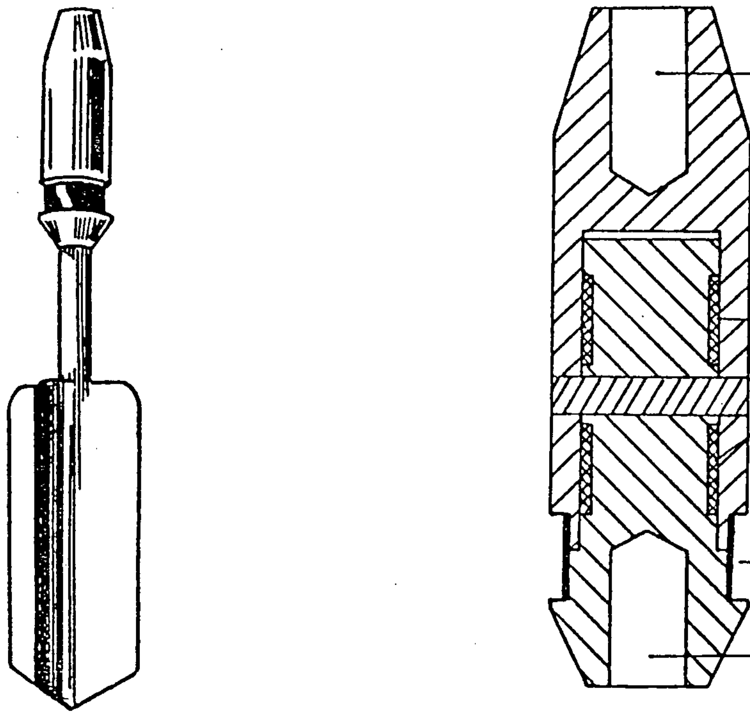

a) Field Vane and Slip Couple   b) Slip Couple Detail

Figure 2.4 - NILCON FIELD VANE AND SLIP COUPLE

deflection needle and follower indicate the maximum torque on an arbitrary scale. There is no permanent record of the test. Calibration charts provide the correlation between the scale reading and the undrained strength.

CHAPTER 3
TEST PROCEDURES AND DATA REDUCTION

3.1 Introduction

Another important aspect of any test is the procedure by which it is conducted. The use of non-standard methods can make the interpretation of the results difficult, if not impossible. It is important to follow a rigorous set of test procedures to achieve repeatable tests and to gain confidence in the results. In this respect, cone penetration can be thought of as having four distinct steps (Gillespie 1981): calibration; saturation; field testing; and data reduction. This chapter describes the test procedures used for the cone penetration and the field vane tests performed for this report.

3.2 Calibration

To maintain a high level of accuracy the various instruments were periodically calibrated. In addition to checking the linearity and stability of the instrument, the influence of each channel on the other cone channels (crosstalk) was recorded. The cone load cells were calibrated in the research vehicle using a configuration identical to that used during field testing. For the non-amplified cones it was of prime importance to calibrate the cone using the same 16 conductor cable used during a sounding. The vane torque recorders were calibrated in the laboratory using a hanging weight and pulley assembly.

A 7 ton loading frame and a 10 ton high quality reference load cell were used for calibration of the bearing and friction load cells. A pressure chamber hydraulically connected to a dead weight pressure tester was used to calibrate the pore pressure transducers. Large volume constant temperature water baths served as references for the thermistors and the inclinometers were calibrated against an adjustable set square and protractor. The outputs from the reference load cell and the non-amplified cone channels were monitored on a 6 digit multimeter having a 1 microvolt resolution and were recorded on a six channel strip chart recorder. Data from the amplified cones were listed directly in engineering units on the printer.

Calibration adjustments for the U.B.C. cones, when required, were relatively easy to make compared to those for the Hogentogler cone. The non-amplified cones required only changes in the attenuation resistor settings. Changes to the calibration of the UBC #6 cone were made by adjusting the individual gain potentiometers. The Hogentogler system uses fixed gain resistors and fixed calibration constants stored in ROM making calibration adjustments difficult.

It was found that the calibration of the cones did not change appreciably unless they were loaded near capacity. There was no significant crosstalk in any of the cones. Campanella and Robertson 1982 report that when the cone is subjected to an all round pressure the measurement of friction and bearing is commonly in error. For friction, unbalanced forces due to unequal end areas of the friction sleeve result in a net force. Therefore, only equal end area cones were used for this report.

Even with an equal end area sleeve, however, a net friction load can exist if the pore pressure distribution around the sleeve is uneven. Being a total stress element the tip should record a bearing equal to the all round pressure. A close examination of any cone will reveal that some transfer of the load takes place resulting in a recorded tip stress less than the applied pressure. Corrections for these pore pressure effects can be made and are discussed in more detail in section 3.5.3.

Campanella and Robertson 1981 also pointed out that load cells are often temperature dependent. Using large volume constant temperature water baths the cones were calibrated for temperature. After reaching temperature equilibrium in the bath the cones were quickly loaded from zero load to near working capacity. The UBC #6 cone was the only one used that was significantly sensitive to temperature. The data from this cone were corrected using the procedures described in section 3.5.2.

An adjustable set square was used to calibrate the inclinometers. The cones were placed on the set square and the output of the inclinometers were monitored as the angle of inclination was changed. Because all penetration tests performed for this report were near vertical corrections were unnecessary.

3.3 Saturation

For proper interpretation of the pore pressure profiles complete saturation of the piezometer tip was essential. Prior to each sounding the porous element and the cavity between the filter and the transducer were carefully saturated with glycerin. Because it develops a high air entry tension and is miscible with water, glycerin has been used as a saturating fluid at U.B.C. for several years. In preparation for saturation a cup was placed over the inverted cone and sealed with an o-ring. With the filter, tip, and access screw removed, the cup was filled with glycerin. Air bubbles were expelled by injecting the cavity with glycerin from a hypodermic syringe. When no more bubbles could be seen the filter was put into place and the screw and tip were replaced. Figure 3.1 illustrates the saturation system used.

3.4 Field Cone Penetration Testing

Prior to saturating the cone and after allowing the electronic systems to warm up, each channel (except for temperature) was checked by applying small loads to the cone. After saturation the cone was attached to the first cone rod and hung from the loading chuck for alignment. When the cone was properly aligned it was lowered to just above the ground surface and held there until the cone came into equilibrium with the surrounding air temperature. Once in equilibrium, the excitation voltage was checked and the cone channels were zeroed. For the amplified cones the baseline readings were taken. Penetration began after the zero load information was recorded.

All tests were performed at a penetration rate of 2 cm/s. Rod changes occurred at one meter intervals during which time pore pressure dissipations were recorded.

An important detail in the test procedure was to check the zeroes for each channel after the completion of a hole. To do this, the electronics were left on as the rods were withdrawn.

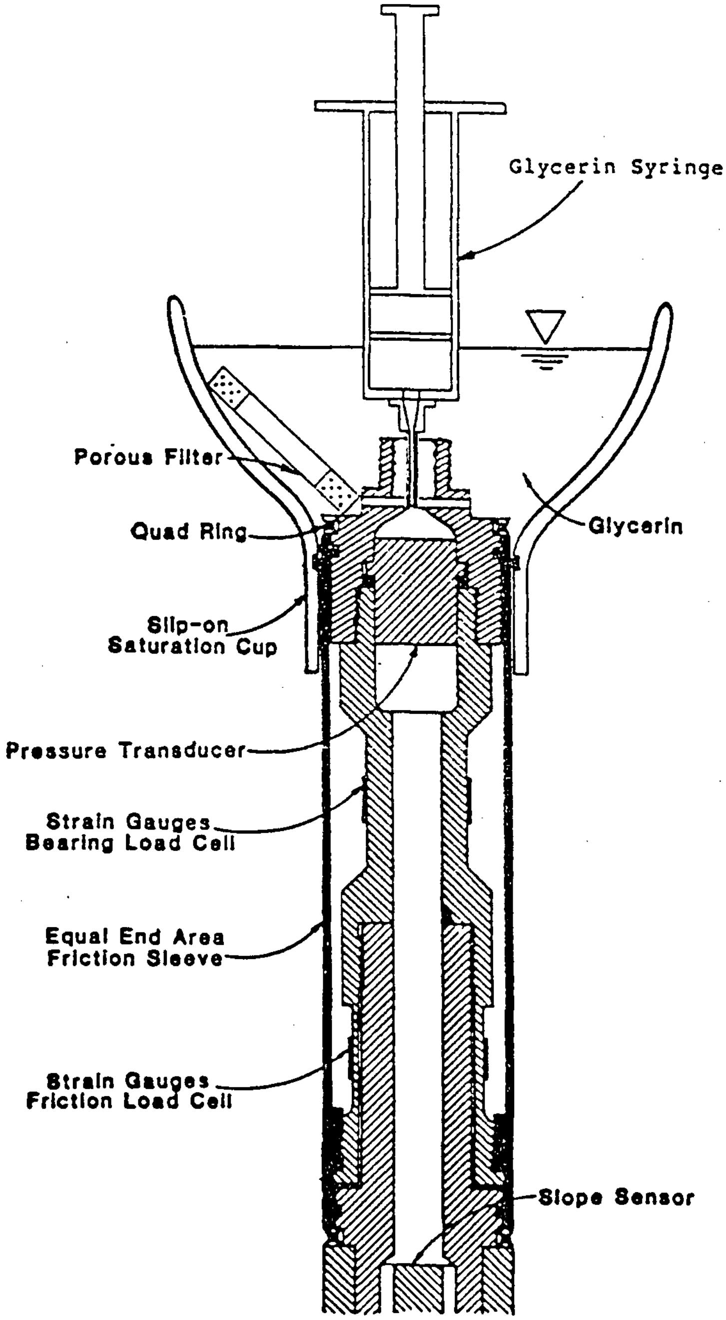

Figure 3.1 - SATURATION PROCEDURE

After removing the cone from the hole it was held vertically just above the ground surface in order to record the zero load information. Zero shifts were occasionally encountered. The thermistor data indicated that the shifts were primarily due to temperature changes. Corrections were made to the data to account for the temperature effects.

3.5 CPT Data Reduction

The method of data reduction was dependent upon the type of data acquisition system used. The digitally collected data was transferred from the Hogentogler unit to an IBM XT microcomputer for manipulation and plotting. The analog records were digitized using a graphics tablet and the U.B.C. mainframe computer. In addition to correcting for temperature and pore pressure effects, the data required manipulation to eliminate incorrect data at rod breaks and spurious data due to electrical power spikes. For interpretation of the data various parameters also needed to be calculated. A discussion of the different corrections applied to the data and the various calculated parameters follows.

3.5.1 Unwanted Data

At each rod break the analog data recorded the drop in bearing load as the loading head was lifted off the rods. This data was simply ignored during digitizing. Due to power surges and for other electrical reasons the digital system occasionally recorded spurious data. A text editor was used to remove these data from the record.

3.5.2 Temperature Corrections

Because the cones had been calibrated for the effects of temperature, corrections to the data were easily made. The temperature calibrations indicated that the load cells underwent a zero shift rather than a change in their calibration. For the most part, only bearing values were affected. To correct the analog data, the depth axis was simply shifted the appropriate amount during digitizing. The digital data were corrected using a program (CPTCORR) which adjusted the data for each channel according to the load cell temperature calibration, the recorded temperature, and the baseline temperature.

Temperature corrections were quite substantial in soft soils as indicated in figure 3.2.

3.5.3 Pore Pressure Corrections

Both bearing and friction measurements were affected by pore pressure. As discussed previously, the bearing load cell does not record all of the pore pressure acting on the tip and the friction sleeve readings can be in error because of end area effects.

Bearing

The configuration of the friction sleeve and bearing load cell leads to an incorrect interpretation of the stress applied to the tip due to pore pressure. Although the load cell records the correct force acting on it, it is incorrectly assumed to be acting over an area equal to that of the tip area (10 cm^2 or 15 cm^2 depending on the cone used). An examination of figure 2.1

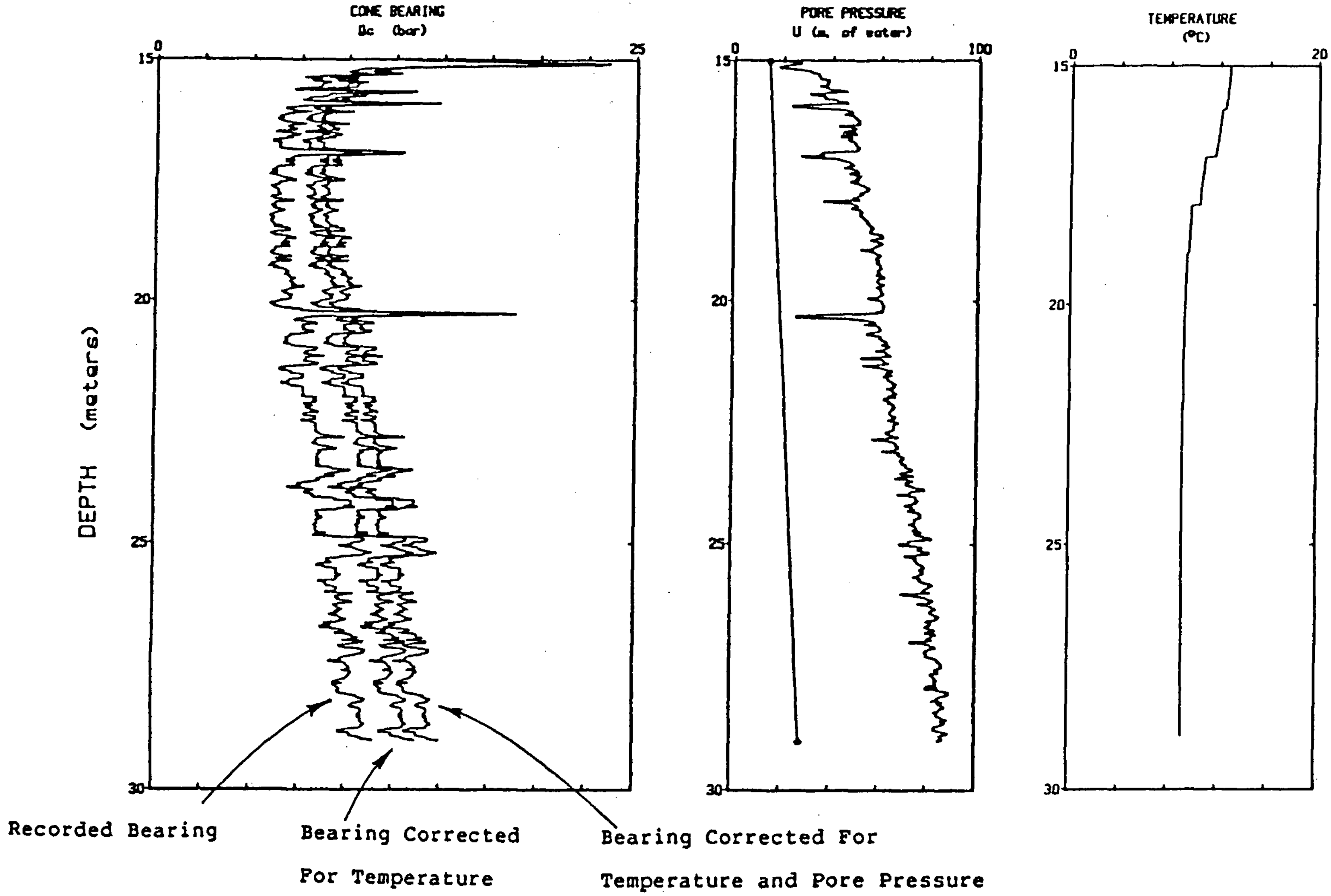

Figure 3.2 - TEMPERATURE AND PORE PRESSURE
EFFECTS ON CONE BEARING

indicates that the effective area of the load cell is less than that of the tip because of the presence of the friction sleeve. The bearing load due to soil stress is, however, correctly interpreted. During calibration the cone is subjected to an all round pressure to determine the ratio of the total applied pressure that is recorded by the tip. This ratio has been termed 'the net area ratio' by Campanella and Robertson 1981. One needs only to add to the recorded pressure that fraction which was not recorded. Campanella and Robertson term the corrected bearing, Qt, and calculate it according to the following expression:

$$Qt = Qc + (1-a) \cdot U \qquad 3.1$$

where
- Qt = corrected bearing
- Qc = recorded bearing
- a = net area ratio
- U = pore pressure measured behind the tip

To properly correct the bearing the pore pressure must be recorded behind the tip. If pore pressures are measured on the face they must be converted to an equivalent behind the tip pore pressure before calculating Qt. Section 5.4 describes how one might make this conversion.

Pore pressure corrections were significant in soft normally consolidated soils as shown in figure 3.2.

Friction

If the two ends of the friction sleeve are of different cross sectional areas the pore pressures will apply a net force on the sleeve. Depending upon which end is larger, the net force may incorrectly be attributed to soil friction or it may subtract from the actual friction. In the latter case, negative friction values have been observed. Even if the ends of the friction sleeve are of equal area, a net force can result if the pore pressure distribution about the sleeve is not uniform. The distribution of pore pressures about the cone is discussed in section 5.4.

3.5.4 Friction Ratio

Friction ratio (Rf) is a calculated parameter that is used as an indicator of soil behaviour type. It is a dimensionless ratio and is defined as:

$$Rf = \frac{Fs}{Q} \cdot 100\% \qquad 3.2$$

where Fs = sleeve friction
Q = cone bearing Qc or Qt

The exact location of where the friction acts is unknown, however, it is usually assumed to act at the center of the sleeve, approximately 10cm behind the tip. The Hogentogler unit assumes the friction/bearing offset to be 10cm and automatically makes this adjustment when recording the data. Because the digital data is recorded at discrete intervals the friction ratios are easily calculated. The analog bearing, friction and pore pressure records are digitized according to the peaks and valleys in their respective records and, thus, the three parameters are not necessarily digitized at corresponding depths. The friction ratios were calculated at the depths of the offset friction values using linearly interpolated bearing values.

3.5.5 Differential Pore Pressure Ratio

Although pore pressure is an indication of soil type, Campanella and Robertson 1981 suggested that differential pore pressure was more fundamental. The differential pore pressure is defined as:

$$\Delta U = Ud - Ue \qquad 3.3$$

where Ud = the dynamic pore pressure (i.e. that measured during a sounding)
Ue = equilibrium pore pressure

An equilibrium pore pressure profile can be determined by conducting complete pore pressure dissipations at selected depths. As a first approximation, a hydrostatic distribution is often assumed. Campanella and Robertson 1981 report that the differential pore pressure ratio ($\Delta U/Q$) is a good indicator of soil type and possibly stress history. The differential pore pressure ratios calculated from the analog records were done so at the depths of the pore pressure measurements using linearly interpolated bearing values.

3.6 Field Vane Testing

The Geonor field vane tests at McDonald Farm (Richmond, B.C.) were performed by the National Research Council (NRC), Division of Building Research under the supervision of the author. Vane tests were conducted at 1 meter intervals with remolded tests being performed at each test depth after 20 turns of the vane rods. The Nilcon vane tests were performed by the author and assistants. The majority of the tests were performed at 0.5 meter intervals at shallow depths (<10m) and at 1 meter intervals at greater depths. Remolded tests were usually performed at alternate tests depths after 20 turns of the vane rods. All vane tests were conducted at a strain rate approximately equal to the generally accepted standard rate of 6^0 per minute. Because the slip couple was designed to return the vane to the correct position after 1 meter of penetration, special attention was paid to rotating the vane rods to regain the 15^0 slip before advancing the vane. Two to three vane tests were recorded on a single wax disk. To avoid confusion it was very important to document each test record on the disk immediately following a test.

3.7 Reduction of Vane Data

All undrained strengths were determined using the standard expression:

$$Su = \frac{6T}{7\pi D^3} \qquad 3.4$$

where Su = undrained shear strength
T = applied torque
D = diameter of the vane

This expression applies only for a vane having a height to diameter ratio of 2. There has been much discussion by researchers (see chapter 4) as to the correct interpretation of the vane test, however, most engineers use the above expression.

Correlation charts based on the above expression were used to determine the undrained strength from the peak readings on the Geonor equipment.

An example of a Nilcon test record is shown in figure 3.3. The radial distance from the outer zero line multiplied by a calibration constant (K) gives the applied torque. The distances Mf and Mp represent the rod friction and the peak applied torque, respectively. The value (Mf-Mp)·K represents the torque

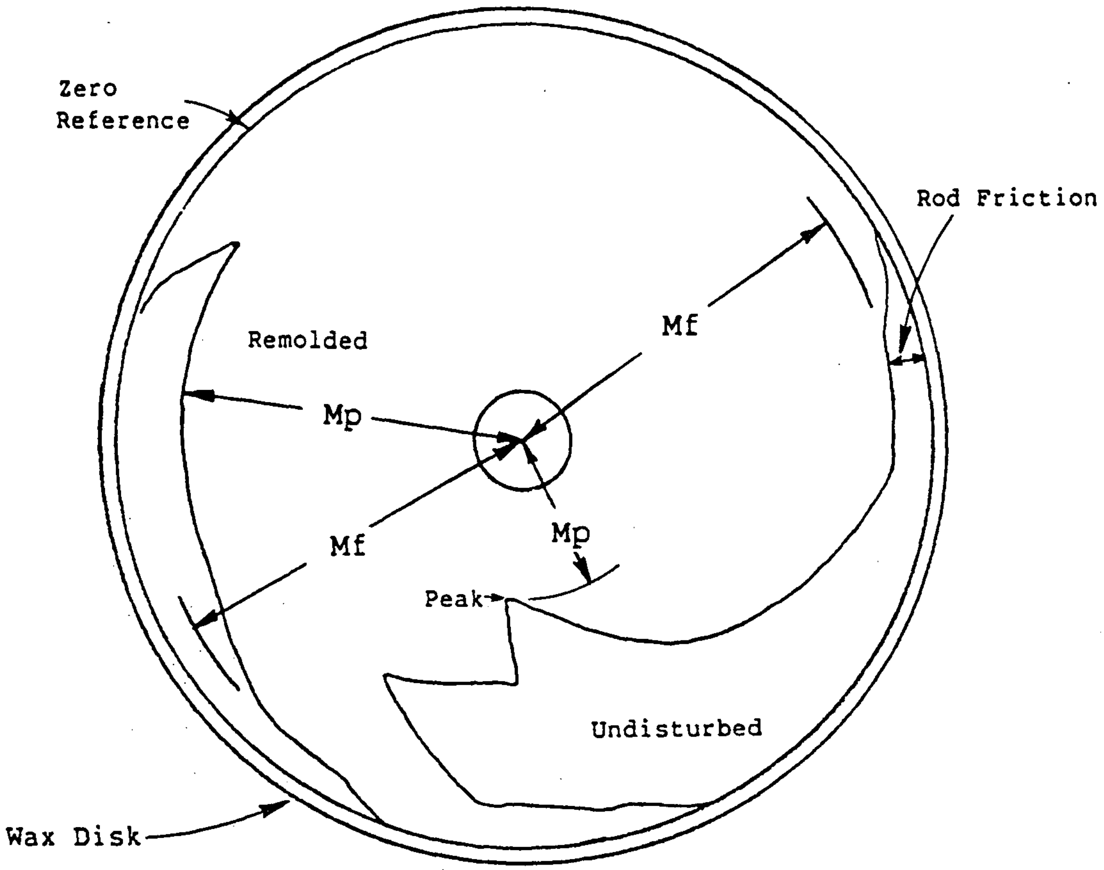

$$Su = (Mf - Mp) \times K \times a$$

where: Su - undrained strength
Mf - as shown in figure
Mp - as shown in figure
K - torque head spring constant
a - vane constant $(6/(7\pi D^3))$

Figure 3.3 - EXAMPLE OF A NILCON TEST RECORD

applied to the vane and is substituted for T in equation 3.4. The determination of undrained strength is sensitive to the ability to accurately define the rod friction. It is therefore important to use the largest possible vane to maximize the output on the disk.

CHAPTER 4
A REVIEW OF THE VANE SHEAR TEST

4.1 Introduction

The field vane test was introduced in Sweden 60 years ago (Bjerrum and Flodin 1960) and has been used by engineers in its present form since 1948 (Cadling and Odenstad 1950). Because of its simplicity, repeatability and relatively low cost of operation it has found wide spread use in practice. A great deal of experience has been gained with its use in the design of slopes, embankments, foundations and other engineering structures. It has only been in the last decade or two that engineers have begun to critically study the vane shear test; Aas 1965, Flaate 1966, Bjerrum 1972 and 1973, Arman et al. 1975, Schmertmann 1975, Donald et al. 1977, Menzies and Merrifield 1980, Wroth 1984 and others. These studies have led to a better appreciation of some of the factors that influence the vane test, however, the ability to incorporate all of these factors and other unquantifiable soil characteristics into the analysis of the vane is still incomplete. In light of this relatively recent research it is felt that a brief review of the main factors influencing vane results is appropriate.

4.2 Evaluation of Undrained Shear Strength

The traditional method of interpreting the vane test assumes that failure occurs over the cylindrical surface circumscribed by the vane with the shear stress being uniformly distributed on the top, bottom, and sides of the cylinder. The material is assumed to be isotropic; the peak shear stress being equal to the undrained strength, Su. These basic assumptions lead to expression 4.1, the derivation of which is shown in figure 4.1.

$$Su = \frac{6M}{\pi D^2 H(3+D/H)} \qquad 4.1$$

where Su - undrained shear strength
M - measured peak torque
D - diameter of vane
H - height of vane
(consistent units)

The most commonly used vane, and that which is the recommended standard according to ASTM (ASTM D2573), has a height to diameter ratio (H/D) of 2. Expression 4.1 thereby reduces to the standard expression shown earlier as 3.4 and repeated here:

$$Su = \frac{6M}{7\pi D^3} \qquad 3.4$$

It is equation 3.4 that is implied in the method of vane interpretation described by ASTM D2573 and in the manuals accompanying vane equipment.

It has recently been showen by Donald et al. 1977 and Menzies and Merrifield 1980 that the distribution of shear stress is likely to be non-uniform, particulary on the ends of the vane. Using a three dimensional linear elastic finite element formulation, Donald et al. derived the stress distribution shown in figure 4.2 for a plane midway between the blades. Their results indicate that a uniform distribution of shear stress is a reasonable assumption on the vertical plane, however, the shear stresses on the horizontal plane increase from zero at the axis of rotation to a maximum at the blade

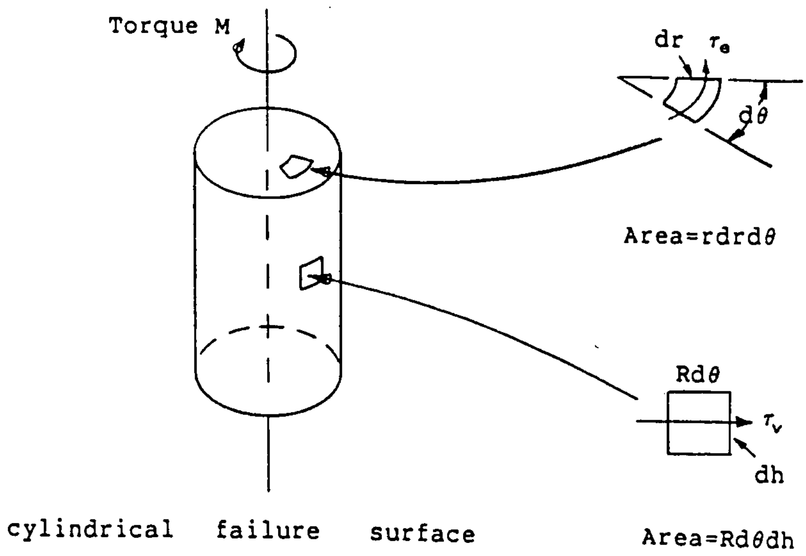

On End (Horizontal Plane)

$$dM_\theta = \tau_\theta \, r\,dr\,d\theta \cdot r$$

$$\int dM_\theta = \tau_\theta \int_0^{2\pi} \int_0^R r^2 \, dr\,d\theta$$

$$M_\theta = \tau_\theta \frac{R^3}{3} 2\pi$$

τ_θ = Su at peak

$$M_\theta = \frac{\pi D^3}{12} Su$$

On Vertical Surface

$$dM_v = \tau_v \, dA \cdot R$$

$$\int dM_v = \tau_v R^2 \int_0^H \int_0^{2\pi} d\theta\,dh$$

$$M_v = \tau_v R^2 2\pi H$$

τ_v = Su at Peak

$$M_v = \frac{\pi D^2}{2} H Su$$

$$M = M_v + 2M_\theta$$

$$M = Su \frac{\pi D^2}{6} H \left(3 + \frac{D}{H}\right)$$

Figure 4.1 - STANDARD ANALYSIS OF THE VANE SHEAR TEST

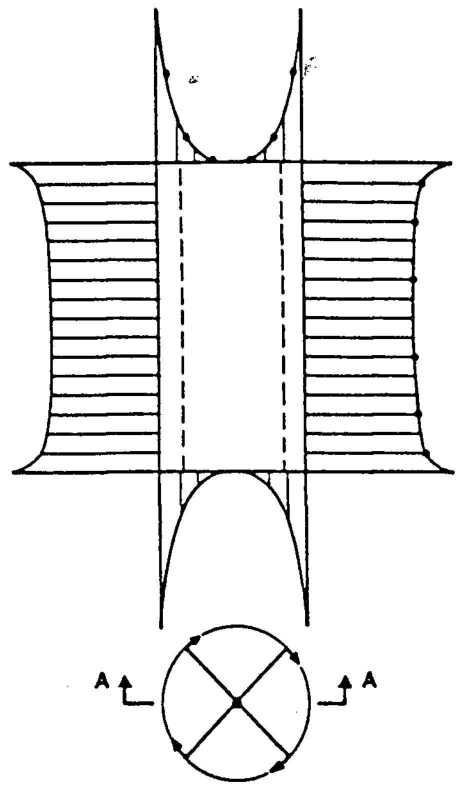

Figure 4.2 - SHEAR STRESS DISTRIBUTION ON A PLANE MIDWAY BETWEEN VANE BLADES USING A 3D FINITE ELEMENT ANALYSIS

(adapted from Donald et al. 1977)

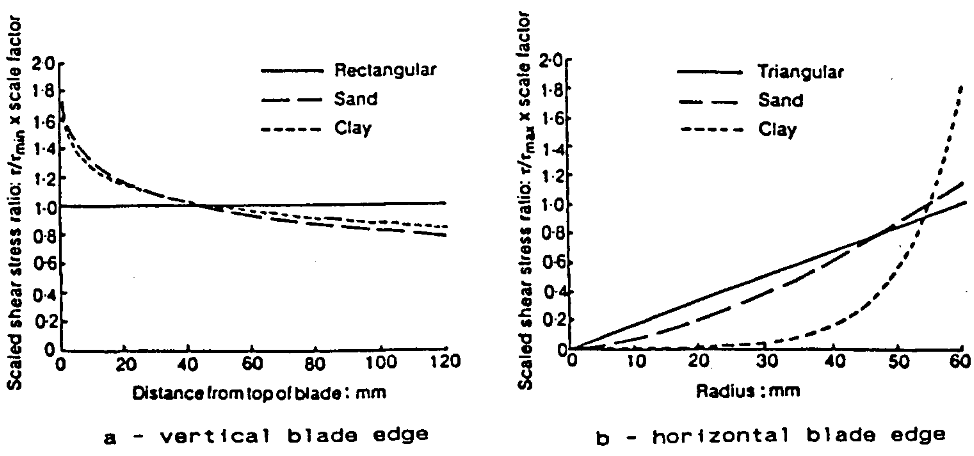

Note: shear stresses have been scaled to give equal torque

Figure 4.3 - DISTRIBUTIONS OF EQUIVALENT SHEAR STRESS ON A VERTICAL AND A HORIZONTAL BLADE EDGE

(adapted from Menzies and Merrifield 1980) edge. Menzies and Merrifield instrumented a vane with close fitting strain gauged cantilevers along the top edge of one blade and along the vertical edge of another. They used this vane to perform tests in a fine sand and in an overconsolidated clay. Their results, shown in figure 4.3, appear to be similar to those of Donald et al. indicating that the distribution along the top of the blade is indeed non-uniform. It is encouraging to see the agreement between the analytical analysis and the field testing, however, one might expect the elastic analysis to adequately predict the behaviour of an overconsolidated clay and, thus, it would be very interesting to see results from tests in a soft normally consolidated clay.

As Wroth 1984 points out, the results just presented suggest that the shear stress distribution on the horizontal planes can be approximated by the expression:

$$\frac{\tau}{\tau_m} = \left(\frac{r}{R}\right)^n \qquad 4.2$$

where τ - shear stress
τ_m - maximum shear stress
R - radius of vane
r - radial distance from axis of rotation

Using this distribution expression 4.1 becomes

$$Su = \frac{2M(3+n)}{\pi D^2 H((3+n)+D/H)} \qquad 4.3$$

For the usual case where H/D=2, equation 4.3 reduces to:

$$Su = \frac{2(3+n)M}{\pi D^3 (2)(3.5+n)} \qquad 4.4$$

Based on the results of Menzies and Merrifield 1980, Wroth 1984 reported that n is approximately 5. Expression 4.4 thereby yields:

$$Su = \frac{16M}{17\pi D^3} \qquad 4.5$$

Comparing equation 4.5 to 3.4 there is an almost 10% underestimation of the undrained shear strength using the standard analysis if one accepts that n is 5.

Several other assumptions are made in the analysis of the vane and are discussed in the following sections:

1) Stress conditions remain unchanged during vane insertion
2) the soil around the vane remains undisturbed
3) shearing takes place under undrained conditions
4) the shear strength is fully mobilized (simultaneously) on all surfaces
5) the soil is isotropic with respect to strength
6) there is no progressive failure

4.3 Effects of Anisotropy

The effect of anisotropy is one of the most commonly studied aspects of the vane test. The resistance to shear can be separated into the contributions by each surface of the cylinder. Denoting the shear strength on the horizontal surface as Sh and that on the vertical face as Sv equilibrium is satisfied by the equation:

$$\frac{2M}{\pi D^2 H} = Sv + \frac{Sh \cdot D}{(3+n)H} \qquad 4.6$$

Equation 4.6 indicates that for the standard vane (H/D=2) the vertical face contributes 86% to 94% of the shear resistance for values of n=0 (uniform shear distribution) and n=5, respectively. In other words, the vane test is strongly dominated by the available strength on the vertical plane.

By using vanes of various proportions several researchers have studied the effects of anisotropy; Aas 1965 and 1967, Eide 1968, Blight 1970, Wiesel 1973, Bjerrum 1973, Richardson et al.

1975, Donald et al. 1977, and Poplin et al. 1978. At least two torque measurements using vanes of different H/D ratios are required at each test depth to solve for Sh and Sv in equation 4.6. Wiesel 1973 recommends using vanes of equal diameter but different lengths to eliminate the problem of the peak strengths not being simultaneously mobilized on the horizontal and vertical planes. Richardson et al. 1975 used diamond shaped vanes (figure 4.4) to determine the anisotropy on planes at various angles. The results from their tests are shown in figure 4.5 and they indicate that the greatest strengths are observed on the vertical plane and the minimum strengths occur on the horizontal planes. They reported that the strengths observed on planes at various angles describe an ellipse having Sv as the radius on the major axis and Sh the radius on the minor axis.

Bjerrum 1973 plotted the ratio of Sh/Sv for several clays against their plasticity index concluding that the ratio decreases with increasing plasticity. In his state of the art address Bjerrum 1973 presents a rationale as to why this relationship should exist. Richardson et al. 1975 added their data to Bjerrum's figure and this is shown in figure 4.6. The trend of decreasing Sh/Sv ratio with increasing PI was also observed, however, they suggest that Bjerrum's curve should be adjusted.

Donald et al. 1977 attempted to analyse the effect of anisotropy by recording the full torque-rotation curves for vanes of various H/D ratios but of equal diameters. From two curves they inferred the side resistance (and thus the end resistance) by multiplying the difference between the two curves

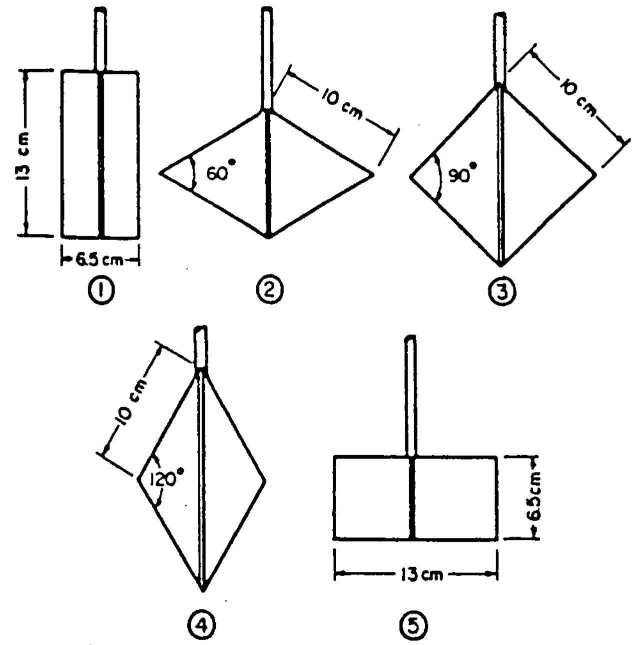

Figure 4.4 - VARIOUS VANE CONFIGURATIONS USED TO MEASURE STRENGTH ANISOTROPY

(adapted from Richardson et al. 1975)

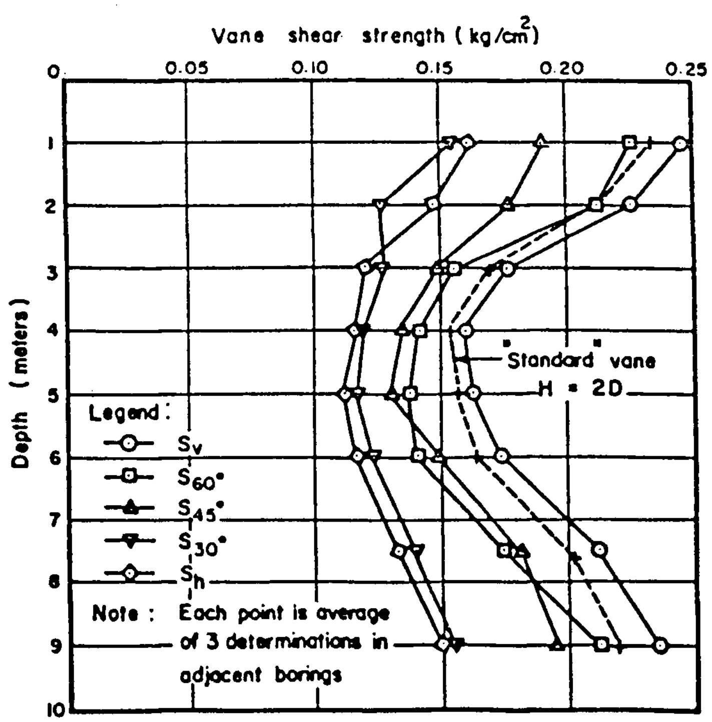

Figure 4.5 - VANE SHEAR STRENGTHS ON PLANES AT VARIOUS ANGLES

(adapted from Richardson et al. 1975)

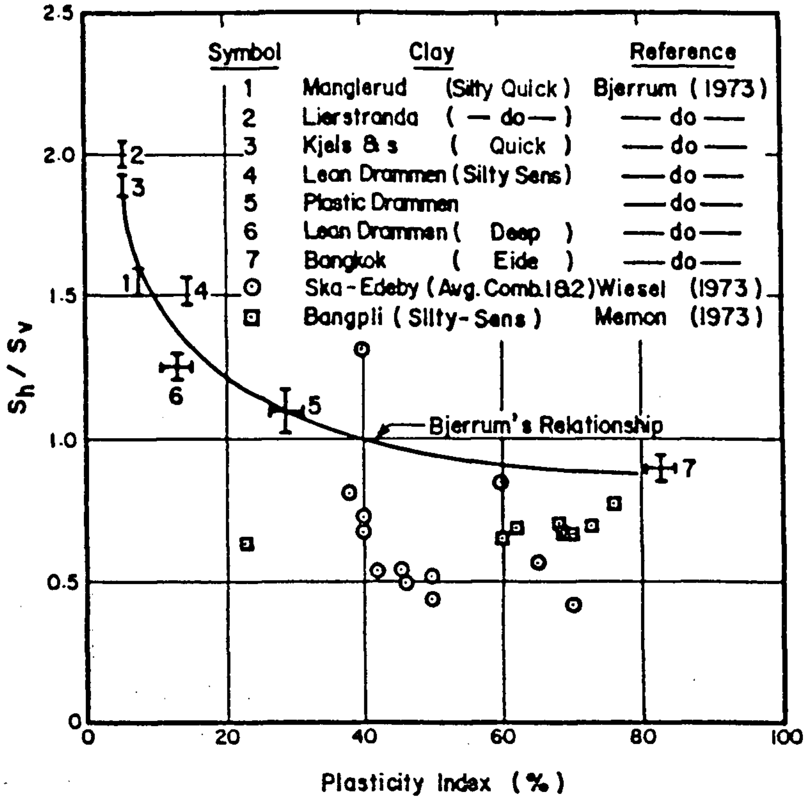

Figure 4.6 - PLOT OF RATIO OF UNDRAINED SHEAR STRENGTHS IN HORIZONTAL AND VERTICAL DIRECTIONS VS PLASTICITY INDEX

(adapted from Richardson et al. 1975)

by the ratio of the length of the first vane to the difference in the lengths of the two vanes. Their analysis indicated that the ends reached their peak strengths before the sides which would mean that the peak torque would be dominated by the strength of the vertical plane even more than considered previously. However, their ability to reasonably estimate the Sh/Sv ratio met with limited success suggesting that this method is unreliable.

Most methods used to estimate the Sh/Sv ratio assume a uniform distribution of stress on both planes. As shown earlier, this may be a reasonable assumption on the vertical planes but is probably not very accurate for the horizontal planes. This assumption has a significant effect on the Sh/Sv ratio. By solving expression 4.3 simultaneously for tests that have recorded different torques T_1 and T_2, used vanes of different diameters D_1 and D_2, and different vane heights H_1 and H_2 it can be shown that:

$$Sh = (3+n)\beta \qquad 4.7$$

$$Sv = \frac{2T_1}{\pi D_1{}^2 H_1} - \left(\frac{D_1}{H_1}\right)\beta \qquad 4.8$$

$$\text{where} \quad \beta = \left(\frac{2T_2}{\pi D_1{}^2 H_1} - \frac{2T_1}{\pi D_1{}^2 H_1}\right) \cdot \frac{H_2 H_1}{H_1 D_2 - H_2 D_1}$$

The value of n does not affect the estimation of Sv but it does have a significant effect on Sh.

4.4 Rate Effects

It has been commonly found that the undrained shear strength is dependent upon the rate of shear; Aas 1965, Flaate 1966, Blight 1968, Bjerrum 1972, Berre and Bjerrum 1973, Wiesel

1973. This effect is illustrated in figures 4.7 and 4.8. Figure 4.7 shows the variation in undrained strength with depth at different rates of vane rotation whereas figure 4.8 shows the correlation between shear stress level and time to failure for undrained triaxial compression tests established by Berre and Bjerrum 1973 for Drammen clay. Bjerrum 1972 states that the rate effect is associated with the cohesive component of shear and that there are good reasons to assume that the rate effect should increase with increasing plasticity of the clay. Tests by Aas 1965, Flaate 1966, Torstensson 1977, and Kimura and Saitoh 1983 indicate that the shear strength can vary with the time delay between vane insertion and the start of shearing. In the results presented by Flaate 1966 a time delay of only 15 minutes led to an increase in the undrained strength by more than 10%. This effect is related to the dissipation of the pore pressures generated during insertion of the vane resulting in the consolidation of the surrounding clay. Blight 1968 proposed a method by which the preselection of a test duration can be made to ensure that the vane test in silty soils is conducted under undrained conditions.

4.5 Disturbance Due to Vane Insertion

It is generally assumed that the soil remains undisturbed during vane insertion, however, it has been documented that high pore pressures can be generated and that the insertion of the blades can partially destroy the natural soil structure. Both of these effects can result in a measured undrained shear strength less than the actual insitu value.

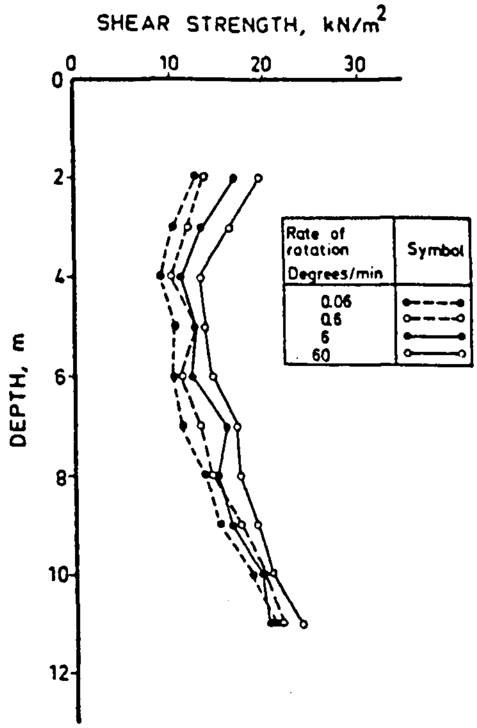

Figure 4.7 - VARIATION WITH DEPTH OF UNDRAINED SHEAR STRENGTH AT DIFFERENT RATES OF ROTATION

(adapted from Wiesel 1973)

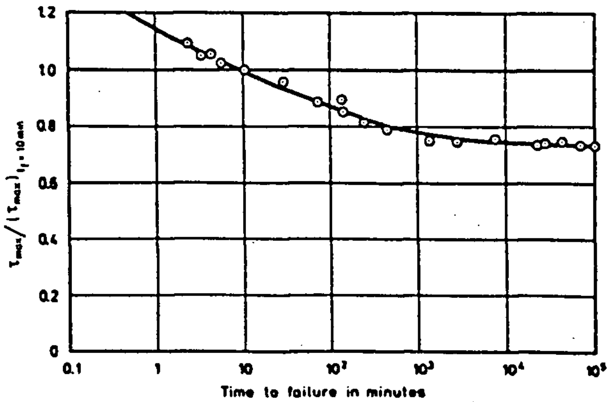

Figure 4.8 - CORRELATION BETWEEN SHEAR STRESS LEVEL AND TIME TO FAILURE FROM UNDRAINED TRIAXIAL COMPRESSION TESTS ON DRAMMEN CLAY

(adapted from Berre and Bjerrum 1973)

La Rochelle et al. 1973 performed tests using four different thicknesses of vane blades to evaluate the effect of disturbance due to vane insertion. By plotting the measured Su values against the vane perimeter ratio (ratio of 4 times the blade thickness e to the vane perimeter - $4e/\pi D$) he was able to extrapolate the results to estimate the shear strength corresponding to a zero blade thickness. His results indicated that the disturbance due to the insertion of the standard vane reduced the apparent strength by about 16%. It is important to note that La Rochelle was testing Champlain clay, a highly sensitive and brittle glacial marine clay characterised by chemical bonds between the clayey platelets. Clays from two different sites were used for his study; one having an average sensitvity of 50, the other having an average sensitivity of 20. He presented the results for only the most sensitive site and stated that the results from the other site were not as marked. This suggests that the effects of vane insertion are probably not as significant in less brittle and less sensitive soils.

Kimura and Saitoh 1983 instrumented a laboratory vane and a triaxial cell with pore pressure transducers to investigate the effects of vane insertion. They found that high pore pressures in the order of 75% of the consolidation pressure were generated during vane insertion. They also found that the pore pressure changes during vane rotation were very small. Evidence of the generation of high pore pressures and their subsequent dissipation confirms that the time delay between vane insertion and the start of rotation can be a controlling factor in the measured undrained strength.

Flaate 1966 also indicated that an unknown degree of disturbance can be caused by soil sticking to the vane blades thereby increasing the area ratio of the vane (ratio of the actual vane blade area to the projected area of the vane πD^2) for tests at other depths.

4.6 Correction Factors

Several papers appear in the literature in which attempts have been made to correlate the results of vane shear tests to those obtained from laboratory tests. These laboratory tests have included unconfined compression, consolidated undrained, K_0 consolidated undrained, direct shear and simple shear among others. Rightly so, no single correlation has been established between the vane and laboratory tests which would help in 'correcting' the vane strength. The discrepencies are not surprising since the failure mechanism of the vane test is unlike that of any other test. More importantly, however, is the fact that there are many examples of vane tests producing non-conservative stability calculations. Back calculations from actual failures should yield the true insitu undrained strength and it has been found that in many cases the vane strength overpredicted the value at failure. This problem has led to the concept of applying correction factors to the vane strength.

Bjerrum 1972 reviewed 14 known failures (FS=1) and discovered that the theoretical factors of safety differed from 1 and varied with the plasticity index of the clay. He therefore introduced a correction factor, μ, with which the vane strength should be multiplied before it is introduced into a stability analysis. Bjerrum's correction factor is illustrated in figure 4.9. He speculated that the discrepancy was due primarily to rate effects and soil strength anisotropy. He did consider that progressive failure may also be a contributing factor but he concluded that it is only a minor one.

Bjerrum 1973 attempted to separate the two effects and this is shown in figure 4.10. He introduced two factors μ_r and μ_a representing the factors for rate effects and anisotropy respectively and stated that the shear strength to be used in a stabilty analysis should be:

$$Suf = Suv \mu_r \mu_a \qquad 4.9$$

where
Suf - field Su
Suv - vane Su
μ_r - correction factor for rate effects
μ_a - correction factor for anisotropy

Bjerrum 1973 points out that μ_r (figure 4.10) represents a correction factor for cases where the minimum factor of safety will be reached in a matter of weeks or months after construction. A different value may be required for shorter time periods. He also indicates that the value of μ_a will vary along the expected failure surface depending on its inclination and can be estimated from figure 4.11.

Azzouz et al. 1983 proposed a new field vane correction curve to be used in the design of embankments to account for their three dimensional mode of failure.

The Swedish Geotechnical Institute (SGI) uses a reduction factor μ based on the liquid limit (W_l) of the soil. The SGI correction curve is compared to Bjerrum's curve (as plotted against W_l) in figure 4.12.

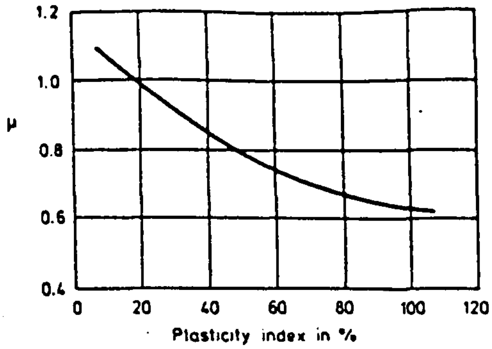

Figure 4.9 - CORRECTION FACTOR FOR UNDRAINED SHEAR STRENGTH DETERMINED FROM FIELD VANE TESTS

(adapted from Bjerrum 1972)

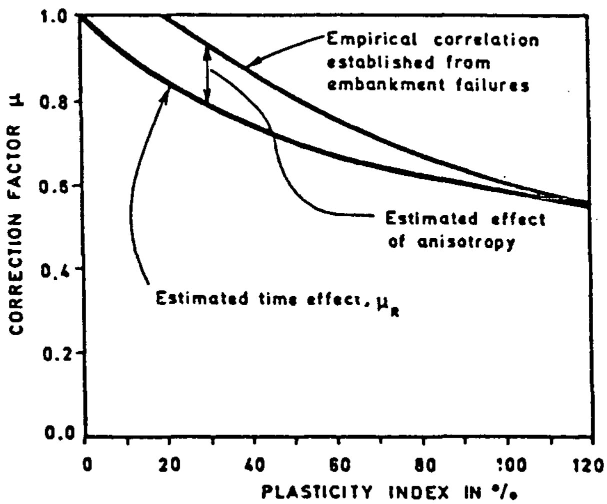

Figure 4.10 - EMPIRICALLY ESTABLISHED CORRECTION FACTORS FOR RESULTS OF VANE SHEAR TESTS

(adapted from Bjerrum 1973)

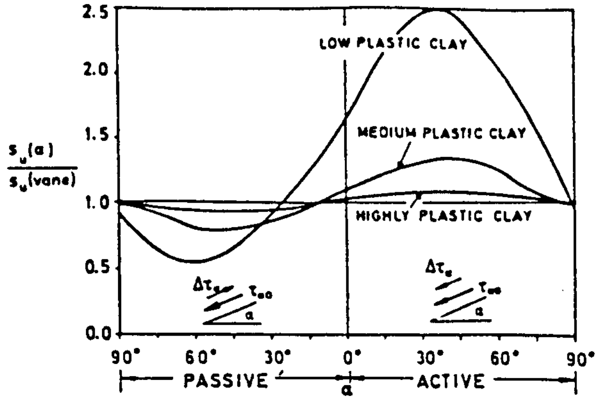

TYP. OF CLAY	I_p (%)	K_0	δ	φ_u	$\frac{p_c}{p_0}$	D_m
LOW PLASTIC	10	0.50	0.03	30°	1.2	0.30
MEDIUM PLASTIC	50	0.65	0.15	15°	1.6	0.45
HIGHLY PLASTIC	100	0.80	0.30	10°	2.0	0.60

Figure 4.11 - RATIO OF UNDRAINED SHEAR STRENGTH TO VANE SHEAR STRENGTH FOR THREE TYPES OF CLAY

(adapted from Bjerrum 1973)

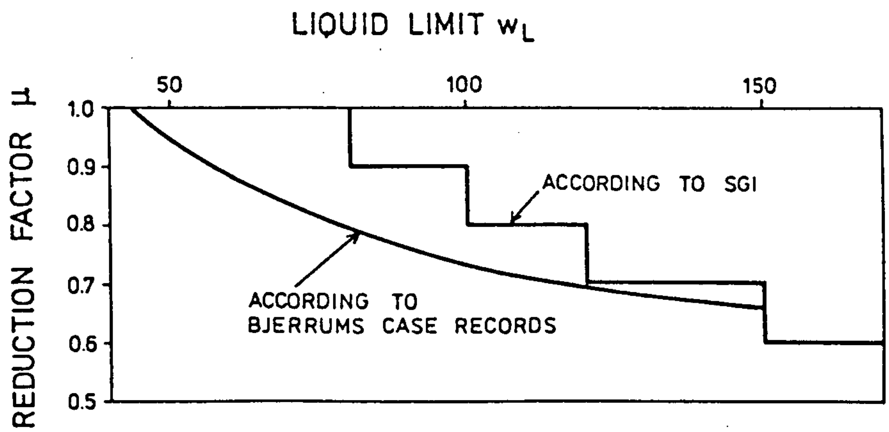

Figure 4.12 - VANE SHEAR TEST REDUCTION FACTOR AS A FUNCTION OF THE LIQUID LIMIT ACCORDING TO THE SWEDISH GEOTECHNICAL INSTITUTE

(adapted from Helenelund 1977)

Helenelund 1977 presents several different methods for reducing the undrained shear strength of clay.

Some engineers are opposed to the application of correction factors to vane strengths. Schmertmann 1975, after reviewing the different factors affecting the vane test, stated that any engineer who desired to apply these state-of-the-art corrections would probably be at a loss as how to use his particular Suv data and he termed this the "current correction crisis". Kenney and Folkes 1979 considered the problem of soft Canadian soils and their unique behaviour and concluded that in the absence of sufficient empirical information, it would be fool hardy to accept the approach of equation 4.9.

This writer has observed that correction factors are often applied without regard to the problem at hand and how it relates to the conditions for which the correction factors were introduced. For example, it does not seem correct to apply Bjerrum's correction to field vane data when it is to be compared to CPT results. Bjerrum's correction is used to reduce the measured strength to account for the effects of the relatively high rate of strain associated with the VST. However, the rate of strain during cone penetration is greater than that in a vane test. If anything, the strength should be increased. Although the effects of anisotropy should vary along the expected failure plane, depending on its orientation, a single correction factor is often applied to vane strength data.

4.7 Summary

The use of the field vane test has a long history and engineers have attained a great deal of experience in the interpretation of VST results. Recent work has shown, however, that the standard method of analysis is likely incorrect. Laboratory studies and finite element analyses suggest that the distribution of shear stress is not uniform, particularly on the ends of the vane. It has also been shown that the vertical face contributes up to 90% of the shear resistance. Using vanes of various shapes and dimensions to study the effects of strength anisotropy, tests indicate a trend of decreasing Sh/Sv with increasing plasticity. The calculation of this ratio, however, is highly sensitive to the assumed shear stress distribution on the ends of the vane. Field vane results are dependent upon the rate of strain with greater strengths being measured at higher rates of strain. Delays between vane insertion and the start of shearing also influence VST results due to the consolidation of the surrounding soil that takes place as the pore pressures induced during vane insertion dissipate.

Because of these problems and due to our lack of complete understanding of the VST, some consider the test to be nothing more than a strength index test (Schmertmann 1975). Despite this feeling, the VST is still used extensively because it is a quick, inexpense and highly repeatable method of determining undrained shear strength.

CHAPTER 5

A BRIEF REVIEW OF THE CONE PENETRATION TEST

5.1 Introduction

The cone penetration test is unequalled in its ability to indentify soil layer boundaries and qualitatively evaluate material types. Because of the complex behaviour of soils and the complex changes in stress and strain around the cone tip, correlations between CPT data and material parameters are necessarily empirical. However, the highly repeatable nature of the test has led to a great deal of confidence in the various correlations.

Comprehensive reviews of the use and interpretation of cone penetration tests have been presented by Schmertmann 1978, Robertson and Campanella 1984, Wroth 1984, Campanella et al. 1985 and Jamiolkowski et al. 1985. Although Schmertmann's report is primarily concerned with the interpretation and application of mechanical cone data, there are many good discussions that are applicable to electronic cone data. These reviews have discussed such topics as equipment design, test procedures, interpretation techniques, applications to geotechnical design and the factors affecting test results and their interpretation. Hence, this review will present only some of the important aspects of cone penetration testing that are relevant to the estimation of undrained shear strength and cone testing in clays.

5.2 Soil Classification

The current method of interpreting soil type from CPT is based on the cone bearing (Qc) and the friction ratio (Rf). Experience has shown that high bearing values and low friction ratios are associated with coarse grained noncohesive materials and lower bearing values and increasing friction ratios are associated with fine grained cohesive materials of increasing plasticity. Douglas and Olsen 1981 describe their work in developing the classification chart illustrated in figure 5.1. They consider that the chart essentially consists of three zones of different soil type: cohesionless coarse grained soils, ductile fine grained soils and mixed soils. Their chart indicates the effect of various soil indices on the penetrometer response. From a practical point of view, Douglas and Olsen's chart is not a very easy one to use. Figure 5.2 shows a simplified version used by U.B.C. for interpreting CPT data.

Douglas and Olsen correctly indicate that cone penetration tests reflect an aggragate behaviour of the soil and that a more appropriate description for soil classification is soil behaviour type rather than just soil type. The cone responds to an interaction of the soil composition, fabric, local stress conditions and soil behaviour within a zone of influence that extends ahead and behind the cone (discussed in more detail in section 5.3).

It should also be pointed out that the classification charts developed to date are all based on uncorrected cone bearing Qc. This is not a serious problem in coarse grained materials (except perhaps offshore), however, it may be of

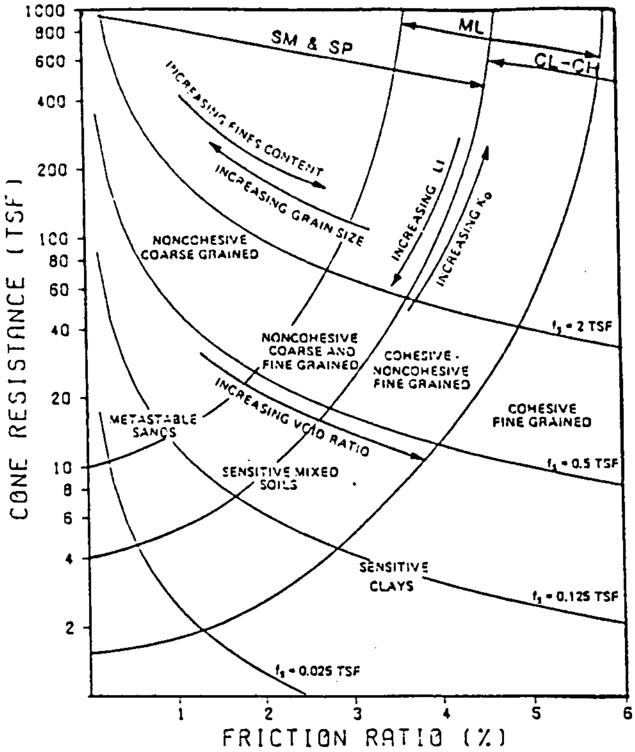

Figure 5.1 CPT SOIL BEHAVIOUR TYPE CLASSIFICATION CHART (adapted from Douglas and Olsen 1981)

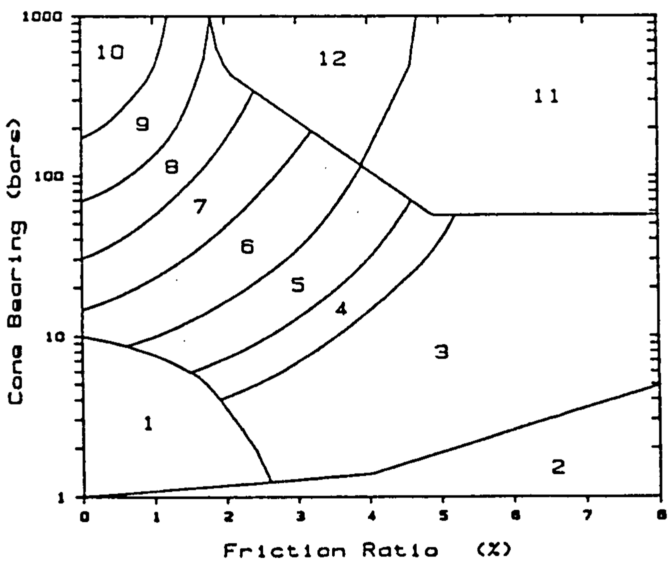

Zone	Qc/N	Soil Behaviour Type
1)	2	sensitive fine grained
2)	1	organic material
3)	1	clay
4)	1.5	silty clay to clay
5)	2	clayey silt to silty clay
6)	2.5	sandy silt to clayey silt
7)	3	silty sand to sandy silt
8)	4	sand to silty sand
9)	5	sand
10)	6	gravelly sand to sand
11)	1	very stiff fine grained (*)
12)	2	sand to clayey sand (*)

(*) overconsolidated or cemented

Figure 5.2 UBC SIMPLIFIED CPT SOIL BEHAVIOUR TYPE CLASSIFICATION CHART FOR THE ELECTRONIC FRICTION CONE significance when interpreting data from soundings in materials that tend to generate high excess pore pressures. These materials generally have low cone bearings and plot in the lower left portion of the chart. Future classification charts should be based on corrected bearing Qt.

Since most classification charts have been developed from soundings that are generally less than 30m, interpretation of data from deep soundings may also present a problem. The effect of high overburden pressure is to increase the cone bearing, consequently, a clay from a deep sounding may be interpreted as a sand. It is recommended that future classification charts use normalized parameters.

Several proposals have been made to include pore pressure data in the interpretation of soil types (Jones et al. 1981, Senneset et al. 1982, Jones and Rust 1982 and Senneset and Janbu 1984). However, until a standard is developed for the pore pressure element location(s) the acceptance of a classification system based on pore pressure is unlikely.

5.3 Soil Profiling

An evaluation of material type and its stress history can often be obtained by considering the entire bearing profile. Some materials are characterized by typical profile shapes. Schmertmann 1978 presented some simplified examples of typical profiles and indicated the likely and possible interpretations. These examples are reproduced in figure 5.3. Of special interest for this report are the typical shapes of bearing profiles in clay deposits. Figure 5.3a indicates that the tip resistance in

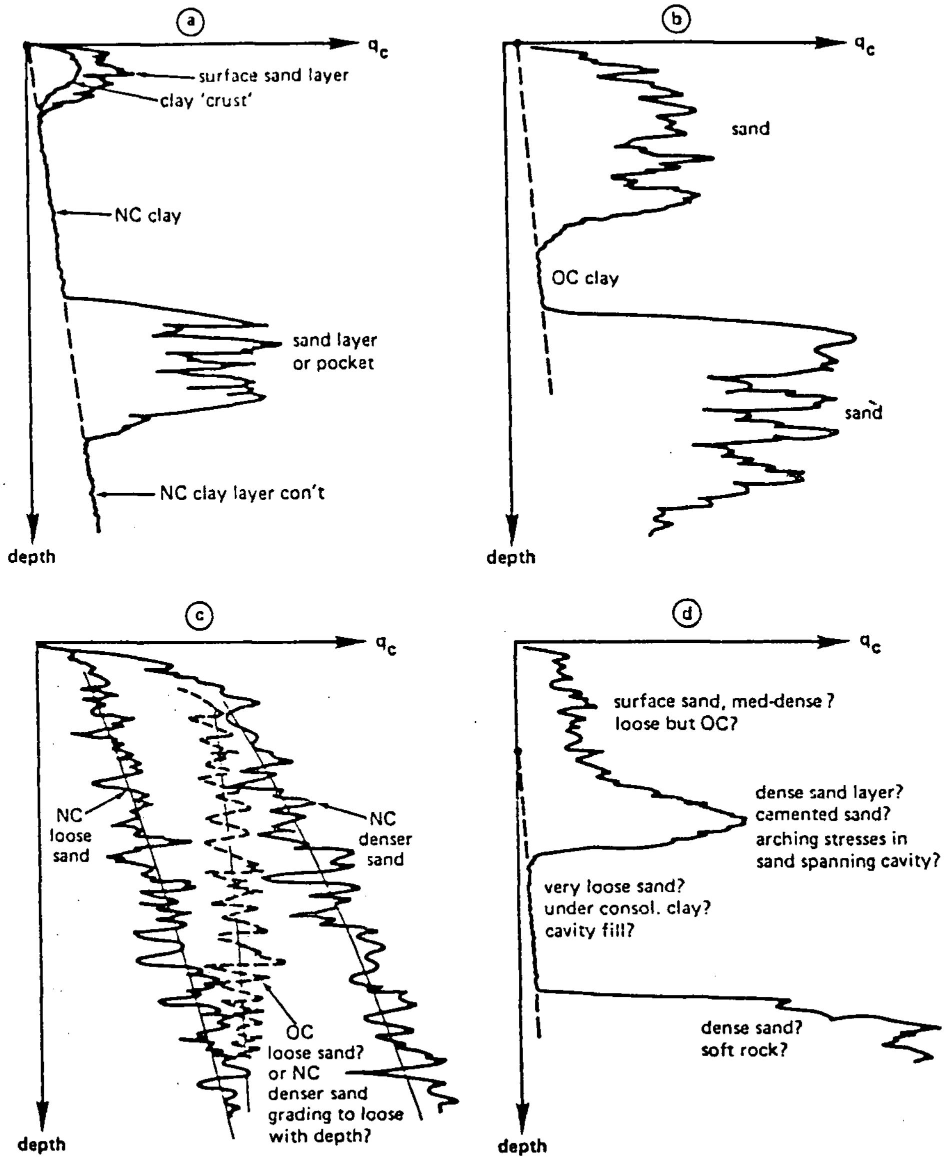

Figure 5.3 SIMPLIFIED EXAMPLES OF CONE BEARING PROFILES SHOWING LIKELY AND POSSIBLE INTERPRETATIONS FOR SOIL TYPES AND AND CONDITIONS

(adapted from Schmertmann 1978)

a normally consolidated clay deposit typically increases linearly with depth (if groundwater conditions are hydrostatic). An extrapolation of the profile should extend through the origin (this idea is modified in section 6.4). Robertson and Campanella 1983 report that for most young clays where overconsolidation has been caused by erosion or dessication, the cone bearing may remain constant or may decrease with depth until the depth where the deposit is normally consolidated. This can be seen in the CPT profile shown in figure 7.3. For aged clays where the OCR is constant with depth, the tip resistance may continue to stay constant with depth.

It has also been found that the friction ratio for some fine grained soils may decrease with increasing overburden stress (Robertson and Campanella 1983). Evidence of this can be seen in the various CPT profiles presented in chapter 7. This result may lead to difficulty when interpreting deep soundings.

Penetration tests performed in a multilayered media by Treadwell 1976 indicated that a transition zone exists at layer boundaries within which the tip resistance is affected by the soil properties of an adjacent layer. It was observed that the tip resistance is significantly influenced by the material ahead and behind the tip. Treadwell considers that this transition zone consists of upper and lower parts; the upper portion being the depth over which the tip resistance is influenced by the next layer and the lower portion being the distance that the tip must advance beyond the layer interface for its resistance not to be affected by the overlying material. Treadwell reports that the upper portion of the transition zone typically begins 3 to 4 cone diameters above the layer interface. The lower portion appears to depend on density, depth and the relative stiffness between the two layers. With regards to the lower portion of the transition zone, he found that the transition was made quickly (in 3 to 5 diameters) when penetrating from a dense layer to a loose layer. However, when penetrating from a loose layer to a dense layer the transition zone was significantly larger, increasing in size with increasing depth. These effects are illustrated in figure 5.4. It can be seen that at a shallow depth the tip resistance in the dense material is almost equal to that for a uniformly dense deposit, however, at greater depth the cone bearing does not attain its full resistance. On the other hand, the tip resistance in the loose layers is equal to or slightly greater than that in a uniformly loose material. Similar work by Schmertmann 1978 shows that the influence of the soil layer interface is felt from a distance of 5 to 10 cone diameters on either side of the layer boundary. Schmertmann found that the greater the difference in strength and compressibilty between the layer to be sensed and the adjacent soil the thinner the layer that can be detected. He added that the smaller the cone diameter the more sensitive the tip is to local variations with depth.

These effects are of great importance when interpreting strength parameters from CPT data. It must be recognized that the cone bearing will not reach its full resistance in thin layers of sand. This can lead to difficulty when estimating such parameters as relative density, modulus and friction angle. On the other hand, much thinner layers of clay are required to

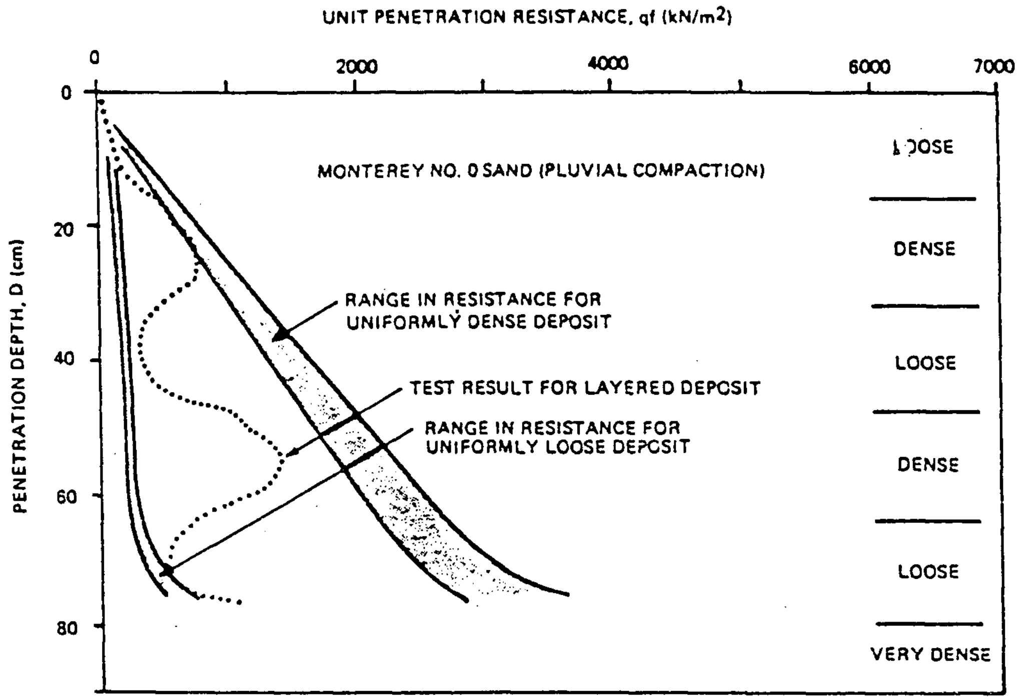

Figure 5.4 CONE PENETROMETER BEARING RESPONSE IN A LAYERED MEDIA

(adapted from Treadwell 1976)

record the true bearing. When estimating shear strength of cohesive materials in stratified deposits, it is best to use the minimum bearing values (i.e. the valleys in the bearing record) rather than an average line drawn through the profile since the local variations in bearing are a reflection of the non-cohesive materials.

These results raise the question as to how thin a layer cone penetration tests can detect. A recent report by Davies 1985 reveals that this can be of interest in the identification of shear planes. Schmertmann's results suggest that a layer must be at least 10 to 20 cone diameters thick (36cm to 72cm for a $10cm^2$ cone) to attain full penetration resistance. Clearly, penetration tests can detect layers thinner than 36cm, however, the interpretation of material parameters may be seriously affected.

The ability of CPT to define soil layers is illustrated in figure 5.5. A portion of a CPT bearing profile is presented alongside a continuously sampled borehole log obtained at the B.C. Hydro railway crossing site (described in chapter 7). The borehole log is based solely on a visual classification of the sampled after it had been extruded from the sample tube and split in half lengthwise. The complete bearing/continuous sample log is included in appendix A, and reference will be made to it in the following discussion. The modified Hogentogler cone (see chapter 2) was used for the CPT and a GMF 67mm diameter continuous sampler was used for the borehole. The CPT was performed 1m from the borehole. During logging of the borehole sample only layers of thickness 1cm or greater were recorded as

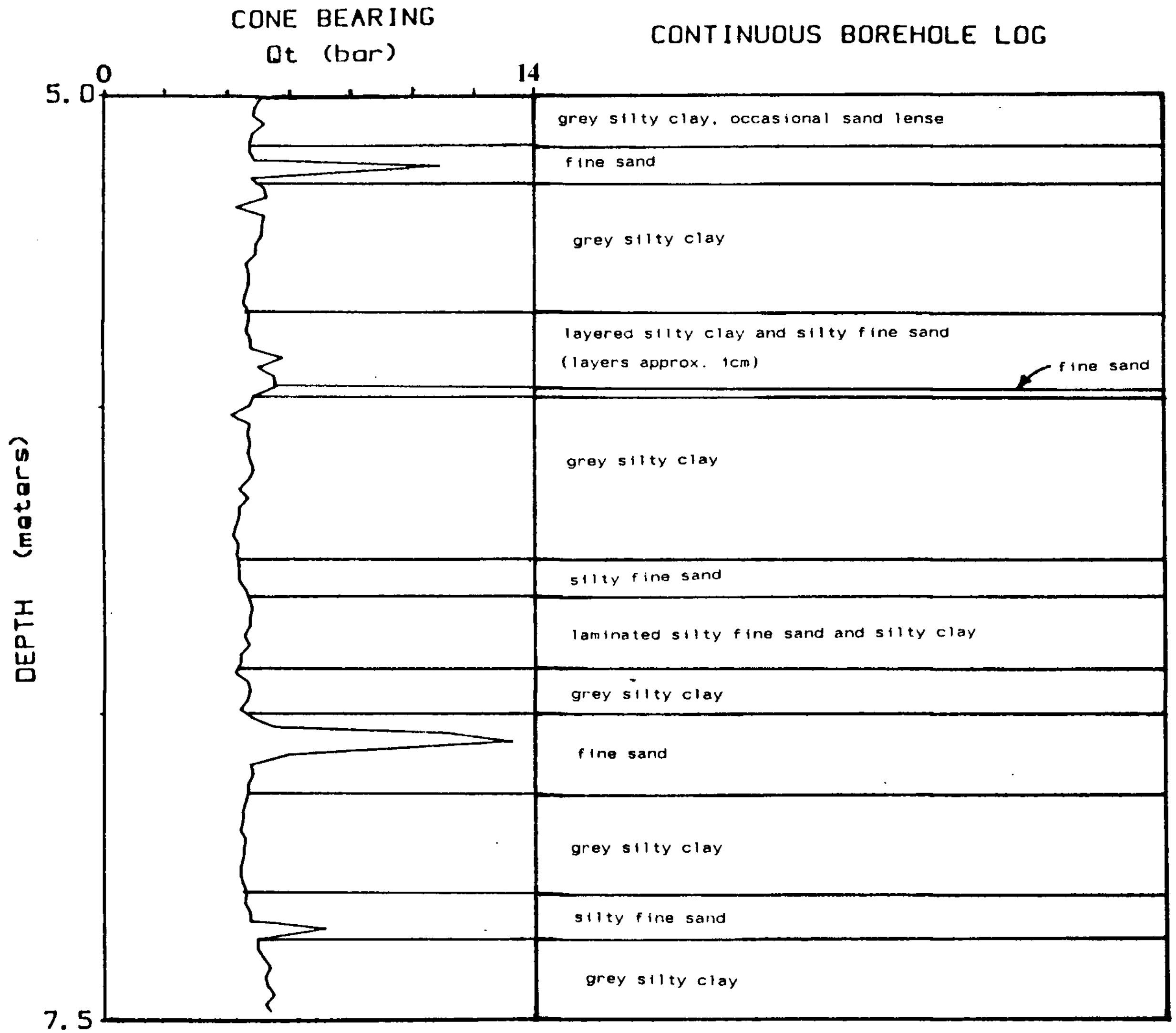

Figure 5.5 COMPARISON BETWEEN A CPT BEARING PROFILE AND A CONTINUOUS SAMPLE LOG

individual layers. It is quite clear from figure 5.5 that layers of the order 10cm thick were easily detected by the tip resistance. There are some examples of thinner layers, possibly as thin as 1cm thick being detected. This can be seen in the layered silty clay and silty fine sand at 5.58m in figure 5.5. The layers of sand were approximately 1cm thick, alternating with layers of silty clay. The increased bearing, however, may be a result of the influence of several thin sand layers that are relatively close together. Had there been only a single sand layer the response of the bearing may not of been as pronounced. The detection of layers less than 10cm thick can also be seen at depths of approximately 9.47m (figure A.1c - inclined sand lense), 11.52m (figure A.1d - sandy clay) and 13.5m (figure A.1e - silty fine sand).

A pore pressure profile should be of considerable help in detecting different layers, unfortunately, the standard Hogentogler porous element used for the CPT at this site had a very small average pore size (approximately 20 microns) which tended to clog, resulting in a poor pore pressure response (Hogentogler & Co. has since changed the material for their porous elements, the new material having an average pore size of 120 microns).

The detection of thin layers is complicated by the sampling rate used during CPT. The profile presented in figure 5.5 was sampled at the U.B.C. standard rate of 2.5cm. Although thin layers may be detected at this rate, many can easily be missed. The ability to confidently identify thin layers also depends upon the relative stiffness between the thin layer and the surrounding material. For example, it may be difficult to identify a thin clay layer within a silt deposit since a small drop in the cone bearing may be attributed to the natural variability of the silt. On the other hand, a thin cemented sand layer may easily be detected. Figure 5.6 illustrates the relative proportions of the $10cm^2$ cone, the likely transition zone required to attain full penetration resistance and the standard U.B.C. sampling rate. For comparison, the three commonly used sizes of field vanes are also shown.

Estimating the thickness of a layer (as opposed to detecting a thin layer) is highly dependent upon the sampling rate. It can be shown that the estimation of layer thickness for layers thinner than the sampling rate is highly speculative and can often be in error. Sampling at discrete intervals can also lead to subdued peaks in the CPT profile. One solution might be to digitize a continuous record obtained from a strip chart recorder. However, this author's experience has shown that the resolution of the digitizing pad can be of the same order as the minor variations of interest in the CPT profile and that the minor variations are often ignored during the digitizing process.

The pore pressure profile can be of considerable use in detecting stratigraphic details. Robertson 1985 indicates that a fully saturated piezometer cone can usually respond to pore pressure changes within a tip advancement of 5mm at the standard rate or penetration of 2cm/sec. However, if the thin layers are discontinuous the drainage conditions may be such that pore pressure response is inhibited. The same sampling rate problems

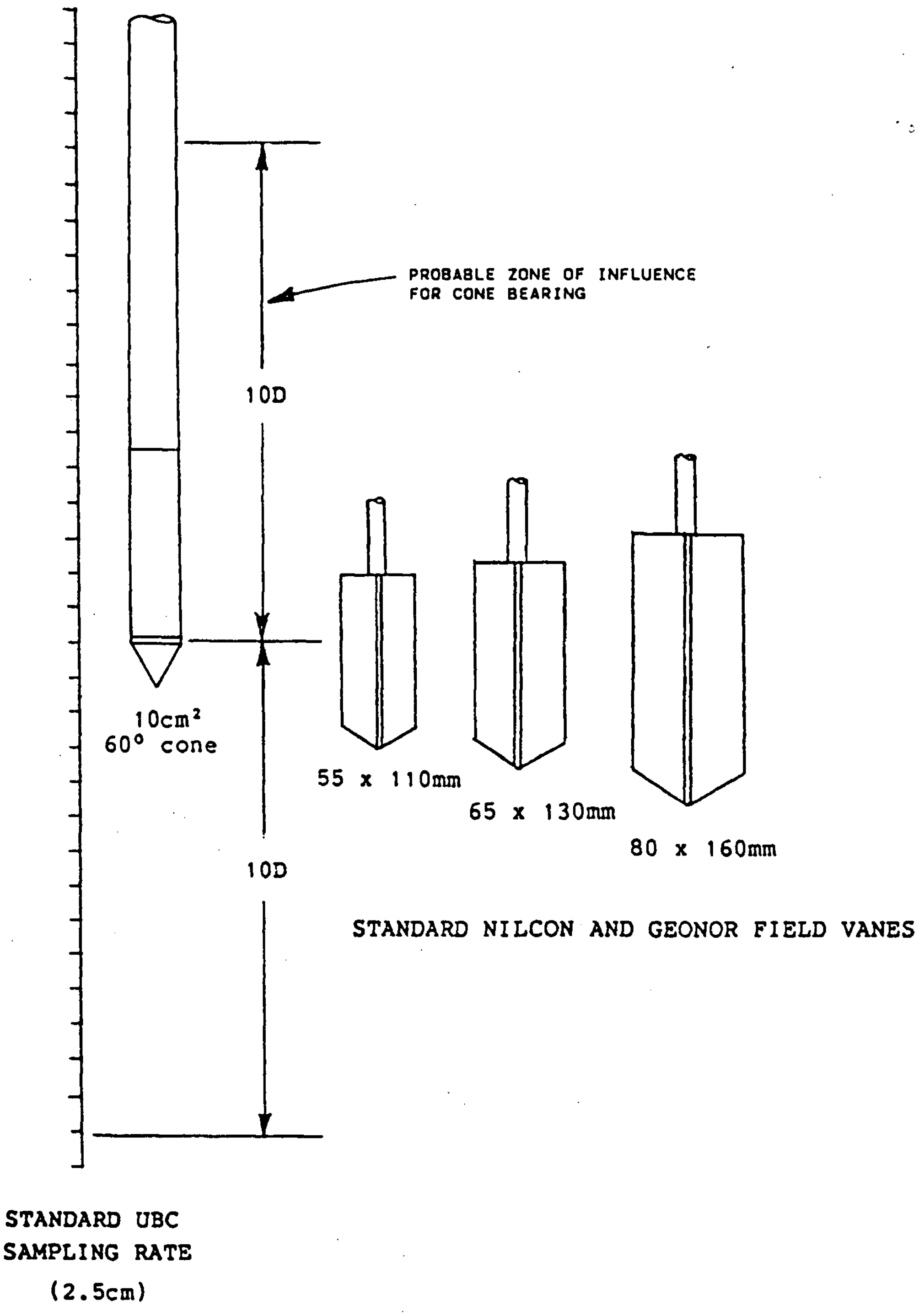

Figure 5.6 RELATIVE PROPORTIONS OF THE $10cm^2$ CONE PENETROMETER, PROBABLE ZONE OF INFLUENCE FOR CPT, UBC STANDARD CPT SAMPLING RATE AND LARGE, MEDIUM AND SMALL FIELD VANES

occur for both the recording of dynamic pore pressures and tip resistance.

5.4 Dynamic Pore Pressure Response

The recording of dynamic pore pressures during cone penetration significantly improves the use, interpretation and application of the electric cone. The measurement of pore pressure aids in soil layer identification and can be used to establish equilibrium groundwater conditions, indicate stress history, evaluate consolidation characteristics and estimate soil permeability and undrained shear strength. A comprehensive review of the uses and interpretation of dynamic pore pressures and the factors that affect their measurement is presented by Robertson and Campanella 1984 and Campanella et al. 1985.

The two main factors affecting the measurement of pore pressures are: saturation and porous element location. Complete saturation of the pore pressure measuring system is essential in order to record high quality and repeatable data. The importance of saturation has been discussed in chapter 3 of this report. The pore pressure response is highly influenced by the porous element location. A conceptual pore pressure distribution around the cone is illustrated in figure 5.7 and clearly shows the dramatic effect that the element location has on the measured response. Campanella et al. 1985 explain that the tip is in a zone of maximum compression and shear, unlike the area immediately behind the tip which is in a zone of normal stress relief. The large normal stresses dominate the pore pressure response on the face and, thus, high positive pore pressures are

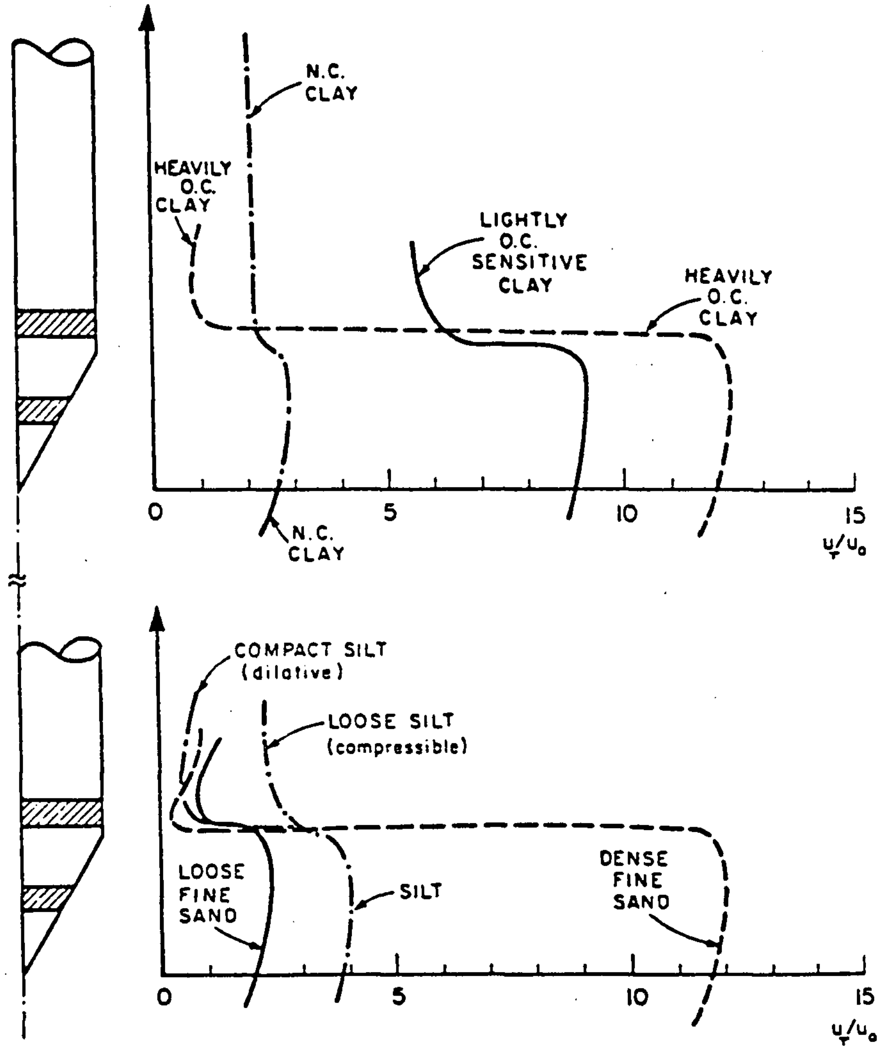

Figure 5.7 CONCEPTUAL PORE PRESSURE DISTRIBUTION IN SATURATED SOIL DURING CPT BASED ON FIELD MEASUREMENTS

(after Campanella et al. 1985)

generally recorded. Large shear stresses dominate the response behind the tip and the recorded pore pressures more closely reflect the volume change characteristics of the soil.

The fact that tremendously different pore pressures are recorded on the face than behind the tip is of significance when correcting the bearing for pore pressure effects. Pore pressures must be recorded behind the tip to properly correct the bearing. If pore pressures are recorded at other locations then an estimate of the ratio of behind the tip to on the face pore pressure must be made before adjusting the bearing data. A similar but much less dramatic situation may occur when correcting friction data. Figure 5.7 indicates that the pore pressure at the top of the friction sleeve is different from that at the bottom. This can lead to an incorrect friction measurement as the imbalance of pore pressures produces a net force on the friction sleeve.

The excess pore pressure is commonly presented as a normalized value and has been found to be a rough indicator of stress history. Robertson and Campanella 1984 list four different definitions and suggest that $\frac{\Delta U}{Q_t - \sigma_{vo}}$ be adopted as a standard. This particular definition has been termed Bq by Senneset et al. 1982.

Work by Gillespie 1981 showed that predicted pore pressure response using cavity expansion theory compared well with measured values. Pore pressures generated on the face were best predicted using spherical cavity expansion whereas pore pressures generated behind the tip and up the sleeve were best predicted using cylindrical cavity expansion.

CHAPTER 6

METHODS OF CORRELATION BETWEEN CPT AND Su

6.1 Introduction

This chapter discusses the different methods that have been proposed for correlating CPT results with undrained shear strength. This topic has been studied by several researchers in the past, however, most have focussed only on the cone bearing as a means of estimating Su. These have been termed the "traditional methods" by this author and they usually employ a cone factor Nk or Nc whose values have exhibited a tremendous range but are often relatively well defined at individual sites. Various theoretical cone factors have also been proposed by different researchers. Recently proposed methods make use of excess pore pressures measured during penetration. Senneset et al. 1982 proposed the use of 'effective' bearing for estimating Su. A semi-empirical approach based on cavity expansion theory has been adopted by Campanella et al. 1985 and various pore pressure parameters and cone factors have been used by Lunne et al. 1985 in an attempt to find a satisfactory correlation technique. Several researchers have also proposed the use of friction measurements to estimate Su.

This chapter concludes with a presentation of some proposed methods of evaluating the stress history of a deposit from CPT and a method for estimating sensitivity from friction ratios.

6.2 Traditional Methods of Correlation

The undrained shear strength of clay has traditonally been evaluated from cone bearing data using a bearing capacity type equation of the form:

$$Qc = Su\ Nk + \sigma \qquad 6.1$$

where Qc is the cone bearing
Nk is the cone factor
σ is a measure of insitu stress

Various forms of insitu stress have been used; total vertical stress, total horizontal stress and octahedral stress. The insitu stress is sometimes ignored, in which case the cone factor is usually defined as Nc. A wide range of values for Nk and Nc have been reported by Brand et al. 1974, Schmertmann 1975, Lunne et al. 1976 Schmertmann 1978, Baligh et al. 1979, Lunne and Klevin 1981 and Jamiolkowski et al. 1982. It was noted in chapter 1 that Su is not a unique parameter as it is dependent on the type of test used. This may partly explain the wide range in reported cone factors since many different types of tests have been used to establish a reference Su.

Table 6.1 summarizes Nc cone factors for various clays from around the world and illustrates the wide range of reported values. Baligh et al. 1979 presented a plot of Nk against depth for nine different clays (reproduced in figure 6.1), the values for Nk ranging from 5 to 28. The lowest and highest values of Nk were recorded for materials of high plasticity and high sensitivity (St>40), respectively. The curves which exhibited a decreasing cone factor with depth correspond to deposits where sensitivity decreased with depth. Table 6.2 presents a summary of material properties and cone factors for some Scandanavian

Reference	Clay	Avg Cone Factor[1]	Clay Properties				
			W%	Wl%	PI%	Su, kPa	Sensitivity
Thomas (1965)	London Clay	18	20-30	80-85	50	49-285⁺	-
Ward et al. (1965)	London Clay	15.5	22-26	60-71	36-43	206-510⁺	-
Meigh & Corbett (1969)	Arabian Gulf Clay	16	30-47	38-62	20-35	4.9-39"	5
Ladanyi & Eden (1969)	Leda Clay (Gloucester)	7.5	50-57	50	23	25"	30 - 50
Ladanyi & Eden (1969)	Leda Clay (Ottawa)	5.5	72-84	40	20	56"	10 - 35
Pham (1972)	Bangkok Clay (City)	16	60-70	70-80	40-50	12.8-28.5"	5 - 7
Anagnostopoulos (1974)	Patras Clay	17	30	35	18	29.4-68.7⁺	1.5 - 3
Brand et al. (1974)	Bangkok Clay (Bangpli)	19	60-130	60-130	60-120	12.8-37.3"	5 - 7
Brand et al. (1974)	Weathered Bangkok Clay (Bangpli)	14	100-130	100-135	60-80	12.8-19.6"	6 - 8
Author	Richmond Clayey Silt	11.9	23-40	25-42	3-20	45-94"	2 - 7
Author	Langley Clay	14.4	27-53	32-59	16-34	19-80"	2 - 19
Author	Haney Clay	14.2	40-45	44	18	33-96"	3 - 13

1 - cone factor calculated from $\bar{Q}c/Su$
⁺ - unconfined compression
" - field vane

Table 6.1 - SUMMARY OF CONE FACTORS (Nc) DETERMINED FOR DIFFERENT CLAY DEPOSITS

(revised from Brand et al. 1974)

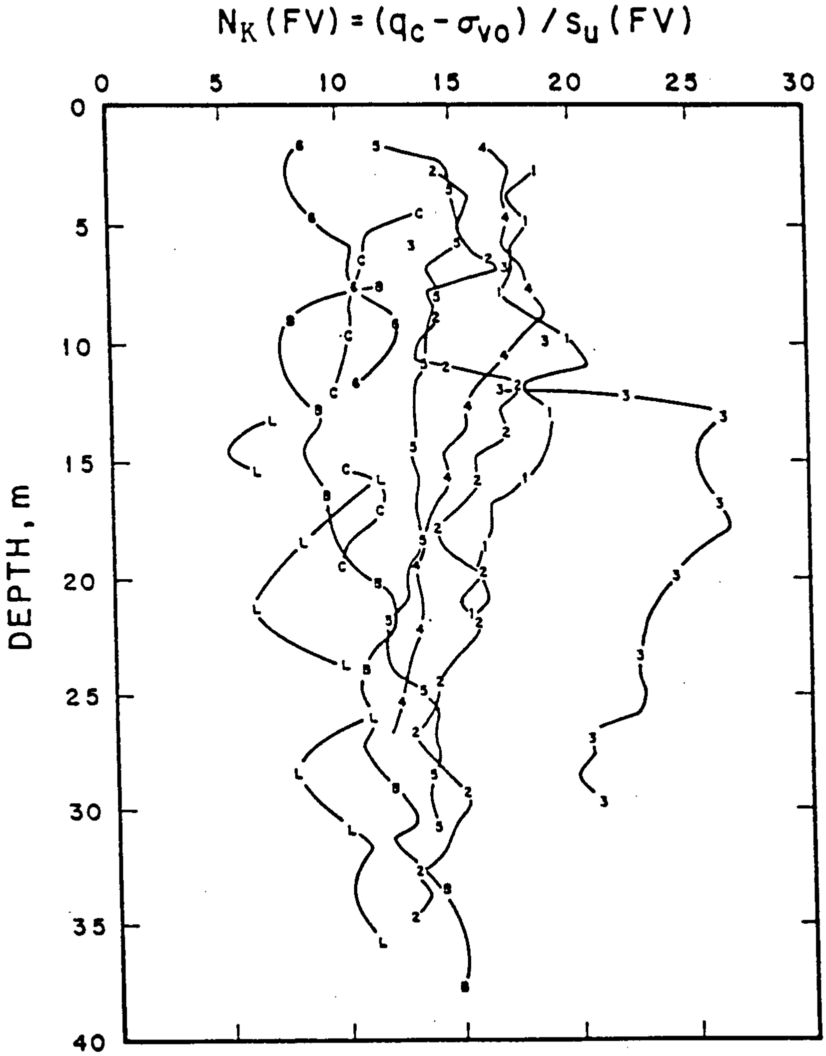

Figure 6.1 - EMPIRICAL CONE FACTOR Nk vs DEPTH FOR DIFFERENT CLAY DEPOSITS

(adapted from Baligh et al. 1979)

Test site	Depth (m)	Range $\tau_f(t/m^2)$	Plasticity $I_p(\%)$	Sensitivity	Cone Factor N_k
Sundland	4-9	2-2.5	22-28	10-15	17-18
Drammen	9-14	2-4.5	~10	~2	20
	14-22	2.5-4	~10	3-4	15.5
Dansvigs gate	5-10	2-3	20-25	6-9	14-15
Drammen	11-30	2-4	10-11	2-4	14-16
Børresens gate	5.5-12	3-2	~15	15-25	16-20
Drammen	12-30	1.3-2.5	~5	50-160	20-24
Onsøy	1-9	1.2-1.4	20-30	5-10	16-18
	10-20	1.8-4.8	35-40	4-7	13-18
Skå-Edeby	1-4	0.6-1.2	45-80	6-10	8-9
	4-12	0.8-2.0	30-50	10-15	10-12
Gøteborg	3-10	1.5-2.5	50-60	15-24	13.5-14.5
	10-21	2.5-4.2	50-55	13-19	13-14
	21-30	4.5-5.5	~40	13-17	13-14

Table 6.2 - SUMMARY OF CONE FACTORS (Nk) FOR SCANDANAVIAN CLAYS

(adapted from Lunne et al. 1976)

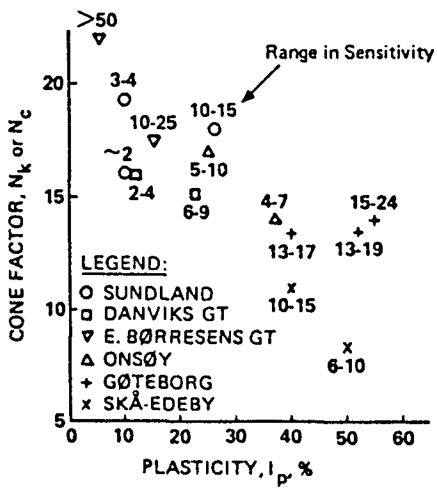

Figure 6.2 - SUMMARY OF CONE FACTORS (Nk) FOR SCANDANAVIAN CLAYS

(adapted from Lunne et al. 1976)

clays. These cone factors were plotted against plasticity index by Lunne et al. 1976 as shown in figure 6.2. There appears to be a general trend of decreasing cone factor with increasing PI. For a given PI there is also a trend of increasing Nk with increasing sensitivity.

Baligh et al. 1979 presented a review of existing theories of cone penetration in clays and reported that there are basically three different approaches: plane-strain slip-line solution, expansion of cavities, or steady penetration analysis. The plain-strain slip-line approach treats cone penetration as a bearing capacity problem where the material is in a state of incipient failure. Various shape and depth factors have been proposed to determine an appropriate cone factor. The second method is based on the expansion of cylindrical or spherical cavities; theories which have been described by Gibson and Anderson 1961, Vesic 1972 and Ladanyi 1972. The steady penetration approach is a combination of the first two methods. A summary of the different cone penetration theories is presented in table 6.3.

Using the steady penetration approach, Baligh et al. 1975 demonstrated the effect of rigidity index G/Su (a parameter central to cavity expansion theory) and cone angle on the penetration resistance of clays. This effect is shown in figure 6.3 and it clearly illustrates that Nk increases with increasing soil stiffness. An estimate of the rigidity index can be made from the curves presented by Ladd et al. 1977 (figure 6.4). Note, however, that Ladd's curves are in terms of Eu and not Gu ($G = E/2(1+\nu)$). Low values of G/Su correspond to highly plastic

Type of Approach	Reference	$q_c = Nk\, s_u + p_o$ Expression for Nk	Nk for $2\delta = 60°$ $G/s_u = 100$	$G/s_u = 400$	p_o
Bearing Capacity	Terzaghi (1943) Meyerhof (1951)	(shape factor)(depth factor) x 5.14	9.25	same	σ_{vo}
	Mitchell and Dorgunoglu (1973)	(shape factor)(depth factor) x $(2.57 + 2\delta + \cot\delta)$	9.63	same	σ_{vo}
	Meyerhof (1961)	(1.09 to 1.15) x $(6.28 + 2\delta + \cot\delta)$	10.2	same	σ_{vo}
Cavity Expansion	Bishop et al (1945)	$1.33(1 + \ln G/s_u)$	7.47	9.30	unspecified
	Gibson (1950)	$1.33(1 + \ln G/s_u) + \cot\delta$	9.21	11.03	σ_{vo}
	Vesic (1975,1977)	$1.33(1 + \ln G/s_u) + 2.57$	10.04	11.87	σ_{oct}
	Al Awkati (1975)	(correction factor) x $(1 + \ln G/s_u)$	10.65	13.28	σ_{oct}
Steady Penetration	Baligh (1975)	$1.2(5.71 + 3.33\,\delta + \cot\delta) + (1 + \ln G/s_u)$	11.02 + 5.61 =16.63	11.02 + 6.99 =18.01	σ_{ho}

Table 6.3 - SUMMARY OF EXISTING THEORIES OF CONE PENETRATION IN CLAYS

(adapted from Baligh et al. 1979)

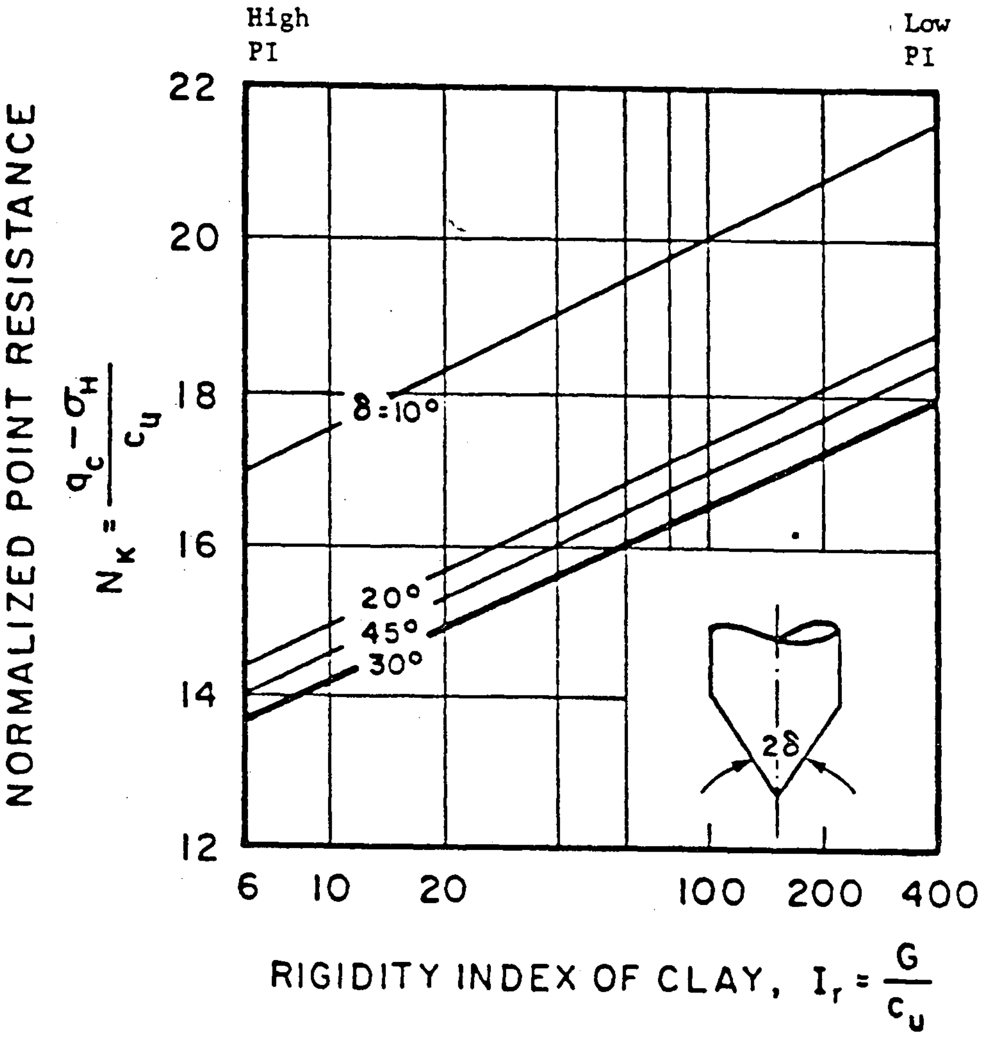

Figure 6.3 - EFFECT OF RIGIDITY INDEX AND CONE ANGLE ON THE PENETRATION RESISTANCE OF CLAY

(adapted from Baligh et al. 1975)

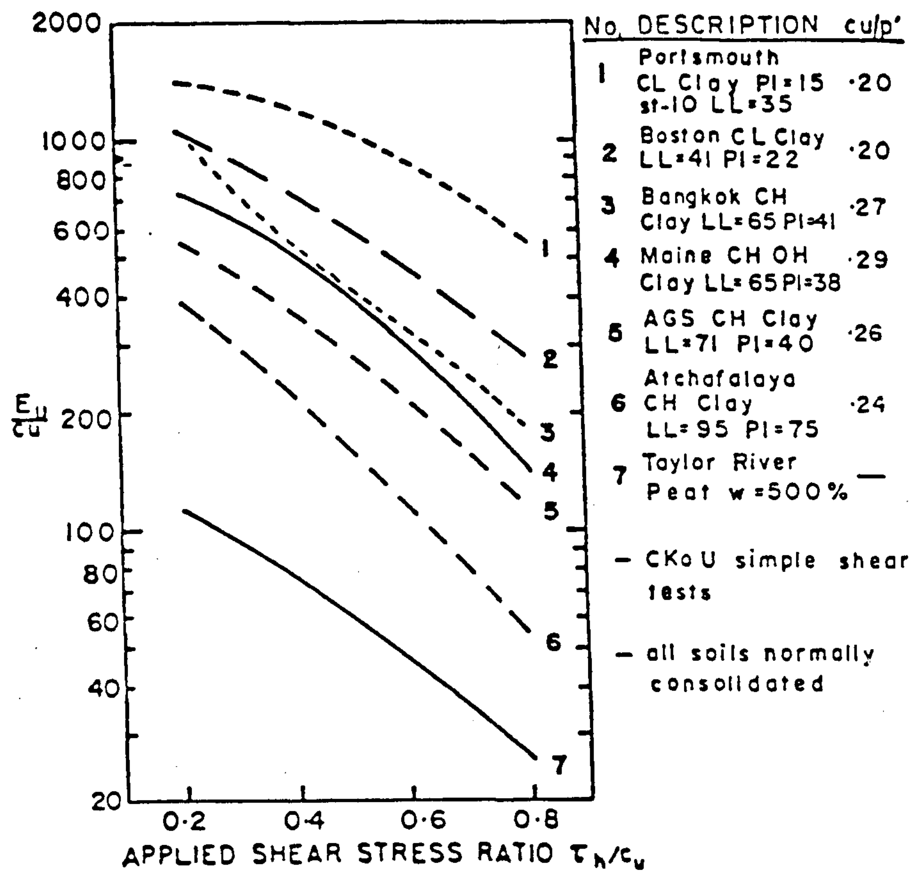

Figure 6.4 - SELECTION OF SOIL STIFFNESS

(adapted from Ladd et al. 1977)

materials. This dependence on soil stiffness explains the trend of decreasing Nk with increasing PI observed in the data from Lunne et al. 1976 (figure 6.2).

6.3 Recently Proposed Methods of Correlation

The data presented in the previous section clearly indicate that correlations between cone bearing and Su are heavily influenced by such soil characteristics as soil stiffness and sensitivity. In addition, the correlations are affected by stress history, strength anisotropy and several factors relating to cone design details. Many of these factors have not or can not be incorporated into the traditional methods of correlation and are the likely reasons for the tremendous range in reported cone factors. The dependence on these factors indicates that there can not be a unique cone factor that is applicable to all clays.

These properties are difficult to quantify and equally difficult to incorporate into analyses. Stress history is generally expressed as overconsolidation ratio but such factors as aging, effects of secondary compression and creep are necessarily omitted. Soil stiffness is usually expressed as a rigidity index, G/Su. Sensitivity is commonly expressed in terms of the vane sensitivity and reflects the structure and fabric of the cohesive material.

As has been mentioned several times throughout this report, the consequences of certain cone design details must be considered when analyzing CPT data. It is now becoming widely accepted that bearing values must be corrected for pore pressure effects. However, results presented in chapter 5 indicate that the recording of pore pressures at locations other than the tip can create problems in making the proper corrections. A great deal of attention must also be paid to details in test procedures, in particular, the saturation procedure and the checking of zeroes before and after penetration. Zero offsets can often be caused by temperature instability. Because bearing values are typically low in normally consolidated clays, numerically small errors in the bearing may actually be quite substantial (see figure 3.2). Another problem is that the tip load cell is usually working in the range of 2% to 5% of capacity and, therefore, the resolution of the data recording system may be inadequate. On the other hand, the pore pressure transducer is generally working near capacity and may be more reliable and consistent than the bearing values.

For these reasons, recently proposed correlation methods make significant use of pore pressure data allowing correlations to be based on semi-empirical methods such as cavity expansion theory. These new methods make an attempt to incorporate stress history, soil stiffness and sensitivity into their analyses.

6.3.1 Using Effective Bearing to Estimate Su

Senneset et al. 1982 recommended the use of effective bearing (Qc') for estimating Su. Effective bearing is defined as

$$Qc' = Qc - Ut \qquad 6.2$$

and Su is to be determined using an effective cone factor Nc' and the expression

$$Su = \frac{Qc'}{Nc'} \qquad 6.3$$

They suggested that an average value of Nc'=9 (±3) should be used. It has been noted earlier that the dynamic pore pressure can often be greater than the recorded bearing which is impossible since the tip is a total stress element. Cone bearing must be corrected for pore pressure effects in order to use this method. The cone factor Nc' was later defined as Nke by Lunne et al. 1985 and is discussed in greater detail in section 6.3.3.

6.3.2 The Use of Excess Pore Pressures and Cavity Expansion Theory

An estimate of undrained shear strength can be made from excess pore pressure data using the charts shown in figure 6.5. These charts were presented by Campanella et al. 1985 and were based on expressions developed by Massarch and Broms 1981.

In a study of pile driving in clay slopes Massarch and Broms presented expressions for the distribution of pore pressures within the plastic zone adjacent to a spherical or cylindrical cavity:

$$\text{spherical} \quad \frac{\Delta U}{Su} = \frac{4}{3}\ln\left(\frac{G}{Su}\right) + 2Af - 0.667 \qquad 6.4$$

$$\text{cylindrical} \quad \frac{\Delta U}{Su} = \frac{4}{3}\ln\left(\frac{G}{Su}\right) + 1.73Af - 0.577 \qquad 6.5$$

These equations incorporate the effects of overconsolidation and sensitivity by using Skempton's pore pressure parameter, Af. The effect of soil stiffness is also included by using the rigidity index G/Su.

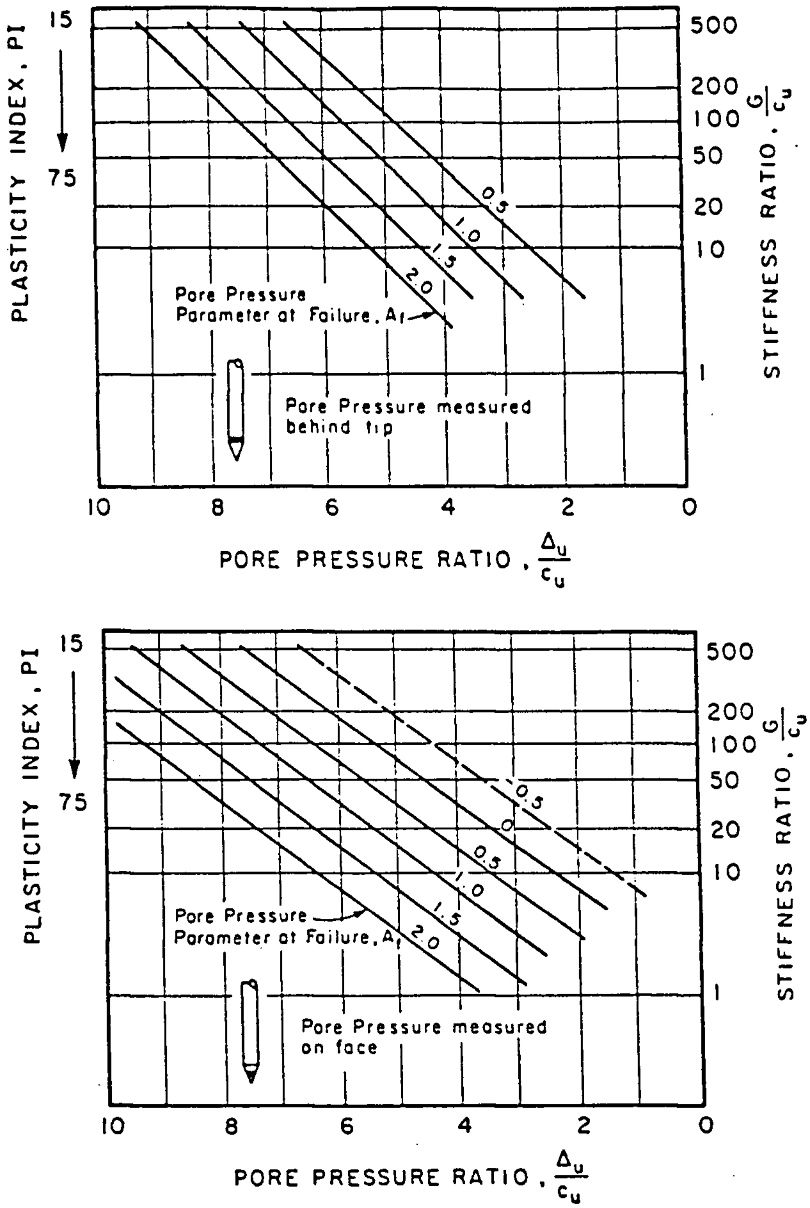

Saturated Clays	Approximate Af Range
Very sensitive to quick	1.5 - 3.0
Normally consolidated	0.7 - 1.3
Lightly overconsolidated	0.3 - 0.7
Highly overconsolidated	-0.5 - 0

Figure 6.5 - PROPOSED METHOD FOR OBTAINING Su FROM EXCESS PORE PRESSURE MEASURED DURING CPT

(after Campanella et al. 1985)

Because measured pore pressures are also dependent on the porous element location, two charts are shown in figure 6.5 reflecting the different porous element locations and the corresponding equation. The face of the cone is often considered to be in a zone of spherical cavity expansion whereas the region behind the tip is thought to be in a zone of cylindrical cavity expansion. Typical values for Af are given below the charts.

A review of the two charts reveals that they describe, qualitatively, the expected pore pressure response. The diagonal lines correspond to different values of Af. Although Af is a parameter associated with triaxial testing, its value should adequately reflect the volume change characteristics of the soil for the purposes of correlation. Sensitive soils tend to generate high pore pressures when sheared and, therefore, have a corresponding high Af value. On the other hand, heavily overconsolidated materials are often dilative and this is reflected by a negative Af value. Given a value for soil stiffness, the charts indicate that $\Delta U/Su$ increases as Af increases, as would be expected. It has been mentioned several times that pore pressure response is also dependent on the soil stiffness, with stiffer soils generating greater pore pressures. This expected behaviour is also predicted in figure 6.5.

6.3.3 Use of Various Pore Pressure Parameters and Cone Factors

A different approach was adopted by Lunne et al. 1985 for correlating pore pressure data with undrained shear strength. Using Senneset's pore pressure parameter Bq ($\frac{\Delta U}{Q_t - \sigma_{vo}}$) they found that it had a rough correlation with overconsolidation ratio. Other dimensionless parameters were defined and attempts were made to correlate these parameters with Bq as a means of isolating stress history.

It was stated in section 5.4 that many researchers have observed that Bq is a rough indicator of stress history. With this in mind, Lunne et al. 1985 plotted values of Bq versus OCR for different North Sea clays (figure 6.6) and concluded that Bq generally decreased with increasing OCR. This conclusion appears to be valid; however, the data define a relatively wide band. This is not surprising since Bq should also be affected by soil stiffness and sensitivity. For a given value of sensitivity the upper part of the band should represent materials of high stiffness (low PI) and the lower part of the band should represent less stiff materials (high PI).

Three dimensionless parameters were defined; Nkt, $N_{\Delta U}$ and Nke:

$$Nkt = \frac{Qt - \sigma_{vo}}{Su} \qquad 6.6$$

$$N_{\Delta U} = \frac{\Delta U}{Su} \qquad 6.7$$

$$Nke = \frac{Qt - Ut}{Su} \qquad 6.8$$

Lunne et al. plotted these dimensionless parameters against Bq in an attempt to isolate stress history. Figure 6.7 shows Nkt (the traditional cone factor) plotted against Bq. The high degree of scatter might be expected since it has been shown that Nkt varies with sensitivity and stiffness in addition to OCR. Plotting $N_{\Delta U}$ against Bq (figure 6.8) provides a more promising correlation as data appear to define a narrow band. Lunne et al.

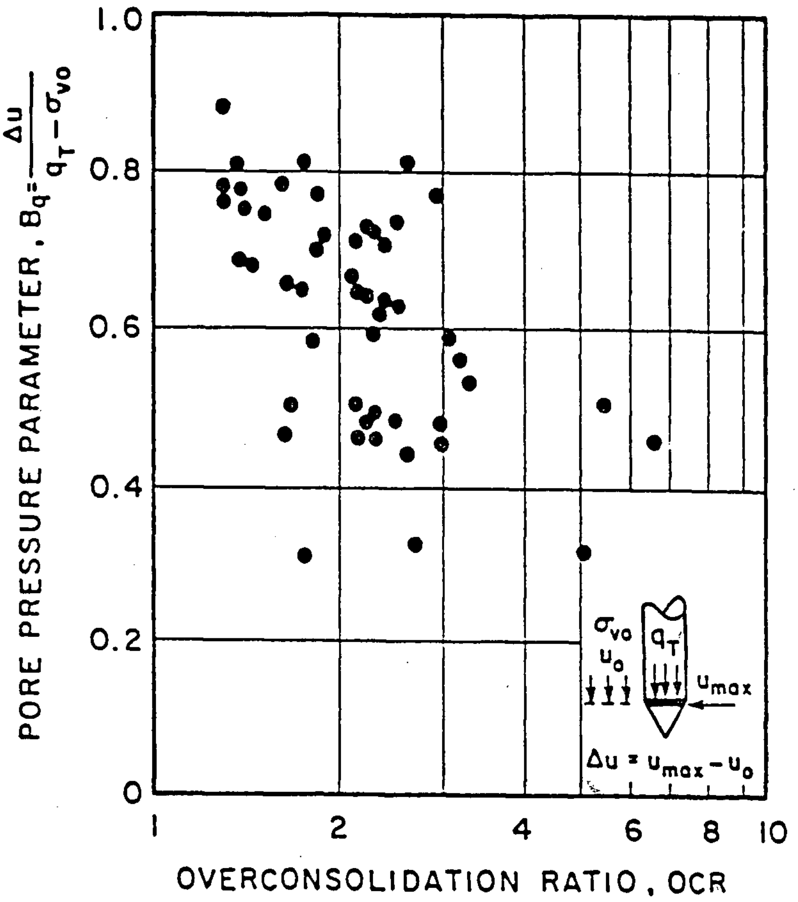

Figure 6.6 - PORE PRESSURE PARAMETER Bq vs OVERCONSOLIDATION RATIO

(adapted from Lunne et al. 1985)

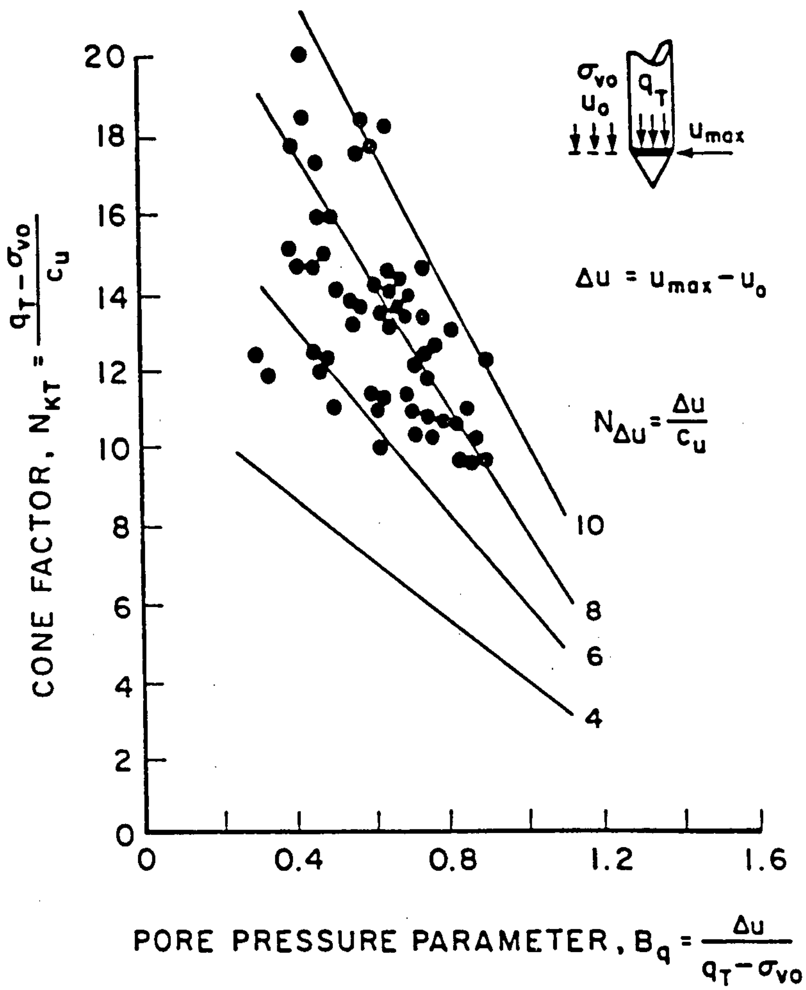

Figure 6.7 - CONE FACTOR Nkt vs PORE PRESSURE PARAMETER Bq

(adapted from Lunne et al. 1985)

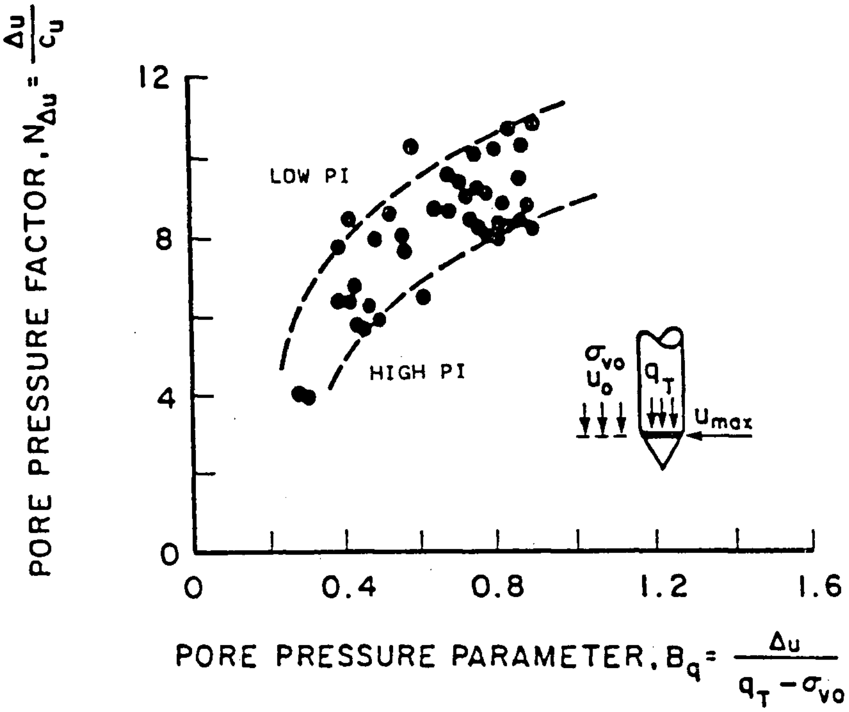

Figure 6.8 - PORE PRESSURE PARAMETER $N_{\Delta u}$ vs PORE PRESSURE PARAMETER Bq

(adapted from Lunne et al. 1985)

recommended using an average line to estimate Su with upper and lower bounds being defined by the outer edges of the band. This author suggests that the band acutally represents varying degrees of soil stiffness with the upper and lower line corresponding to materials of low and high PI respectively. The most promising correlation is shown in figure 6.9 where an 'effective' cone factor Nke is plotted against Bq.

This author cautions that the calculation of Nke can present some problems. Lunne et al. stress that corrected bearing must be used when calculating Nke. In addition, they correctly indicate that pore pressures measured on the face (FPP) must be converted to an equivalent behind the tip pore pressure (BTPP). Therein lies a problem. Lunne et al. adopted a single conversion value (k) of 0.8 for converting FPP to BTPP (i.e. BTPP=0.8·FPP) for penetration tests in different clay types. Figure 5.7 clearly shows that a unique value of k does not exist. Aside from the difficulties of correcting for pore pressure effects, the problems of low bearing values previously discussed may exist. However, Lunne et al. likely did not experience this problem because of the great depth of water under which the tests were made. Because of these problems, tests on land may result in a greater degree of scatter than was found for the offshore tests. Despite the problems, correlations between Nke and $N_{\Delta u}$ do show considerable promise.

6.4 Using Friction Sleeve Measurements to Estimate Su

Some researchers have proposed the use of friction sleeve measurements to estimate undrained shear strength. Begeman 1965

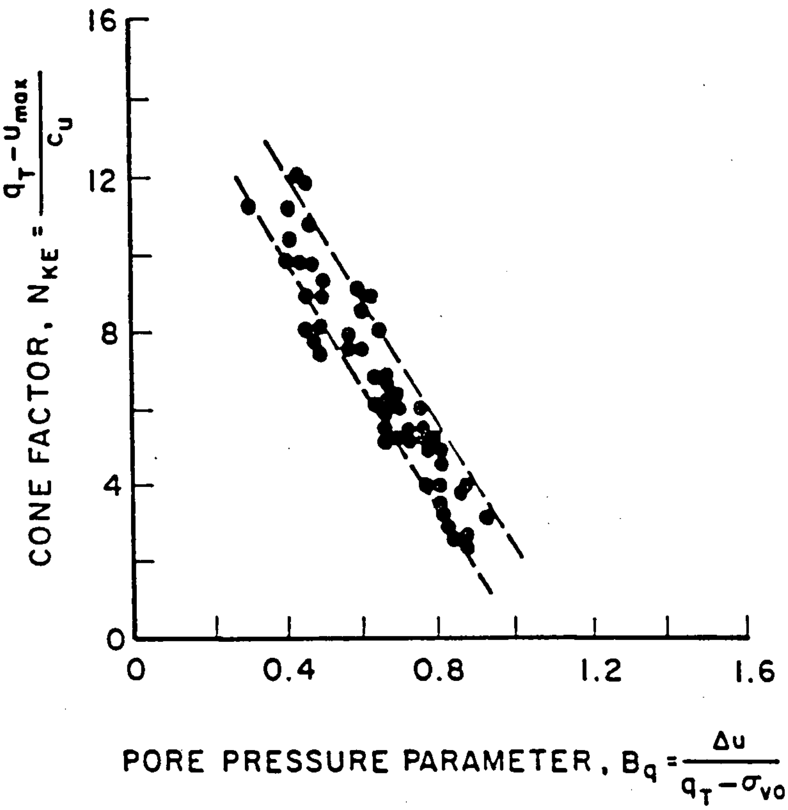

Figure 6.9 - CONE FACTOR Nk vs PORE PRESSURE PARAMETER Bq

(adapted from Lunne et al. 1985)

suggested that the friction measurement, Fs, should be approximately equal to Su. Drnevich et al. 1974 presented some results from tests using a mechanical friction cone and consolidated undrained triaxial tests. They concluded that the friction measurements were slightly greater than the undrained shear strength. They cited work by Cleveland 1971 and Wesley 1967 that showed similar results, indicating that Fs=(1.19-1.28)·Su. Schmertmann 1978 considered Fs to be an average between peak strength and remolded strength. Robertson and Campanella 1984 suggested that the friction measurement is equal to the remolded strength.

It seems unlikely that the friction measurement should be greater than the undrained shear strength of the soil. Considering the extent of remolding that must take place during penetration, this author suggests that Fs should reflect a value close to the remolded strength of the soil, particulary in sensitive materials. It is important to note that all of the above conclusions, except for that by Robertson and Campanella, were based on experience with the mechanical friction cone. Friction measurements made with this type of cone are usually relatively high because of the end bearing on the friction sleeve. The friction measurements are, therefore, not a true reflection of the stress on the friction sleeve. This problem does not occur with the electric friction cone; hence, one must be cautious when using existing correlations between Fs and Su.

6.5 Stress History

An estimation of the extent of overconsolidation of a clay deposit can be made using CPT results. Schmertmann 1978 proposed two methods for estimating the overconsolidation ratio and maximum past pressure of clay. The first method made use of a correlation between normalized undrained shear strength ratio and overconsolidation ratio from laboratory tests. The second method employed a graphical technique to estimate OCR.

Using data from Ladd and Foott 1974 and Koutsoftas and Fischer 1976, Schmertmann presented a correlation of the ratio of the current normalized undrained shear strength (normalized with effective overburden pressure; Su/P') to the normalized undrained shear strength for the normally consolidated material, (Su/P')/(Su/P')nc, with overconsolidation ratio (on a logarithmic scale). This correlation is illustrated in figure 6.10. Ladd et al. 1977 suggested that the curve in figure 6.10 can be represented by the following expression:

$$\frac{(Su\ /\ P')}{(Su\ /\ P')nc} = OCR^{m} \qquad 6.9$$

with m=0.8. Wroth 1984 presented a theoretical argument based on Critical State Soil Mechanics theory as to why this correlation should exist. He indicated that the theory relates the exponent, m, with physical properties of clay; in particular, m is the volumetric strain ratio.

Based on the curve in figure 6.10 and the undrained shear strength determined from the cone bearing, Schmertmann suggested using an average normally consolidated Su/P' of 0.33 to estimate OCR. Robertson and Campanella 1983 slightly modified Schmertmann's method by suggesting that the undrained shear strength can also be estimated from the dynamic pore pressure profile and that the normally consolidated Su/P' be established

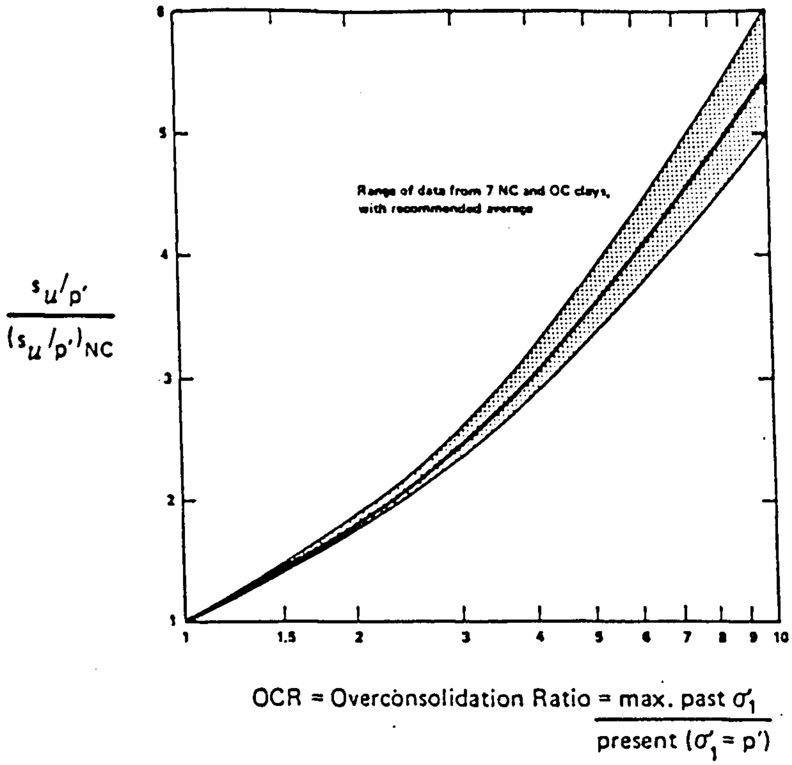

Figure 6.10 - NORMALIZED Su/P' RATIO vs OVERCONSOLIDATION RATIO FOR USE IN ESTIMATING OCR

(adapted from Schmertmann 1978)

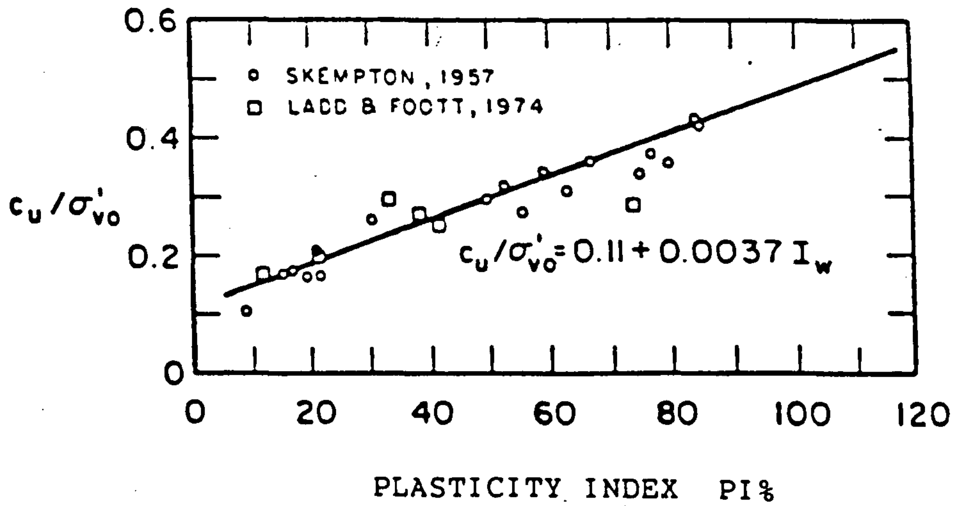

Figure 6.11 - STATISTICAL RELATION BETWEEN Cu/σ'_{vo} RATIO AND PLASTICITY INDEX FOR NORMALLY CONSOLIDATED CLAYS

using the well known (but controversial) Skempton correlation between (Su/P')nc and plasticity index shown in figure 6.11. However, Robertson and Campanella's method does require a knowledge of PI. This author further suggests that the normally consolidated Su/P' can be determined from the cone bearing or pore pressure profile. As described earlier in section 5.3, the tip resistance is linearly increasing with depth in normally consolidated clay deposits with hydrostatic groundwater conditions. From the linearly increasing portion of the cone bearing profile or the corresponding portion of the pore pressure profile an estimate of (Su)nc can be made using one of the methods previously described. Hence, from this value and from an estimate of the effective overburden pressure (Su/P')nc can be calculated. If the overconsolidated and the normally consolidatd material have the same origin (i.e. are the same deposit) this (Su/P')nc value can be applied in the overconsolidated material. Using this method an estimate of PI is not required (except possibly for estimating Su from the pore pressure profile).

Schmertmann 1978 offered an alternative method for estimating OCR in sufficiently thick and homogeneous clay layers. By extrapolating the linearly increasing Qt profile to the intersection of the depth axis (Qt=0) one can define the highest probable past ground surface. The difference in elevation between this surface and the existing ground surface suggests past erosion and overconsolidation due to this depth of material. This method is shown in figure 6.12. For a homogeneous normally consolidated material this extrapolation should pass

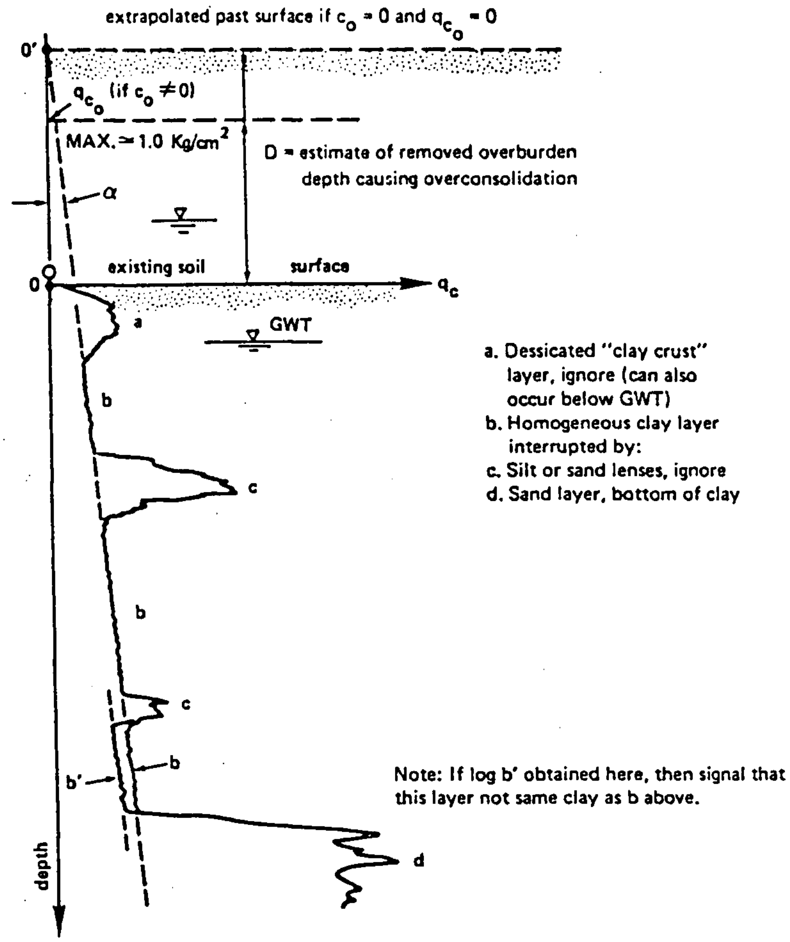

Figure 6.12 - EXTRAPOLATION OF THE Qc PROFILE AS AN ALTERNATIVE METHOD TO ESTIMATE OVER-CONSOLIDATION IN THICK, HOMOGENEOUS CLAY LAYERS

(adapted from Schmertmann 1978)

through the origin. However, the unit weight of the material overlying the clay deposit and the position of the water table can affect the location of the intersection of the extrapolated Qt profile and the depth axis. In order to determine the depth of erosion, the existing ground surface should be repositioned by replacing the overlying material with an equivalent depth of the normally consolidated material on the basis of bouyant weight. Figure 6.13 shows the bearing profile from one the sites used by the author and discussed in greater detail in chapter 7. The site consists of an upper 2m layer of organic silty clay γ=18.4 kN/m^3) which is underlain by approximately 11m of loose to dense sand (avg. γ=20 kN/m^3). Below 13m is a 2m transition layer of silty sand to clayey silt followed by a thick deposit of normally consolidated clayey silt (avg. γ=18.8 kN/m^3). The water table is at a depth of 1m. The effect of the position of the water table and the denser overlying material is to cause the point of intersection to be at an elevation greater than the existing ground surface. An equivalent depth of the normally consolidated material would be 17.5m; 2.5m above existing ground surface. The extrapolated Qt profile in figure 6.13 intersects the depth axis approximately 2m above the existing ground surface.

Because the closure angle, α, indicated in figure 6.12 is typically small, this method of estimating OCR is sensitive to the extrapolation of the bearing profile. Very erratic bearing values in the linearly increasing portion of the profile or insufficiently thick deposits make the extrapolation of the profile difficult. Therefore, the author recommends using the

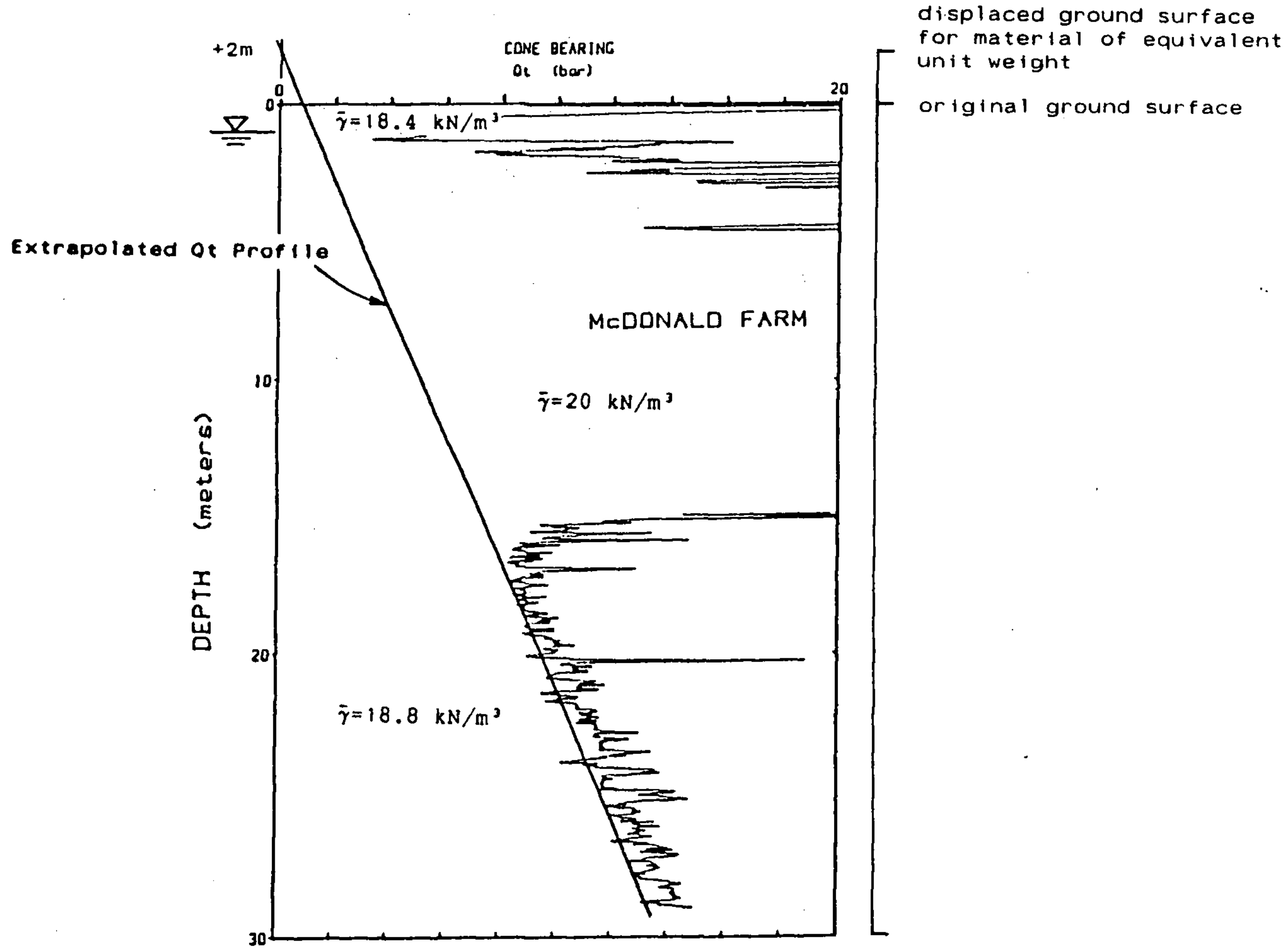

Figure 6.13 - THE EFFECT OF DENSER OVERLYING MATERIALS ON THE EXTRAPOLATED Qt PROFILE FOR A NORMALLY CONSOLIDATED CLAY LAYER

first method for estimating OCR from cone penetration tests.

6.6 Sensitivity

Sensitivity is defined as the ratio of undrained shear strength of undisturbed clay to undrained shear strength of totally remolded clay. Its value is dependent upon the test method used. However, the most common value quoted is that obtained from field or laboratory vane tests.

Schmertmann 1978 proposed a method for obtaining a rough estimate of the vane sensitivity for the Begemann mechanical cone. Robertson and Campanella 1983 proposed a similar method for use with the electric cone:

$$St = \frac{10}{Rf\%} \qquad 6.10$$

This method implies that the stress on the friction sleeve is close to the remolded shear strength of the soil. Equation 6.10 also ignores the effect of overburden pressure.

CHAPTER 7

FIELD PROGRAMME AND DISCUSSION OF RESULTS

7.1 Introduction

The field programme consisted of cone penetration and field vane shear tests at five lower mainland sites:

1) McDonald Farm
2) B.C. Hydro Railway Crossing
3) Upper 232nd St.
4) Lower 232nd St.
5) Haney Slide

The general locations of the sites are shown in figure 7.1 and a summary of the field tests conducted for this investigation is presented in table 7.1. A summary of the material properties for the different sites is given in table 7.2.

This chapter presents the test results from each site and discusses them in relation to the various correlation methods described in chapter 6. A summary compares the results from the five sites. In addition, correlations between friction sleeve measurements and vane shear strength are presented. Lastly, estimating vane sensitivity from CPT data is discussed.

7.2 McDonald Farm Research Site

7.2.1 General Geology and Site Description

McDonald Farm is located at the northern edge of Sea Island in the municipality of Richmond. The island is one of several that make up the Fraser River delta. The general geology consists of deltaic distributary channel fill and overbank

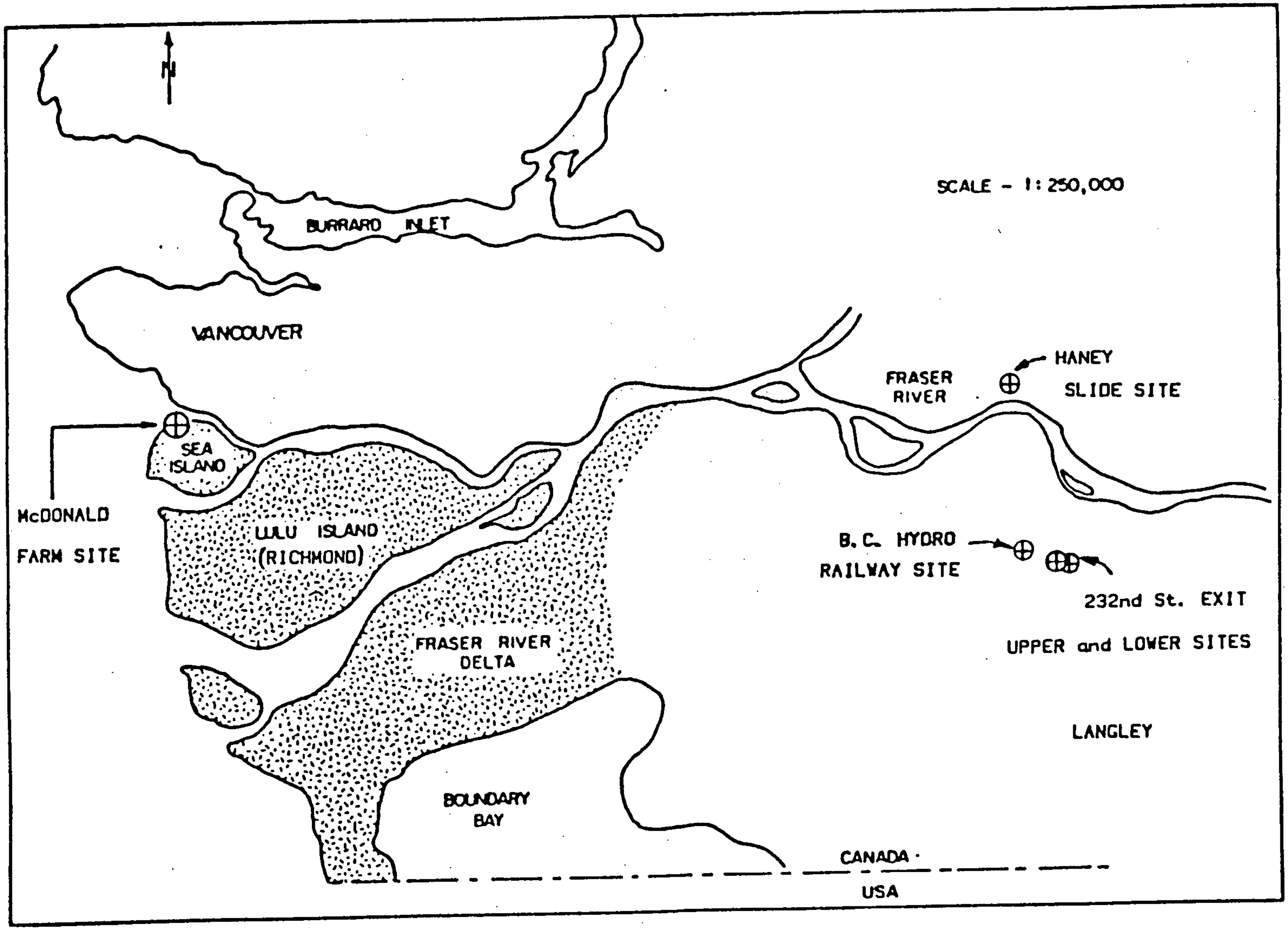

Figure 7.1 GENERAL LOCATION OF RESEARCH SITES

SITE	CPT PROFILE	CPT DATE	CONE	VST	VST DATE	VANE TYPE
McDONALD FARM RICHMOND	1 2 3* 4 5	April 15 1981 July 23 1982 Aug. 04 1982 Jan. 26 1984 May 05 1984	UBC #4 UBC #4 UBC #4 UBC #6 UBC #6	1 2	Sept 27 1983 Sept 29 1983	GEONOR GEONOR
B.C. HYDRO RAILWAY SITE LANGLEY	1 2	Nov. 04 1982 Oct. 24 1982	UBC #4 MOD. HOG.	1	Feb. 15 1984	NILCON
232nd St. - Upper LANGLEY	1	Dec. 08 1983	UBC 15cm^2 (UBC #5)	1 2	Feb. 10 1984 Feb. 10 1984	NILCON NILCON
232nd St. - Lower LANGLEY	1 2	Nov 17 1984 July 17 1984	UBC #4 UBC #6	1 2 3	Nov. 17 1984 Jan. 11 1984 Jan. 20 1984	NILCON NILCON NILCON
HANEY SLIDE SITE	1	June 22 1984	UBC #6	1	June 22 1984	NILCON

* pore pressure measured on face

Table 7.1 SUMMARY OF THE FIELD PROGRAMME

SITE	S.G.	Wl		Wp		Wn		PI		St	
		range	avg	range	avg	range	avg	range	avg	range	avg
McDONALD FARM	2.8	25-42	35	22-25	24	23-40	34	3-20	15	2- 7	5
B.C. HYDRO RAIL. SITE	2.8	32-59	42	16-27	21	27-53	45	16-34	24	7-10	9
232nd St. SITE	2.8		40		20	42-47	45		19	2-19	11
HANEY SLIDE SITE	2.8		44		26	40-45	42		18	3-13	6

S.G. = specific gravity Wl = liquid limit (%) Wp = plastic limit (%)
Wn = natural water content (%) PI = plasticity index (%) St = sensitivity

Table 7.2 SUMMARY OF MATERIAL PROPERTIES AT THE DIFFERENT SITES deposits which overlie post glacial estuarine and marine sediments (Armstrong 1978). A typical CPT profile from the site is presented in figure 7.2 and shows that the general stratigraphy consists of:

0-2m	soft organic silty clay
2-13m	loose to dense coarse sand; some layers of fine sand
13-15m	fine sand, some silt; transition zone
15-300⁺m	soft normally consolidated clayey silt

This report is concerned only with the clayey silt below 15m.

Corrected bearing and dynamic pore pressure profiles from four soundings in the clayey silt are shown in figure 7.3. Note that higher pore pressures were recorded for the profile where the pore pressures were measured on the face. These profiles illustrate the repeatability of CPT and that both cone bearing and pore pressure increase linearly with depth in a normally consolidated material. Note in figure 7.2 that the friction ratio tends to decrease with depth.

Undrained shear strength and vane sensitivity profiles from two VST soundings are shown in figure 7.4. The undrained shear strength increases linearly with depth (Su/P'=0.34) and the sensitivity is relatively constant with depth (avg. St=5).

7.2.2 Correlations Between Su and CPT

The results of the various correlation techniques for McDonald Farm are shown in figures 7.5 through 7.9. Plots of Qc/Su and Qt/Su vs depth (figure 7.5) provide a fairly reasonable estimate of Su. The scatter is reduced when corrected

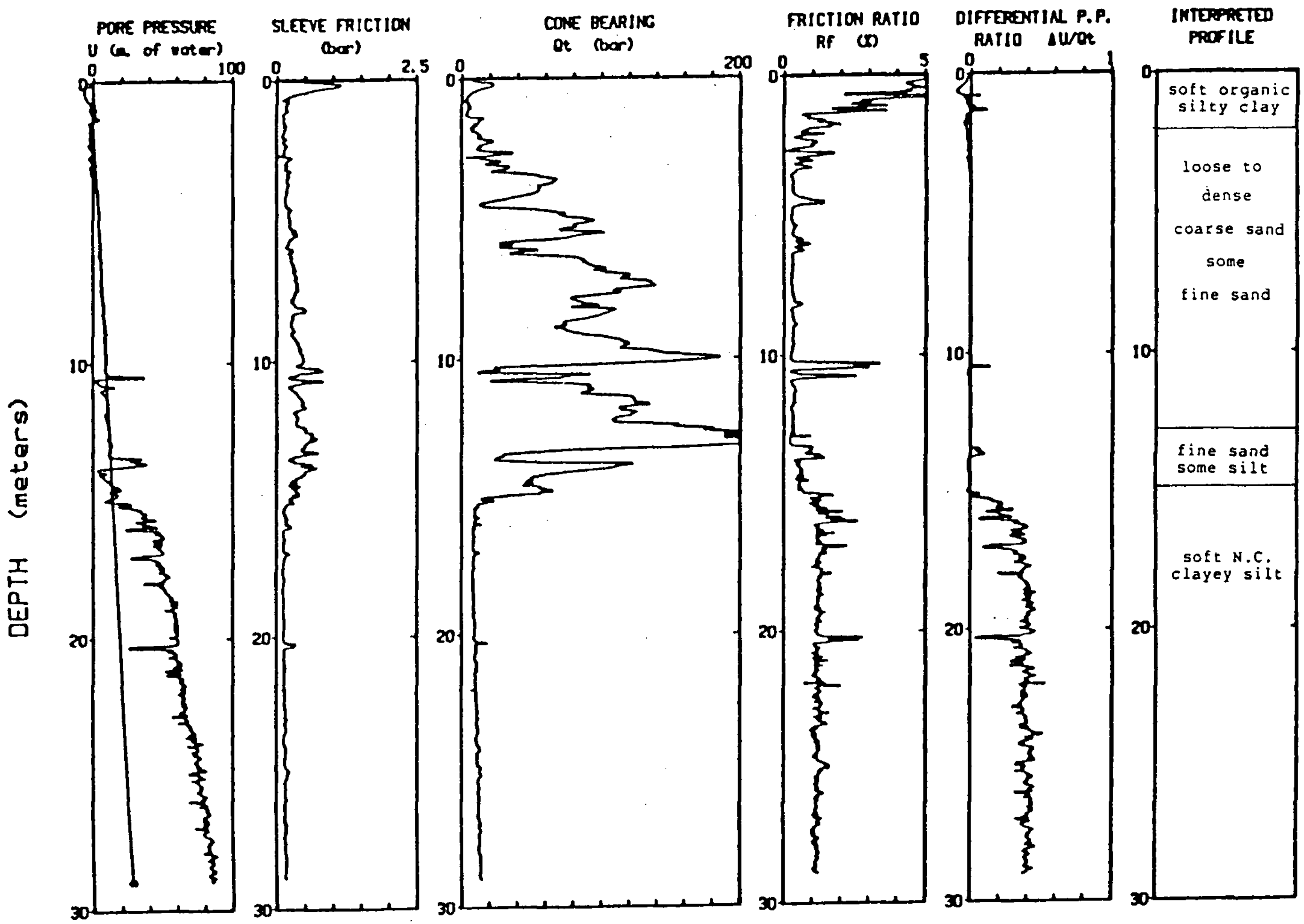

Figure 7.2 TYPICAL CPT PROFILE AT McDONALD FARM

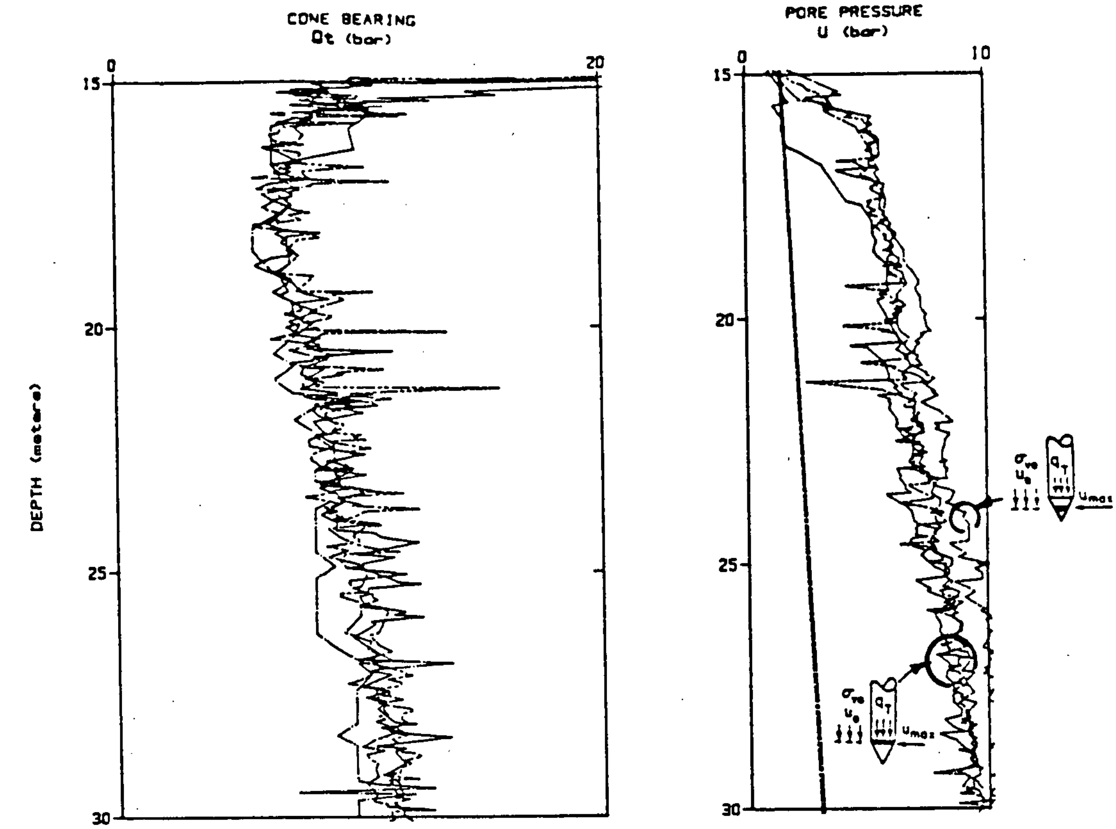

Figure 7.3 PROFILES FROM 4 CPT SOUNDINGS IN McDONALD FARM CLAYEY SILT

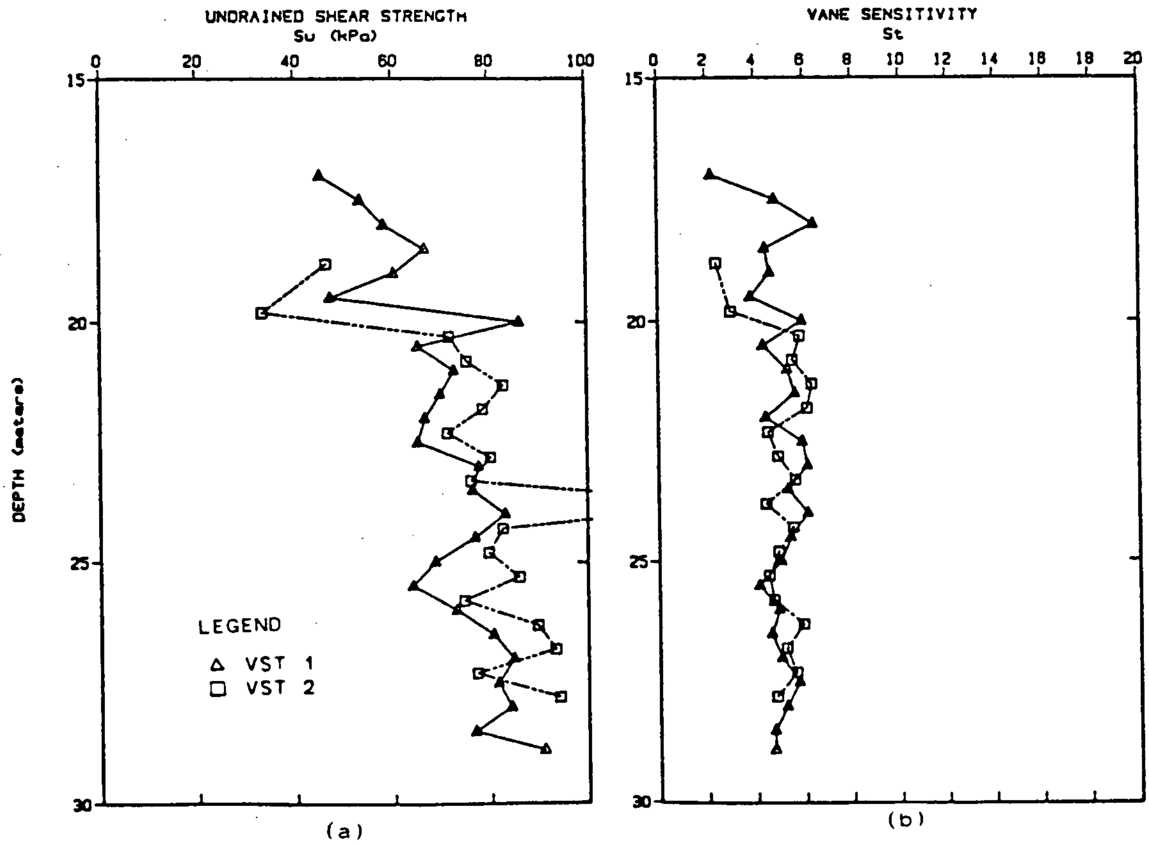

Figure 7.4 FIELD VANE STRENGTH AND SENSITIVITY PROFILES AT McDONALD FARM

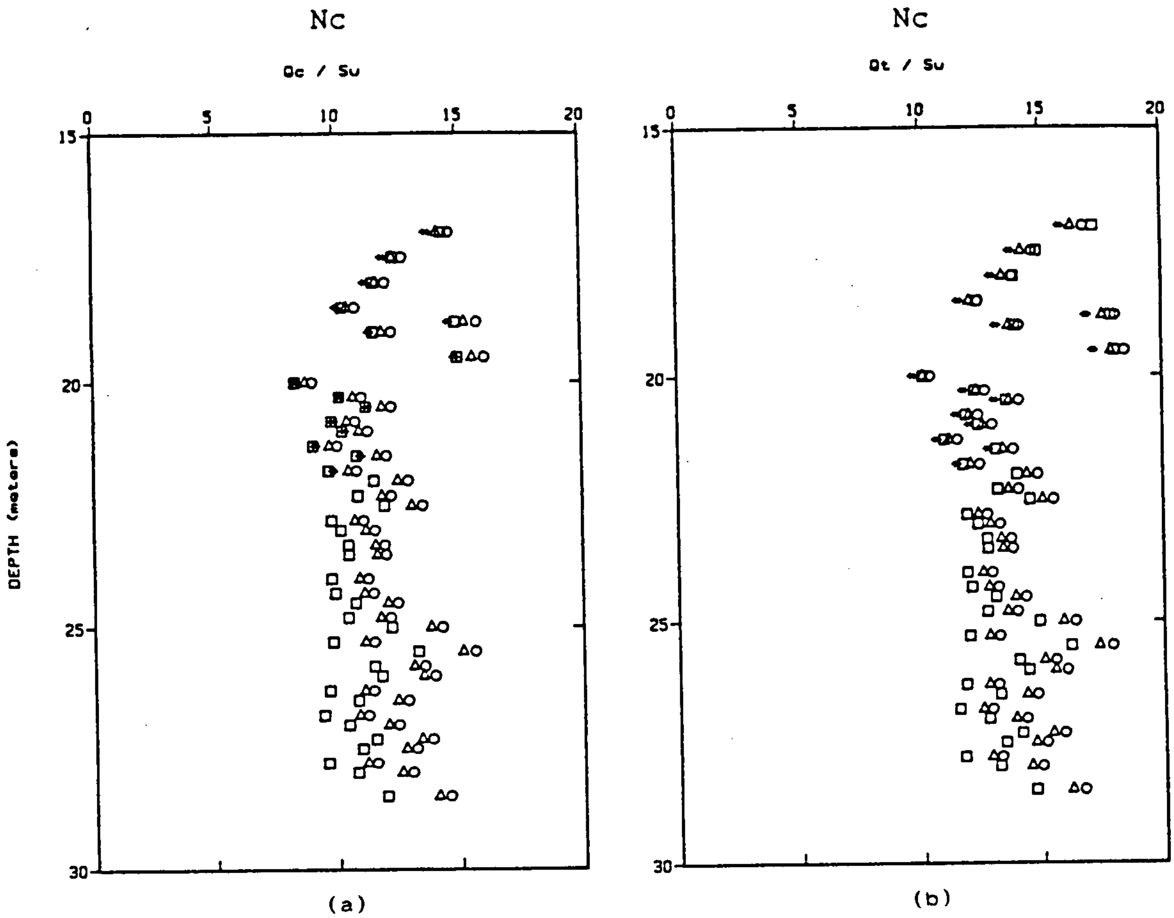

LEGEND

□ CPT 1 - VST 1 & 2
△ CPT 2 - VST 1 & 2
○ CPT 3 - VST 1 & 2
• CPT 4 - VST 1 & 2

Figure 7.5 Qc/Su AND Qt/Su vs DEPTH AT McDONALD FARM

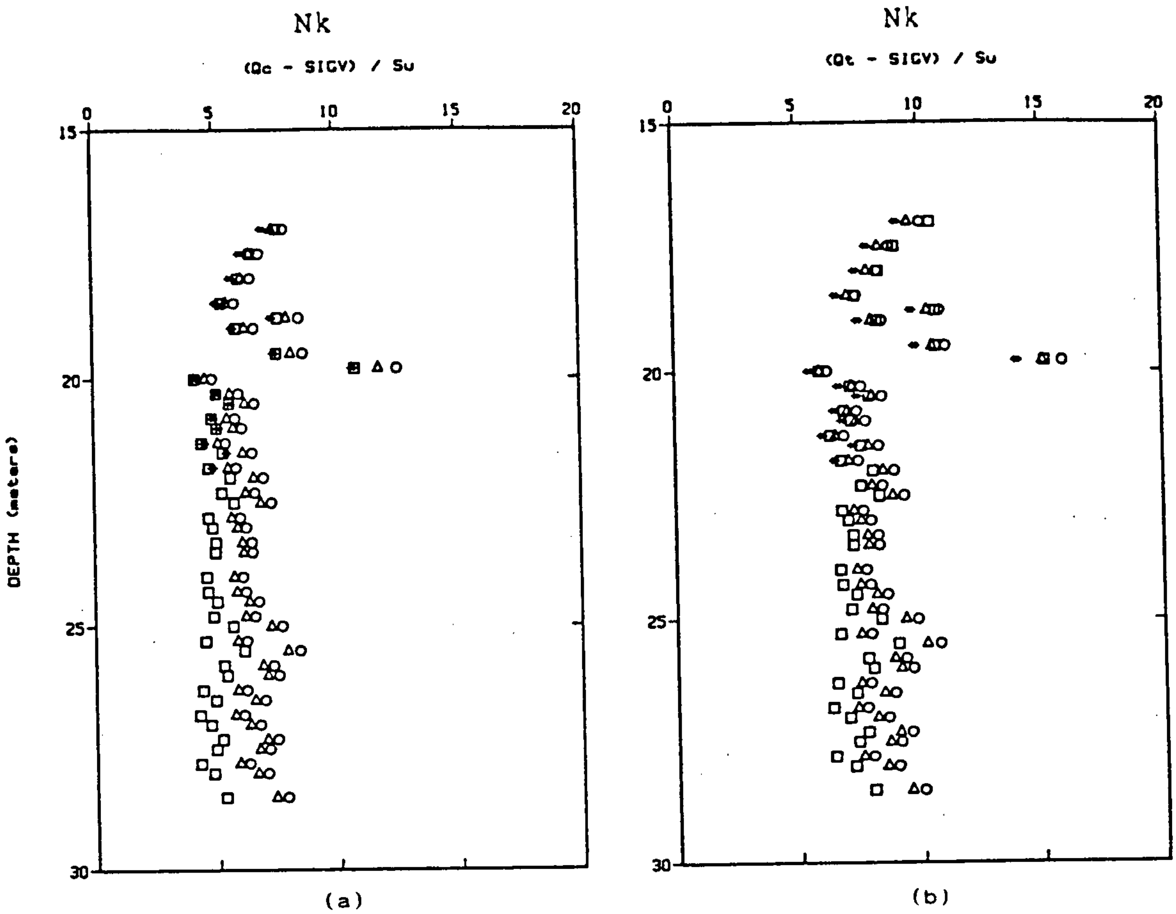

LEGEND

□ CPT 1 - VST 1 & 2
△ CPT 2 - VST 1 & 2
○ CPT 3 - VST 1 & 2
+ CPT 4 - VST 1 & 2

Figure 7.6 $(Qc-\sigma_{vo})/Su$ AND $(Qt-\sigma_{vo})/Su$ vs DEPTH AT McDONALD FARM

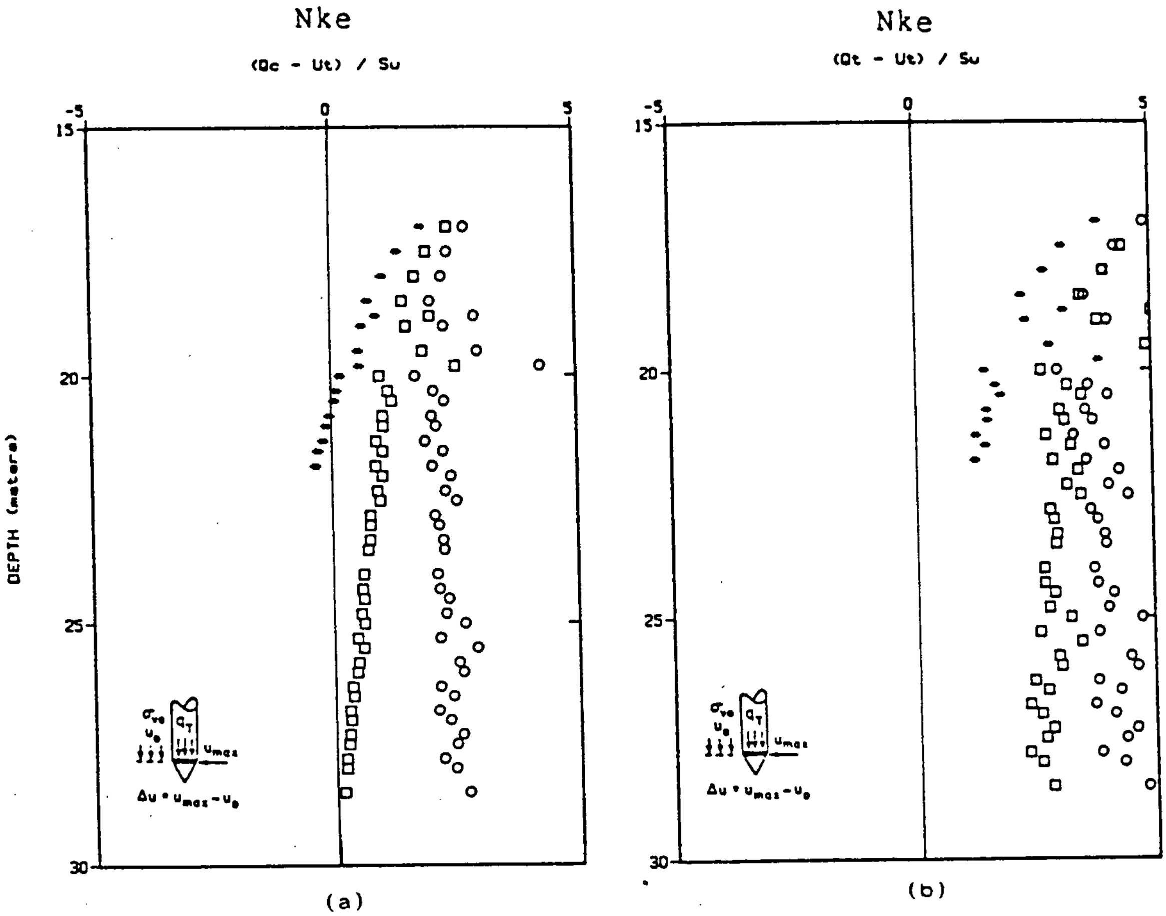

LEGEND

□ CPT 1 - VST 1 & 2
○ CPT 2 - VST 1 & 2
• CPT 4 - VST 1 & 2

Figure 7.7 (Qc-Ut)/Su AND (Qt-Ut)/Su vs DEPTH AT McDONALD FARM

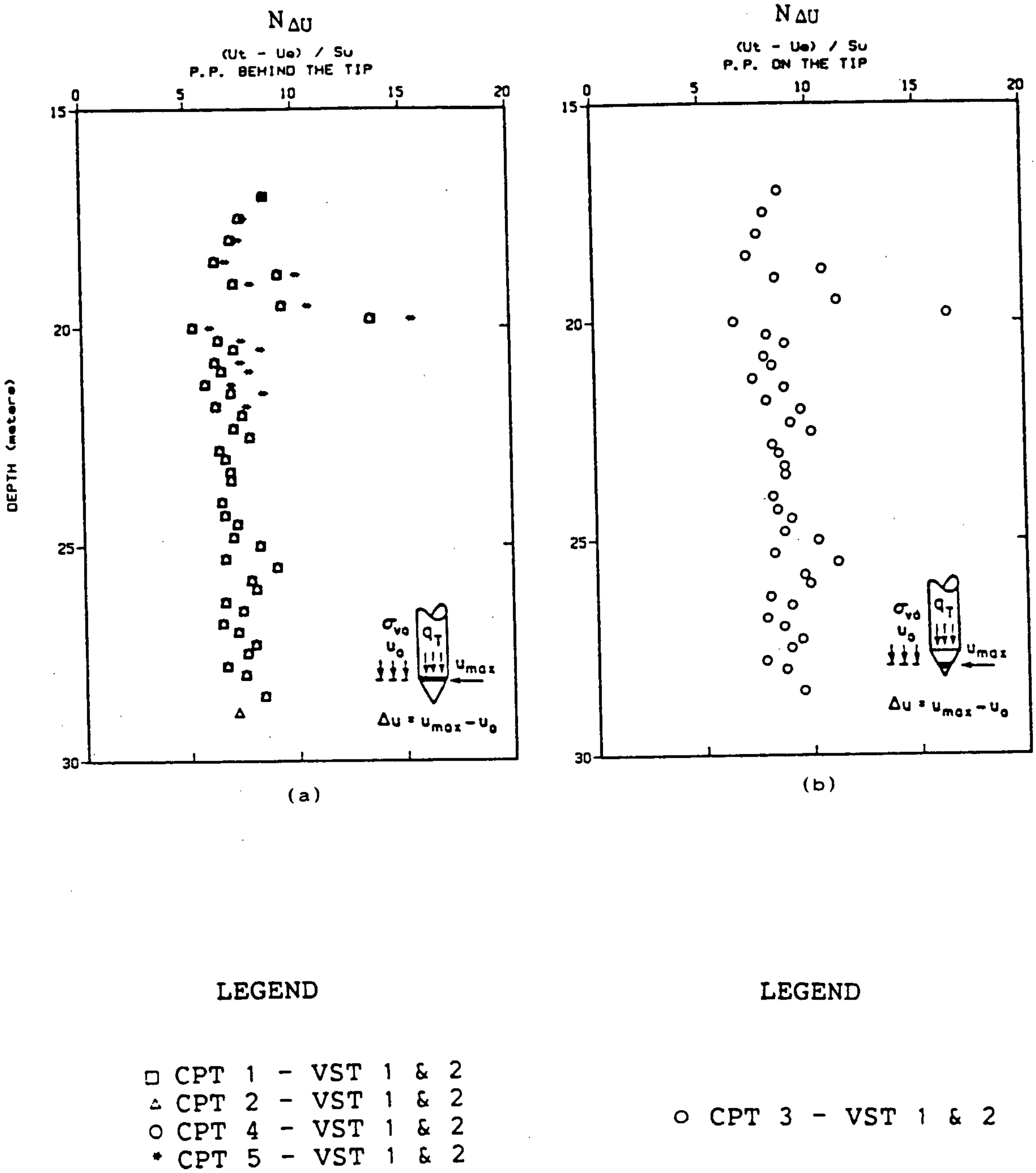

Figure 7.8 ΔU/Su vs DEPTH FOR DIFFERENT POROUS ELEMENT LOCATIONS AT McDONALD FARM

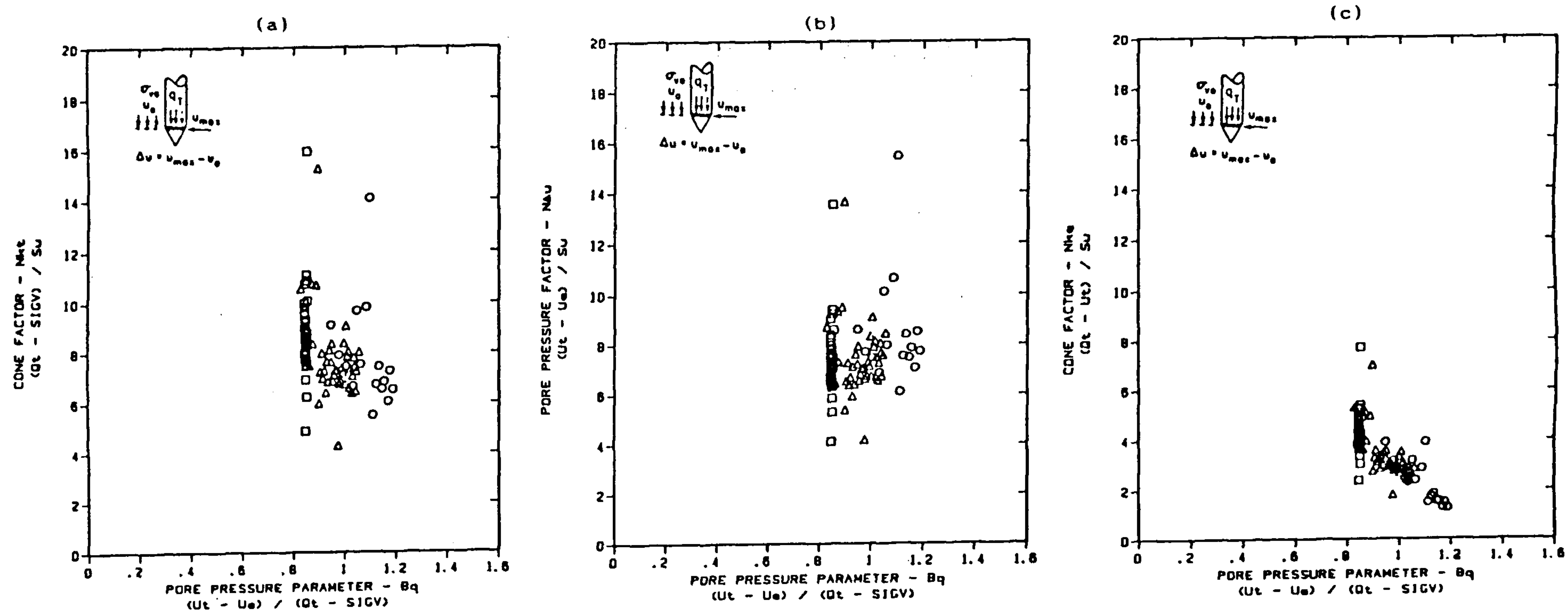

LEGEND

□ CPT 1 - VST 1 & 2
△ CPT 2 - VST 1 & 2
○ CPT 4 - VST 1 & 2

Figure 7.9 Nkt, $N_{\Delta u}$ and Nke vs Bq AT McDONALD FARM bearing, Qt, is used. An even better estimate can be made if overburden stress is included as shown in figure 7.6. Again, the scatter is reduced when Qt is used. Figure 7.7a illustrates the necessity for using corrected bearing when employing Senneset's effective bearing approach. A fairly uniform cone factor is attained using this method, however, the scatter appears to be slightly greater than that observed for the traditional methods (figures 7.5b and 7.6b).

The use of excess pore pressure provides a very good means of estimating Su as shown in figure 7.8 where ΔU/Su is plotted against depth for two different porous element locations. Plots of Nkt, $N_{\Delta U}$ and Nke vs Bq are shown in figure 7.9. There is no discernible correlation, except possibly for Nke vs Bq, as the data tend to cluster in one area. This is due to the small variation in Bq, which might be expected since the material is normally consolidated and its properties are fairly uniform. In section 7.7 the data are compared to those from the other sites where the range in Bq is greater.

7.3 B.C. Hydro Railway Crossing Site

7.3.1 General Geology and Site Description

This site is located at the base of a 5m cut adjacent to the Trans Canada Highway in Langley. It is situated approximately 100m west of the B.C. Hydro railway overpass. The site is located at the eastern extent of the Capilano sediments which consist of raised deltas, intertidal and beach deposits and glaciomarine sediments (Armstrong 1978). The CPT profile in figure 7.10 shows that the site stratigraphy is:

0-2.5m	mixed gravel and sand fill
2.5-10 m	lightly overconsolidated silty clay with occasional silty sand layers
10-30 m	normally consolidated silty clay with occasional silty sand layers

A detailed log from a continuously sampled borehole (to 14.4m) is provided in appendix A. Profiles of index properties and undrained strength and sensitivity from laboratory and field vane tests are shown in figure 7.11. Note that the laboratory values tend to be less than the insitu values indicating possible sample disturbance or size effects. The plasticity index decreases slightly with depth. Sensitivity does not vary much and has an average value of 9. The undrained strength increases with depth having Su/P'=0.31 in the normally consolidated region.

7.3.2 Correlations Between Su and CPT

The results of the various correlation methods are shown in figures 7.12 through 7.16. The cone factor, Nc (Qc/Su or Qt/Su; figure 7.12), initially decreases with depth to a depth of 10m. Below this, Nc tends to increase with depth. A similar trend is observed for Nk ($(Qc-\sigma_{vo})/Su$ or $(Qt-\sigma_{vo})/Su$; figure 7.13). Note the significant reduction in scatter when corrected bearing is used. The initial decrease in Nc and Nk may be a result of the decreasing overconsolidation of the clay. The subsequent increase in cone factor with depth may be a reflection of the decrease in plasticity and the slight increase in sensitivity of the material with depth.

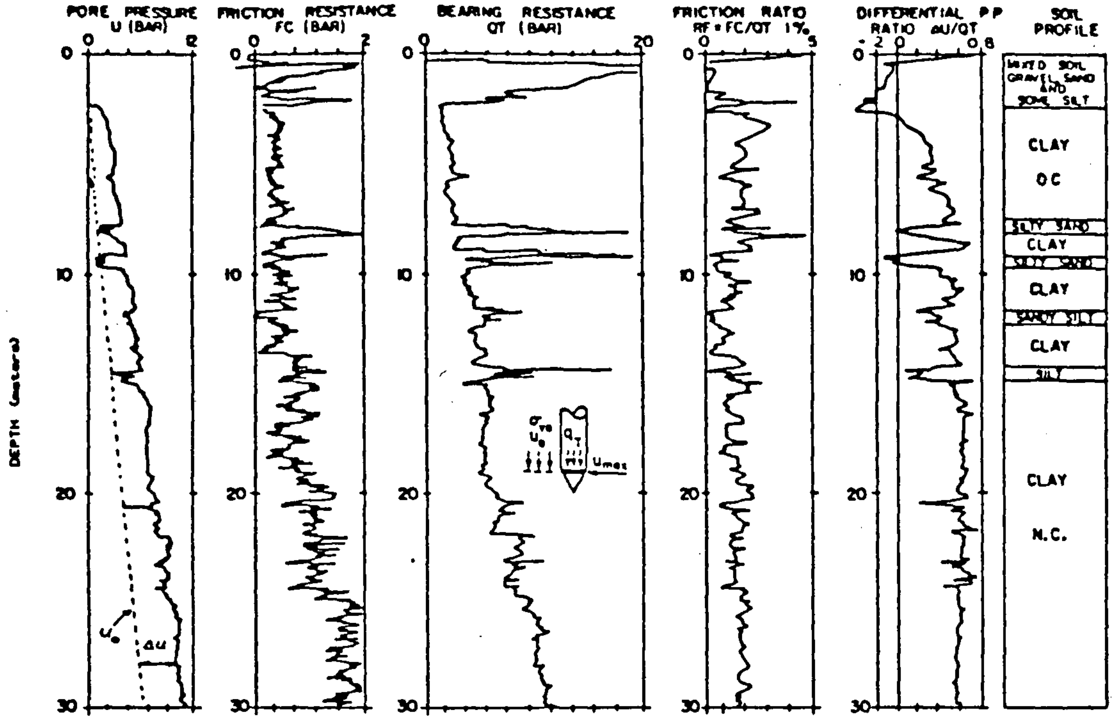

Figure 7.10 TYPICAL CPT PROFILE AT B.C. HYDRO RAILWAY SITE

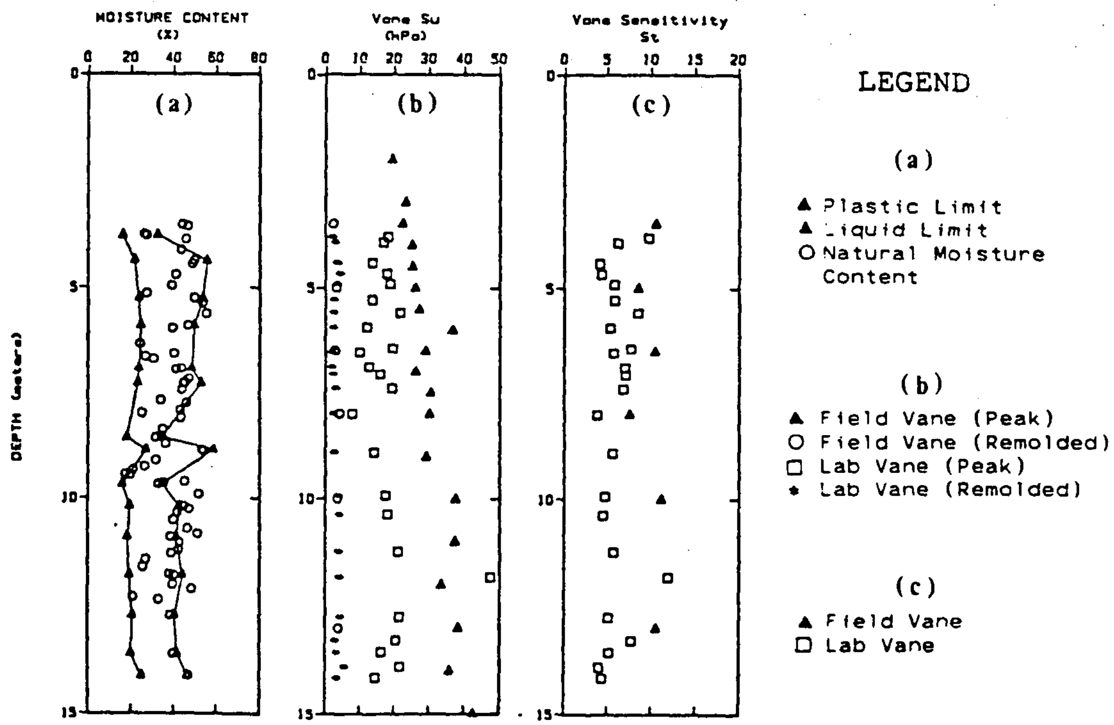

Figure 7.11 INDEX PROPERTIES, FIELD VANE STRENGTH AND SENSITIVITY PROFILES AT B.C. HYDRO RAILWAY SITE

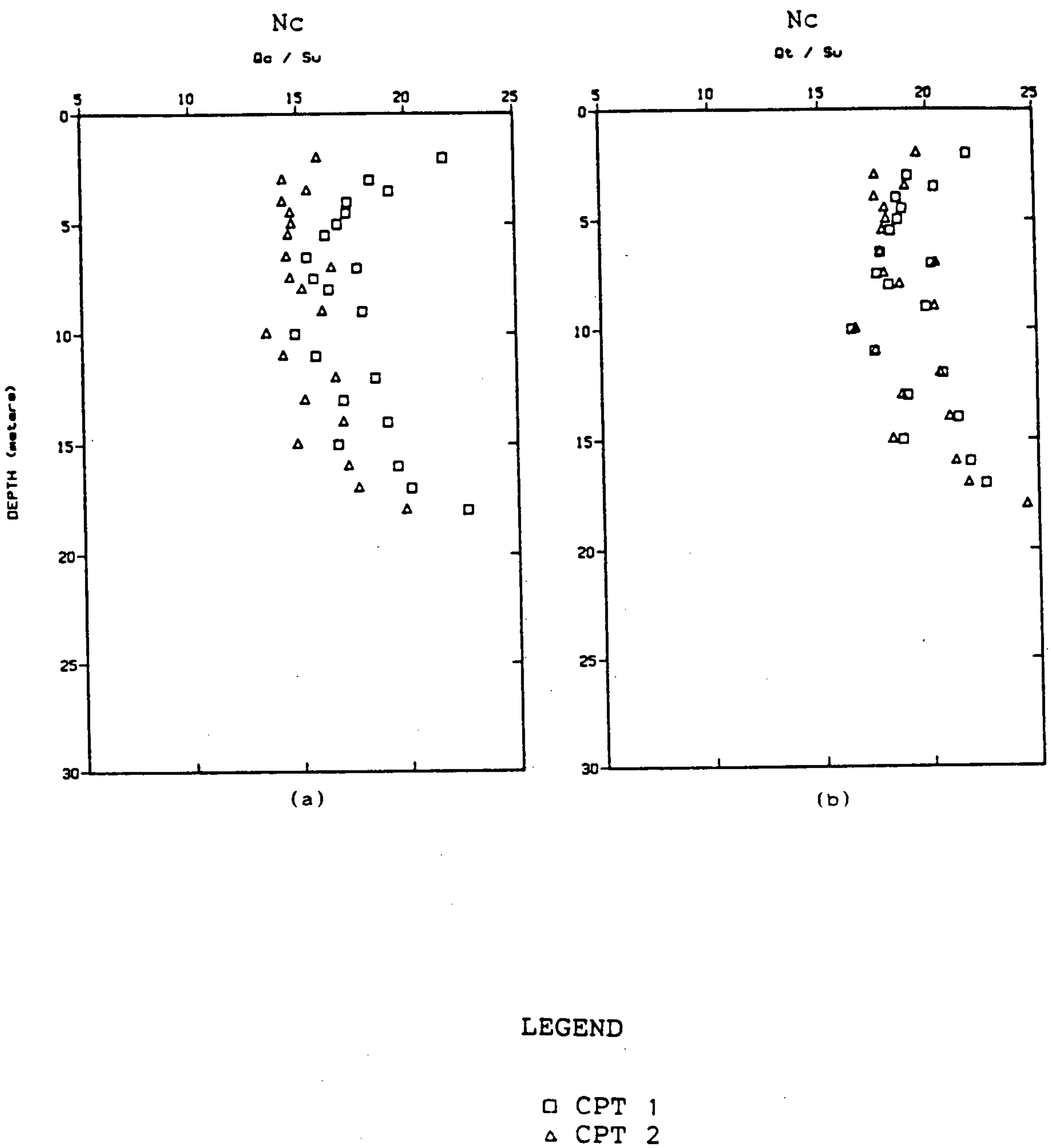

Figure 7.12 Qc/Su AND Qt/Su vs DEPTH AT B.C. HYDRO RAILWAY SITE

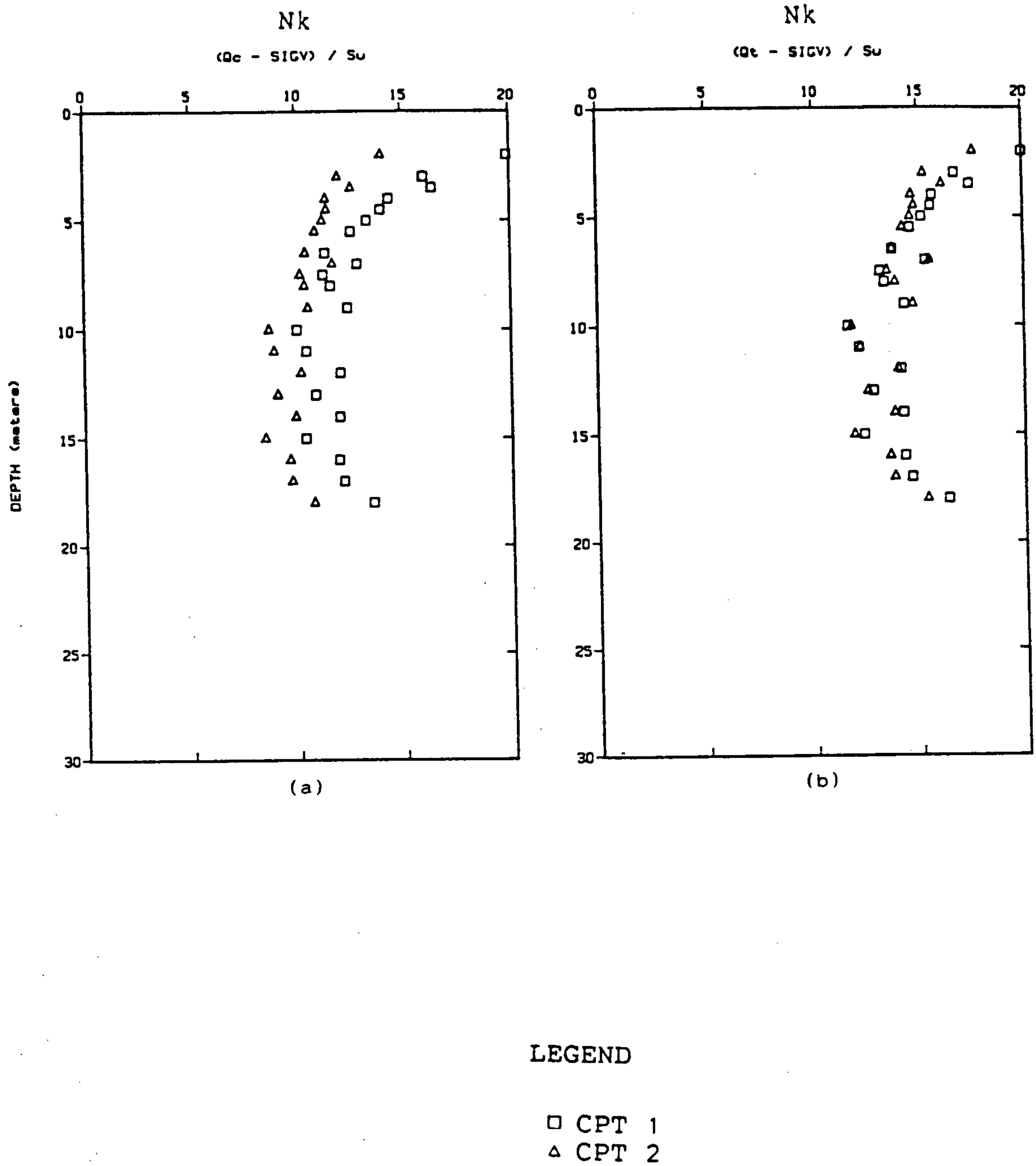

Figure 7.13 (Qc-σ_{vo})/Su and (Qt-σ_{vo})/Su vs DEPTH AT B.C. HYDRO RAILWAY SITE

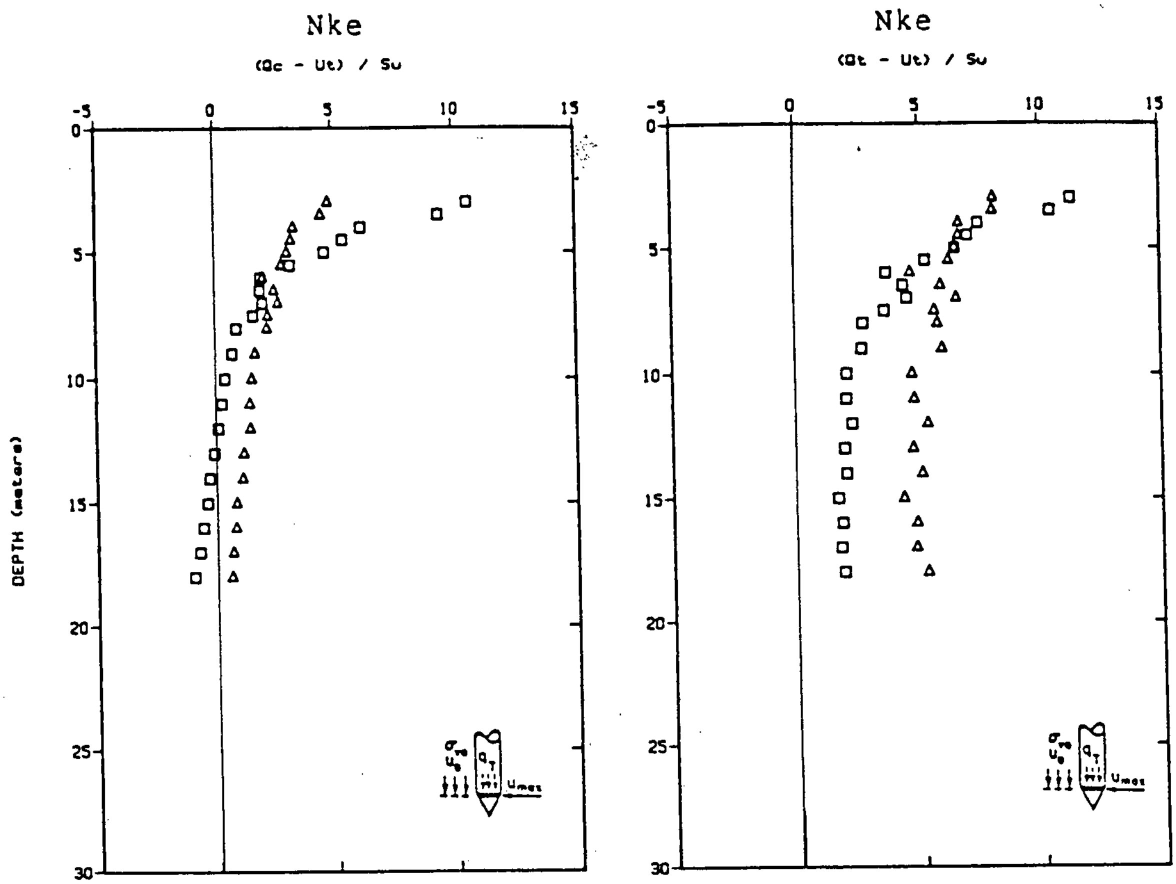

(a) (b)

LEGEND

□ CPT 1
△ CPT 2

Figure 7.14 (Qc-Ut)/Su AND (Qt-Ut)/Su vs DEPTH AT B.C. HYDRO RAILWAY SITE

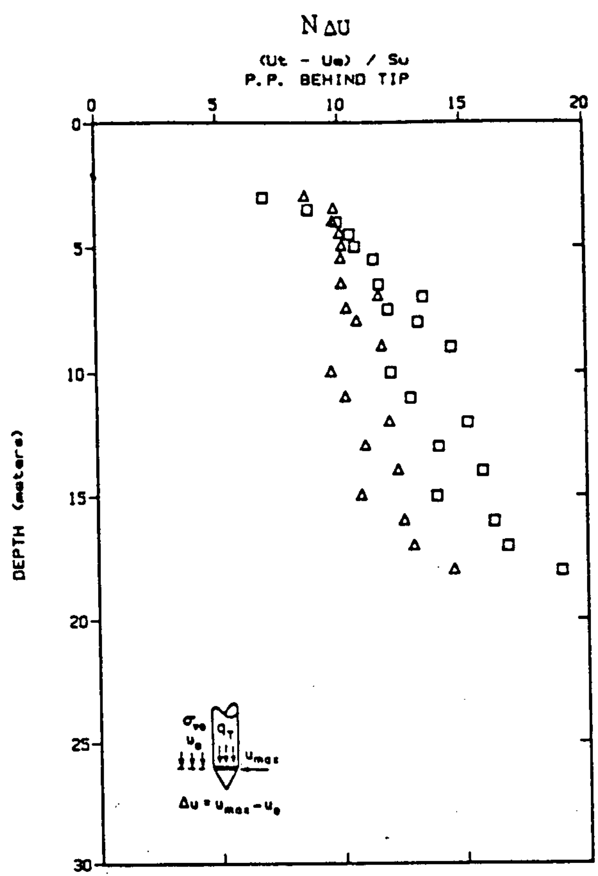

LEGEND

□ CPT 1
△ CPT 2

Figure 7.15 ΔU/Su vs DEPTH AT B.C. HYDRO RAILWAY SITE

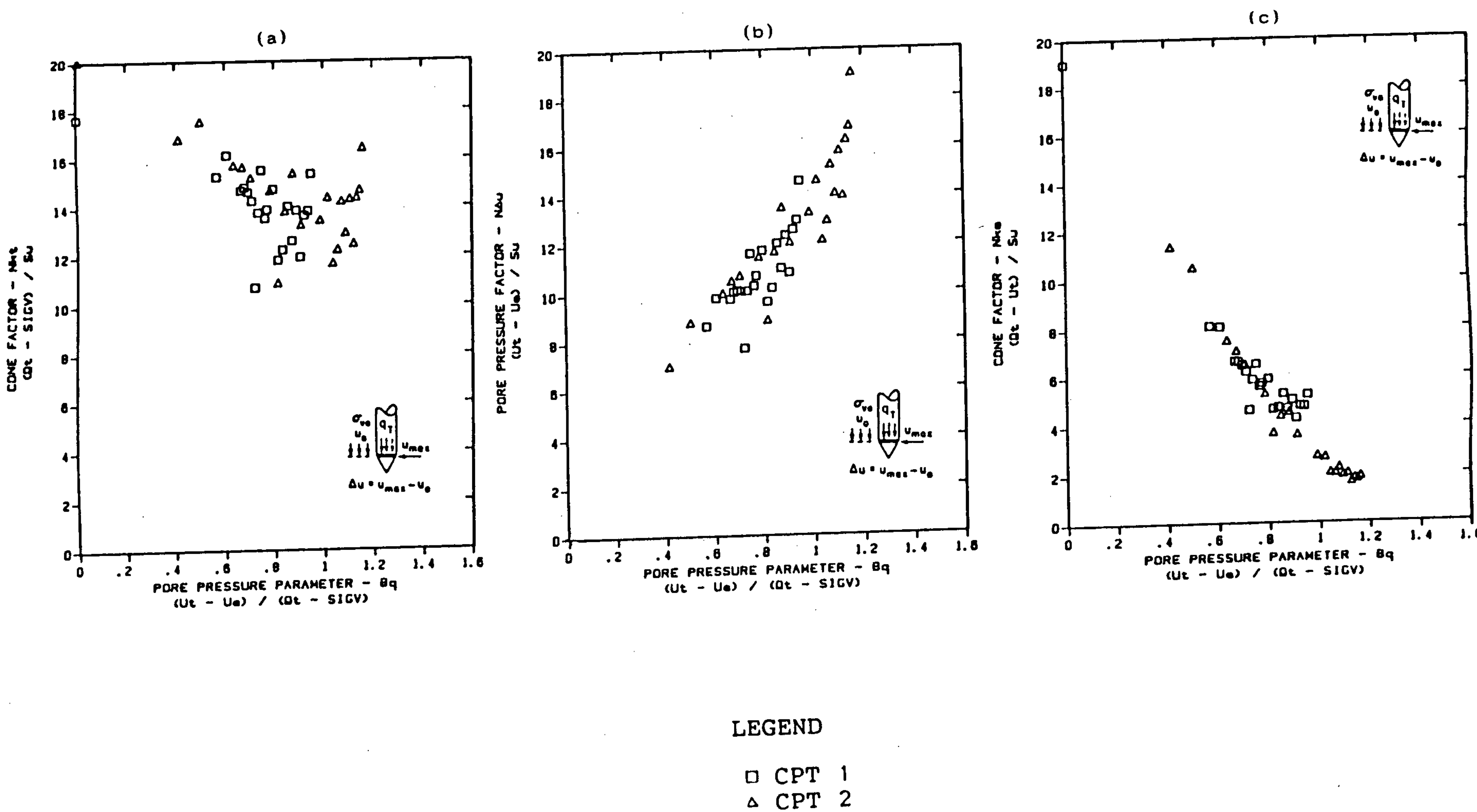

Figure 7.16 Nkt, NΔU and Nke vs Bq AT B.C. HYDRO RAILWAY SITE

Two distinct curves are observed in figure 7.14b where the ratio of effective bearing to Su (Nke) is plotted against depth. The separation between the two curves might reflect the problem of accuracy discussed in section 6.3.3; two similar numbers, Qt and Ut, are subtracted to attain a small number which may be prone to error. However, the trends in the curves are similar and suggest that the use of effective bearing works well in normally consolidated deposits. The cone factor tends to increase with increasing OCR. This is as expected since Qt should increase and Ut (measured behind the tip) should decrease with increasing OCR. The value of $\Delta U/Su$ increases with depth as shown in figure 7.15. Again, this might be a reflection of the decrease in plasticity and the slight increase in sensitivity with depth. Although the data are scattered, there appears to be a distinct kink in the curve above 5m. A noticable decrease in $\Delta U/Su$ is observed because of the lower excess pore pressure in the overconsolidated material. Consistent trends are observed for $N_{\Delta U}$ and Nke vs Bq in figure 7.16, the latter having the least scatter. No correlation is observed for Nkt vs Bq.

7.4 Upper 232nd St. Site

7.4.1 General Geology and Site Description

This site is located at the 232nd St. exit of the Trans Canada Highway in Langley. It is approximately 1km east of the B.C. Hydro railway site. Two sites have been designated at the 232nd St. interchange; the upper and lower sites. The lower site is discussed in section 7.5. The upper site is situated on a compacted clay fill that forms the approach for the 232nd St. overpass. The site lies at the western extent of the Fort Langley Formation. This formation has recorded at least three advances and retreats of a valley glacier and consists of interbedded marine, glaciomarine and glacial sediments (Armstrong 1978). A CPT profile from the upper site is shown in figure 7.17 and the field vane profiles are shown in figure 7.18. Note that the cone bearing clearly indicates the overconsolidation of the upper 7m. The statigraphy consists of:

0-2.5m	compacted clay fill; organic
2.5-7.5m	overconsolidated silty clay
7.5-20+m	normally consolidated silty clay with occasional sand lense; increasing in sand content with depth

The cone bearing is compared with the field vane results and the overconsolidation ratio in figure 7.19. The OCR was calculated using the first method described in section 6.5. Note how both the cone bearing and vane strength decrease with depth in the overconsolidated material. Both increase linearly with depth in the normally consolidated region ($Su/P'=0.23$).

7.4.2 Correlations Between Su and CPT

The results for the upper 232nd St. site are shown in figures 7.20 through 7.24. The cone factor Nc exhibits considerable scatter and generally increases with depth (figure 7.20). It does appear that Qc/Su initially decreases with depth reflecting the decrease in OCR, however, this is not observed for Qt/Su. There is significantly less scatter for Nk vs depth

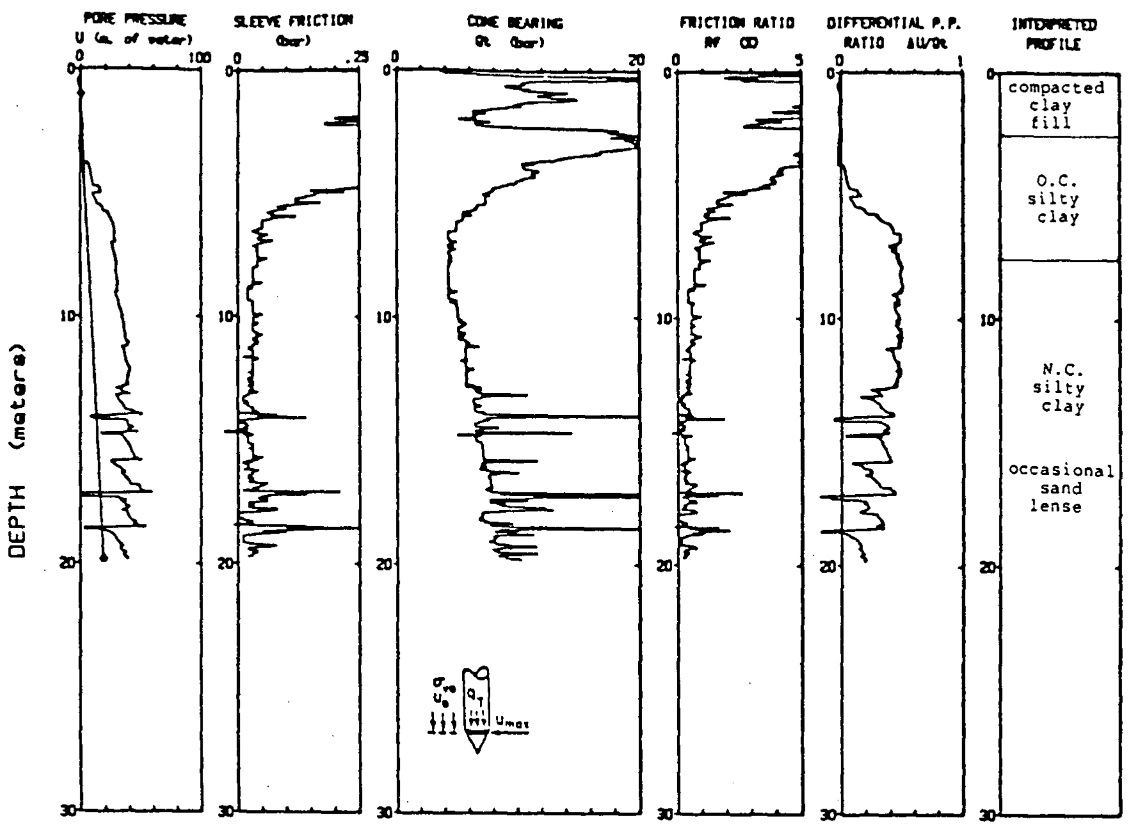

Figure 7.17 TYPICAL CPT PROFILE AT UPPER 232nd St. SITE

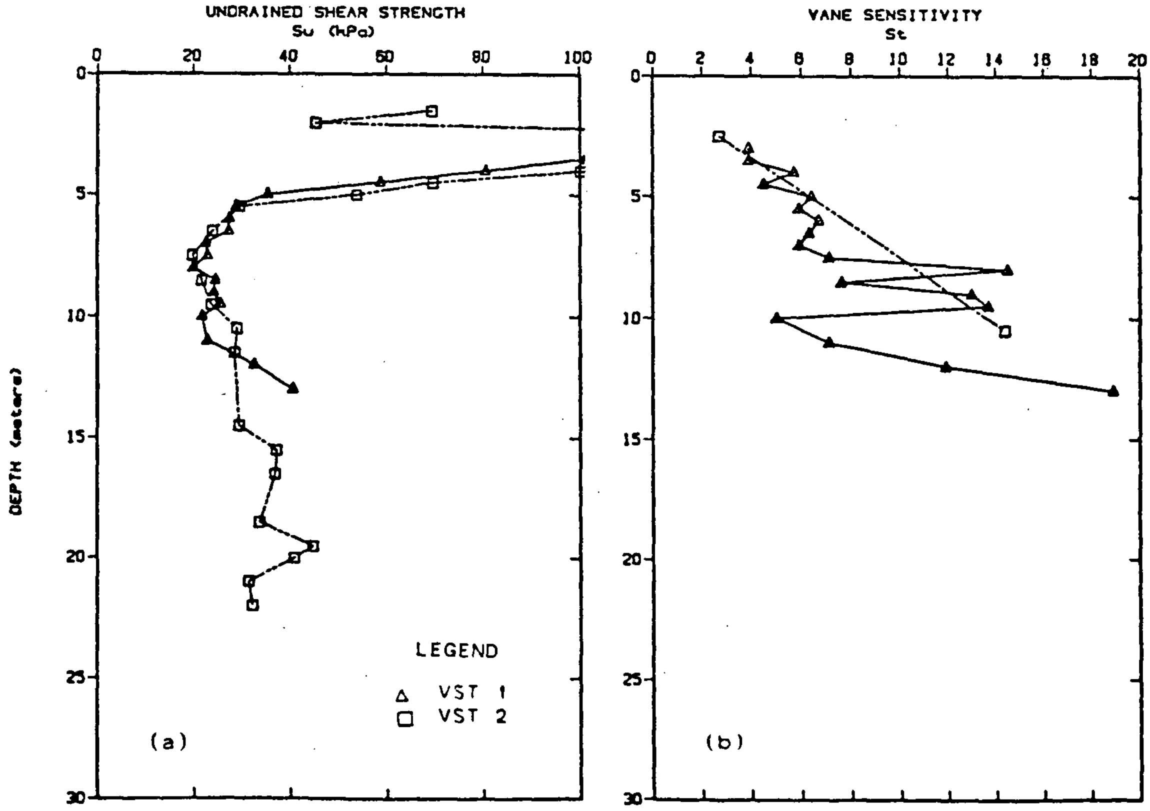

Figure 7.18 FIELD VANE STRENGTH AND SENSITIVITY PROFILES AT UPPER 232nd St. SITE

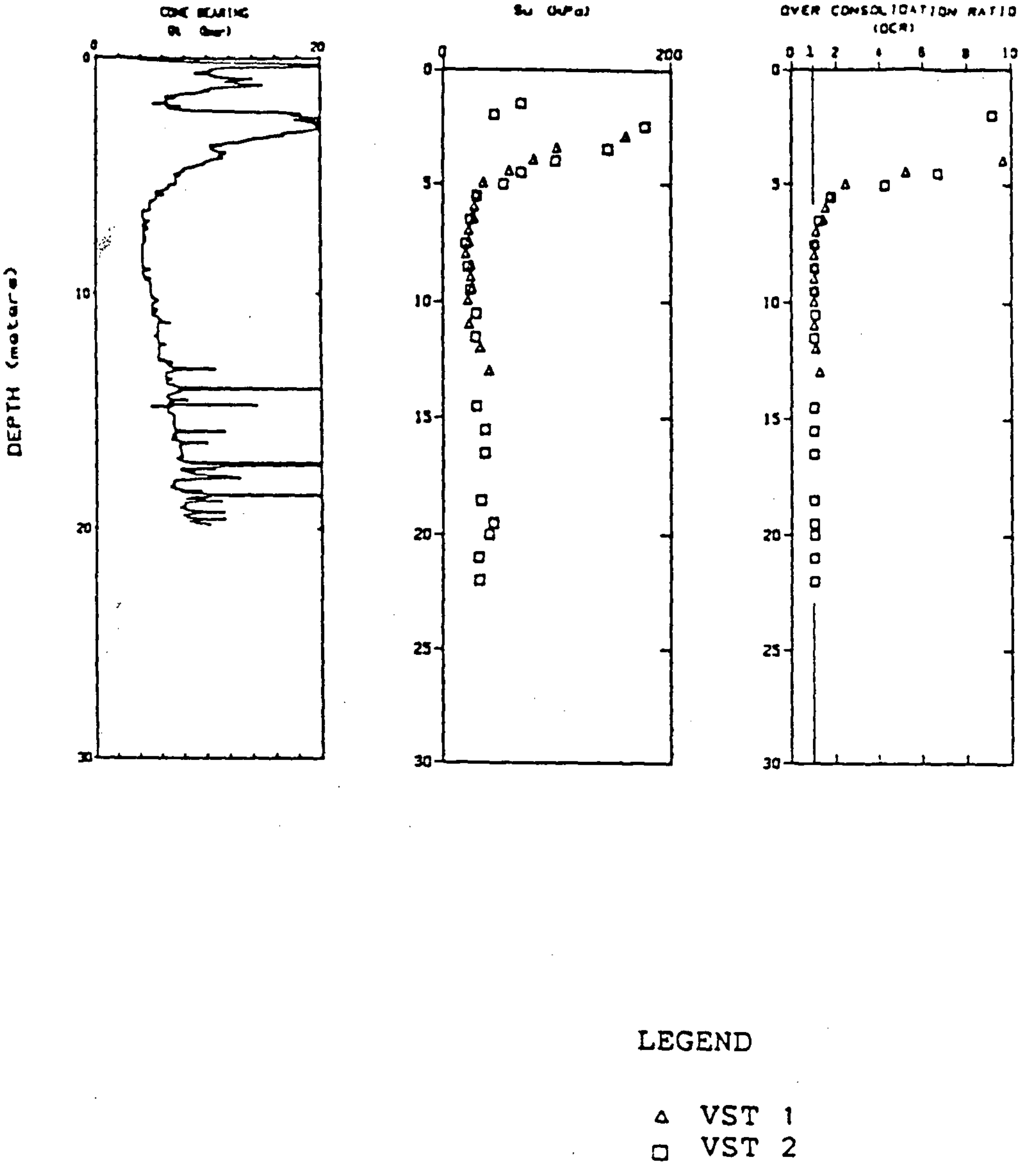

Figure 7.19 COMPARISON BETWEEN CONE BEARING, VANE SHEAR STRENGTH AND OVERCONSOLIDATION RATIO AT UPPER 232nd St. SITE

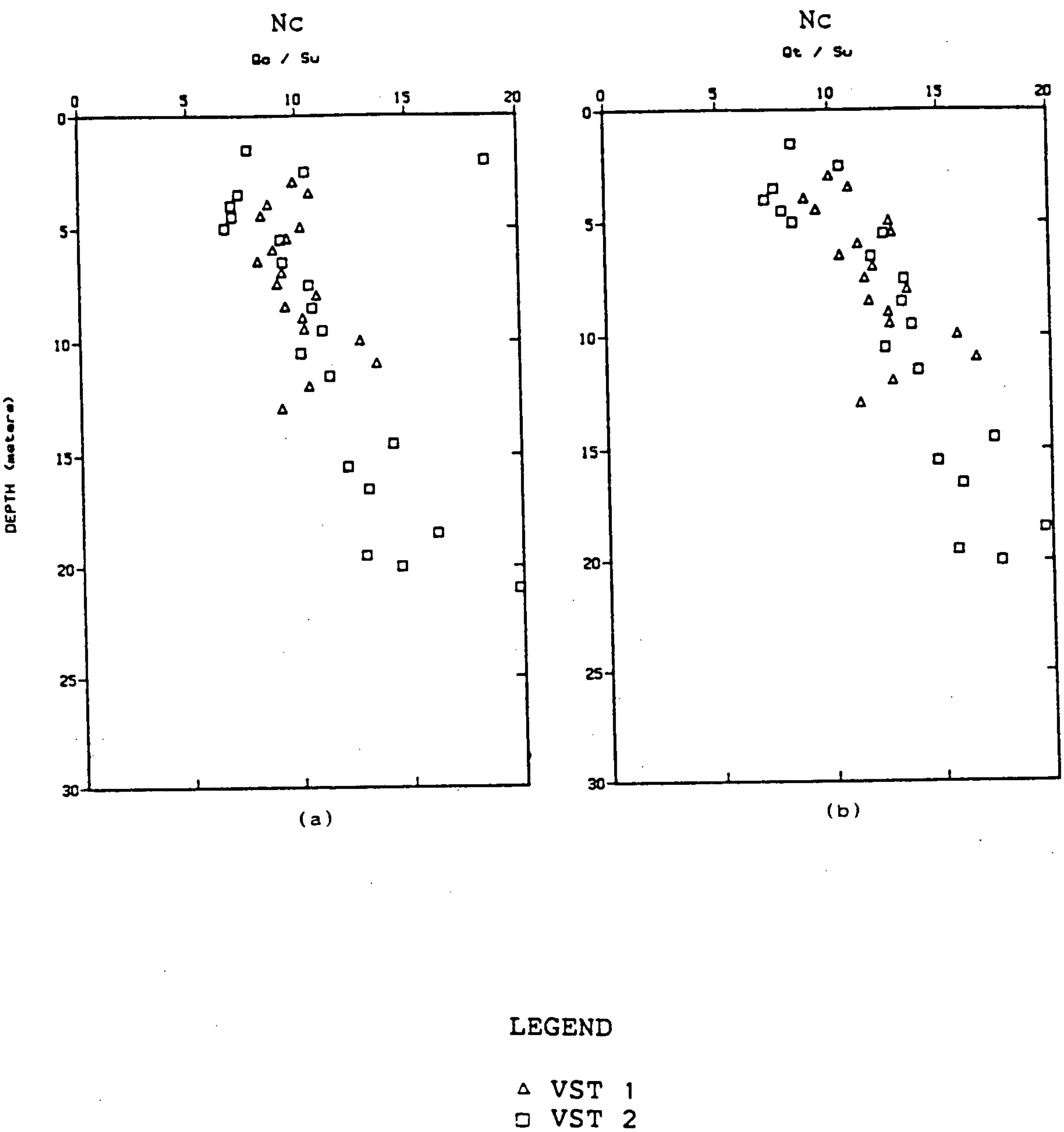

Figure 7.20 Qc/Su AND Qt/Su vs DEPTH AT UPPER 232nd St. SITE

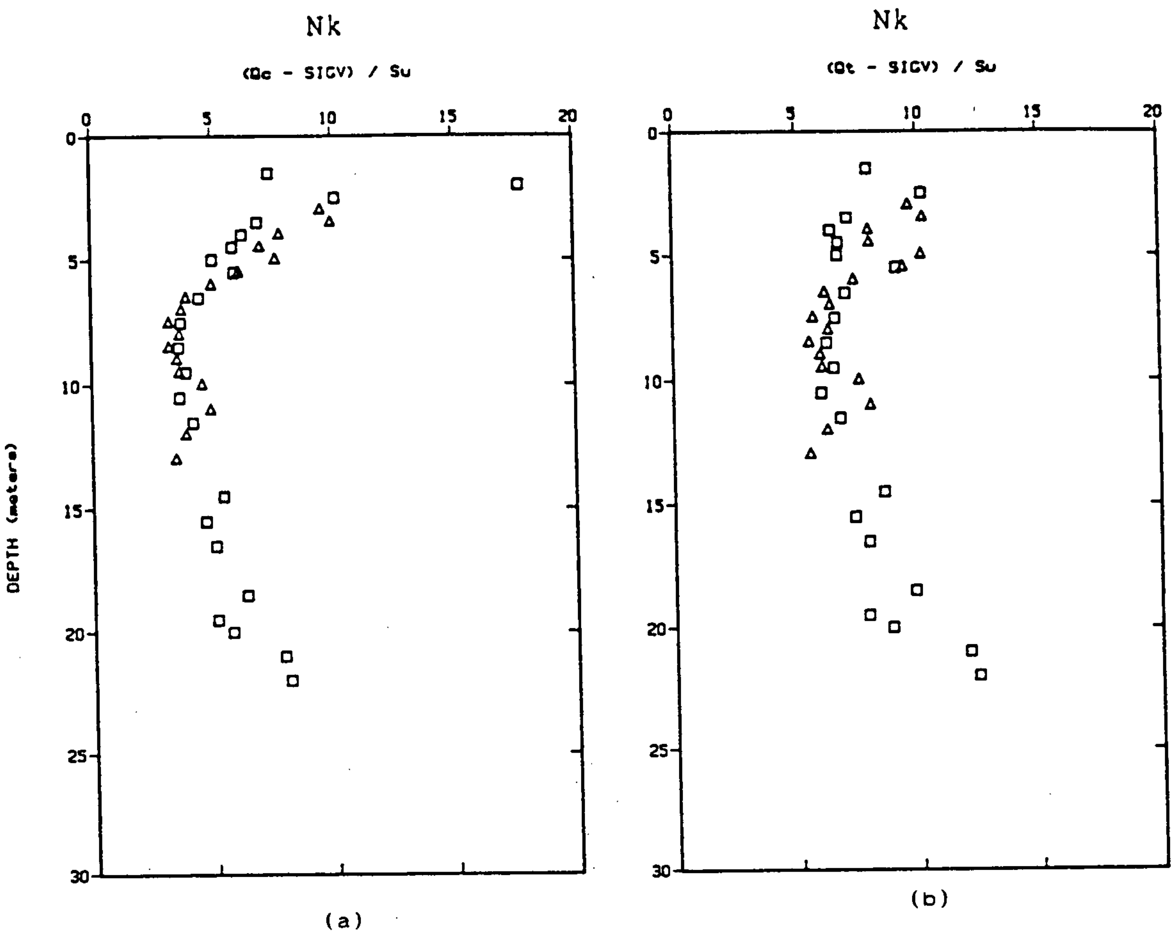

LEGEND

□ VST 1
△ VST 2

Figure 7.21 $(Qc-\sigma_{vo})/Su$ and $(Qt-\sigma_{vo})/Su$ vs DEPTH AT UPPER 232nd St. SITE

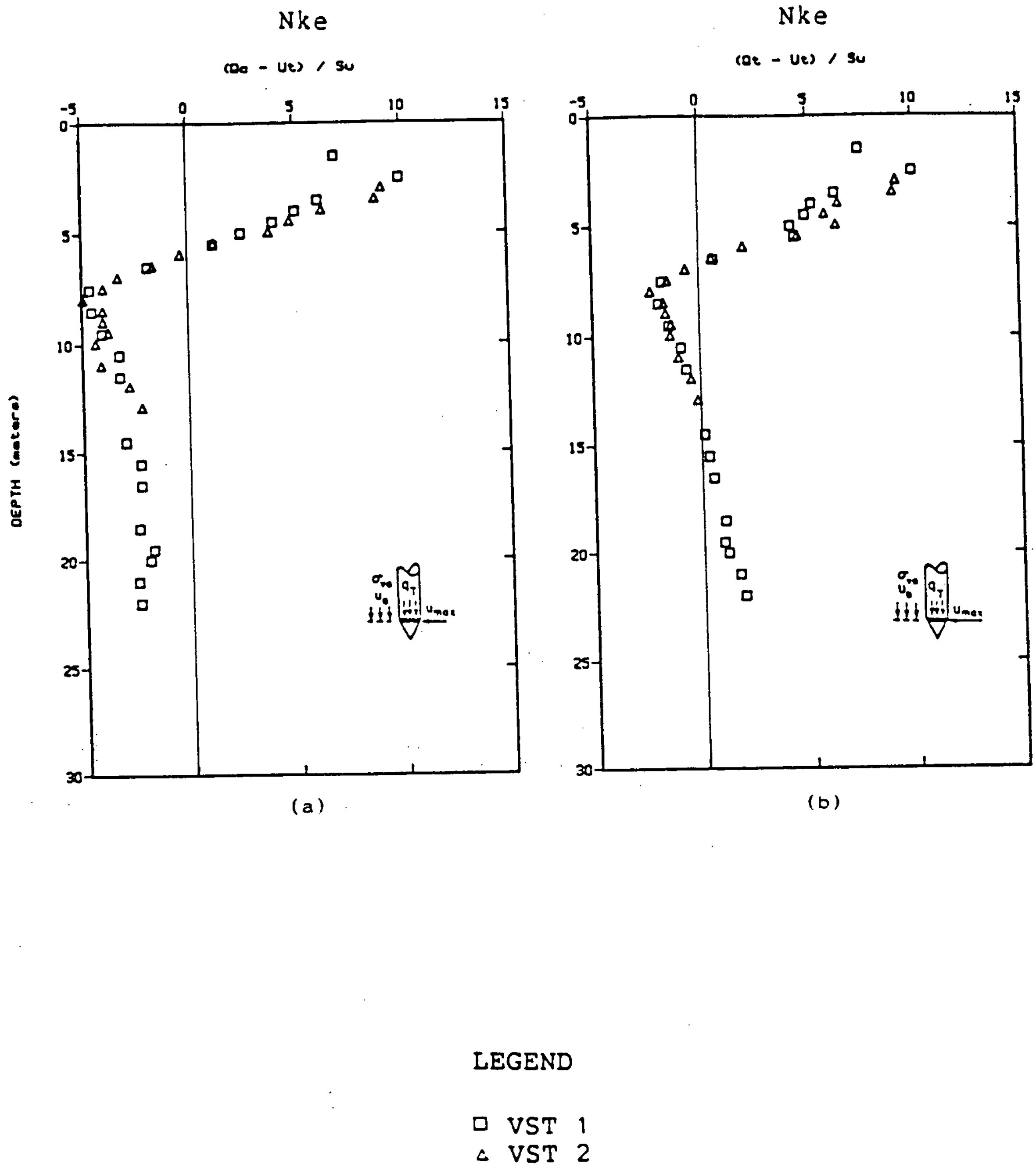

Figure 7.22 (Qc-Ut)/Su AND (Qt-Ut)/Su vs DEPTH AT UPPER 232nd St. SITE

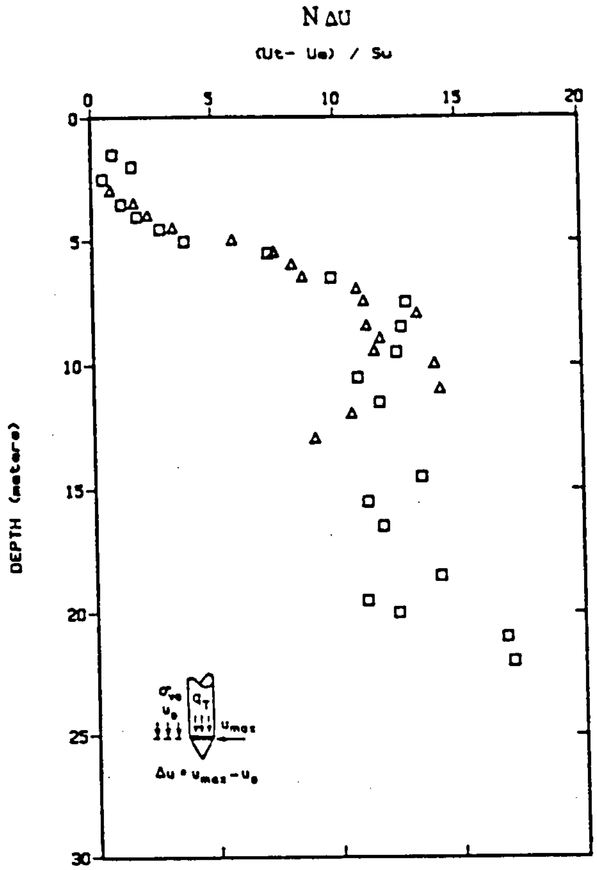

LEGEND

□ VST 1
△ VST 2

Figure 7.23 ΔU/Su vs DEPTH AT UPPER 232nd St. SITE

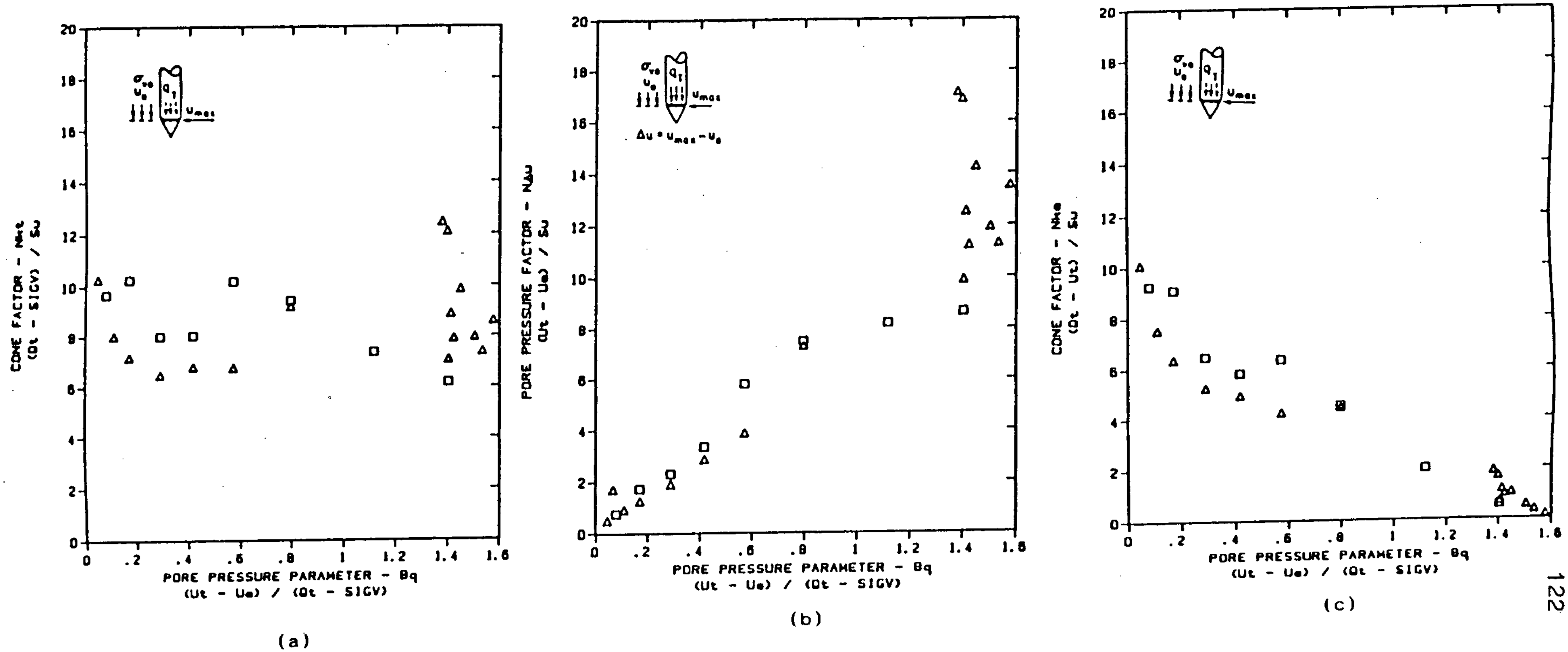

LEGEND

□ VST 1
△ VST 2

Figure 7.24 Nkt, NΔu and Nke vs Bq AT UPPER 232nd St. SITE (figure 7.21). Nk initially decreases with depth to approximately 8m where the material is essentially normally consolidated. Below 8m, Nk increases with increasing sensitivity.

Figure 7.22a clearly illustrates the need to correct bearing data for pore pressure effects when using the effective bearing approach as the value of Nke is negative which, of course, is. impossible. A dramatic decrease in Nke with decreasing OCR can be seen in figure 7.22b. In the normally consolidated range Nke increases with increasing sensitivity. $N_{\Delta U}$ (ΔU/Su) vs depth is shown in figure 7.23 and is observed to increase dramatically with depth in the overconsolidated silty clay. Again, a fairly consistent trend is observed for $N_{\Delta U}$ and Nke vs Bq. There does not, however, appear to be a correlation between Nkt and Bq.

7.5 Lower 232nd St. Site

7.5.1 General Geology and Site Description

The lower site is situated slightly above highway level and about 5m below the elevation of the upper site. The near surface material is overconsolidated due to dessication. A typical CPT profile is shown in figure 7.25 and the field vane results are shown in figure 7.26. The undrained shear strength profile generally increases with depth (Su/P'=0.23) but takes a curious jump at a depth of 15m. This increase in Su is likely due to the influence of sand lenses.

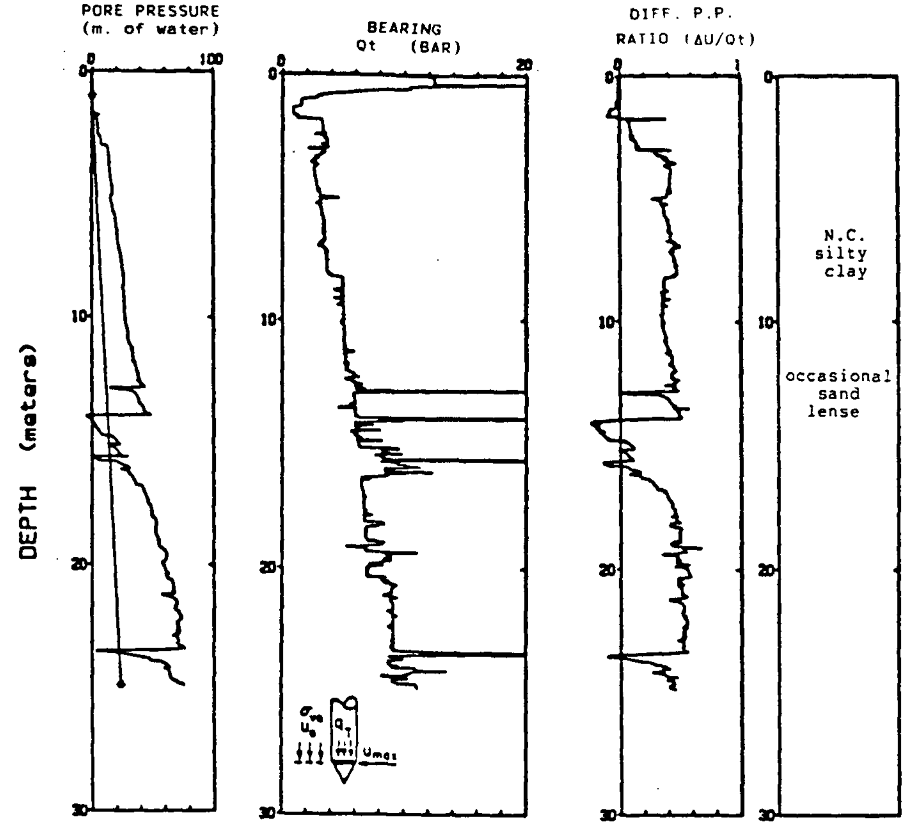

Figure 7.25 TYPICAL CPT PROFILE AT LOWER 232nd St. SITE

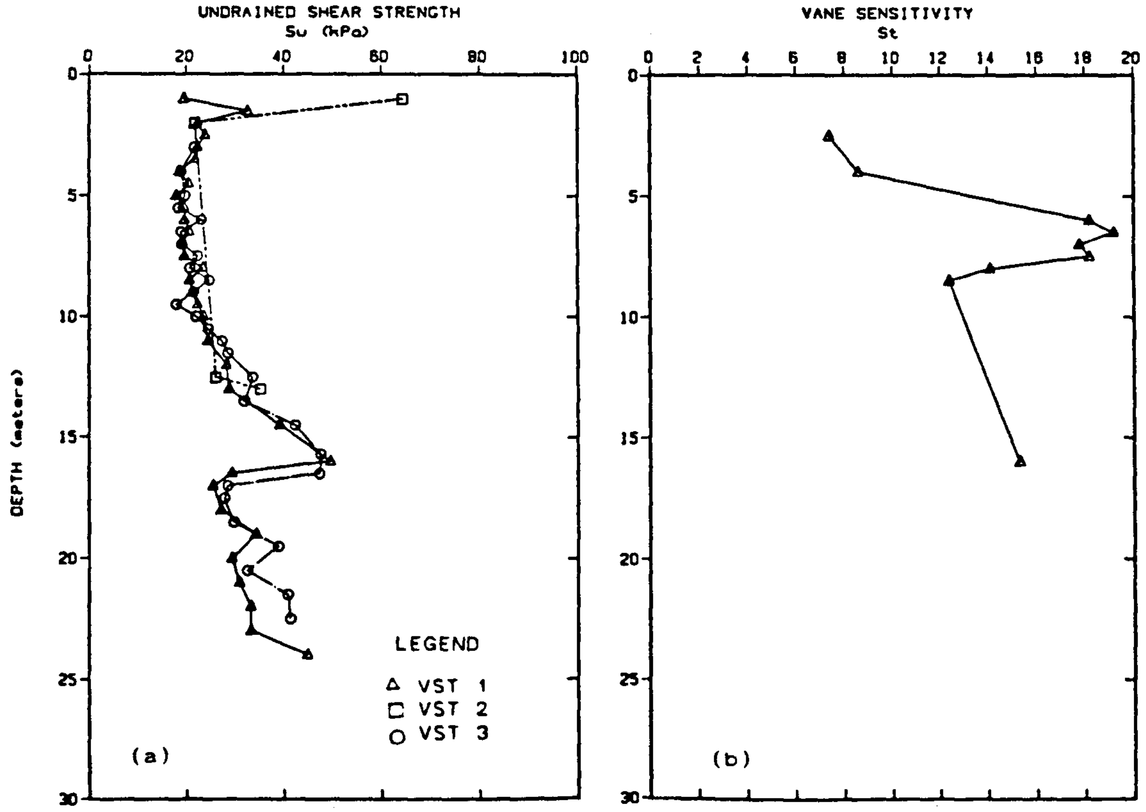

Figure 7.26 FIELD VANE STRENGTH AND SENSITIVITY PROFILES AT LOWER 232nd St. SITE

7.5.2 Correlations Between Su and CPT

Results for the lower 232nd St. site are shown in figures 7.27 through 7.31. The traditional cone factors, Nc and Nk (figures 7.27 and 7.28 respectively) show considerable scatter even though the scatter is reduced when Qt is used. The general trend is consistent with the results from the other sites; Nc or Nk increasing with increasing sensitivity. There is a decrease in Nc and Nk between 13m and 17m due to the unrealistically high Su values. The plot of Nke vs depth in figure 7.29b shows considerable scatter; again likely due to the influence of the sand lenses on the measured pore pressures. The plot of $N_{\Delta U}$ vs depth in figure 7.30 indicates the same trends observed at the other sites. Consistent trends are also observed for $N_{\Delta U}$ and Nke vs Bq in figure 7.31.

7.6 Haney Slide Site

7.6.1 General Geology and Site Description

The Haney Slide site is located approximately 30km east of Vancouver almost directly below the town centre of Haney. The site is a remnant of the Haney slide of January 30, 1880. It features a hummocky topography made up of the slide blocks from the retrogressive failure (Davies 1985). The general geology consists of interbedded marine, glaciomarine and glacial sediments of the Fort Langley Formation. The CPT profile from a sounding adjacent to the FV boring is shown in figure 7.32. The soil profile consists of:

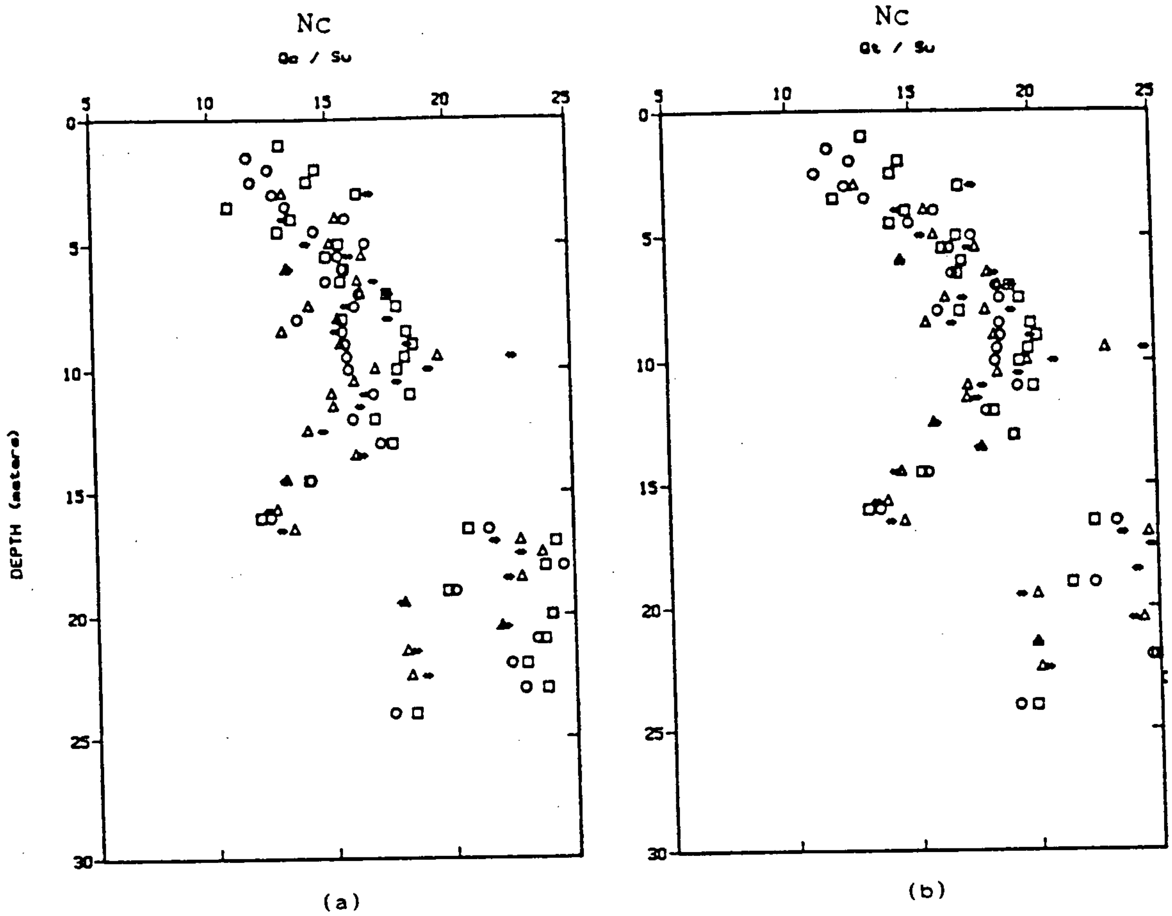

LEGEND

□ CPT 1 - VST 1
△ CPT 1 - VST 3
○ CPT 2 - VST 1
• CPT 2 - VST 3

Figure 7.27 Qc/Su AND Qt/Su vs DEPTH AT LOWER 232nd St. SITE

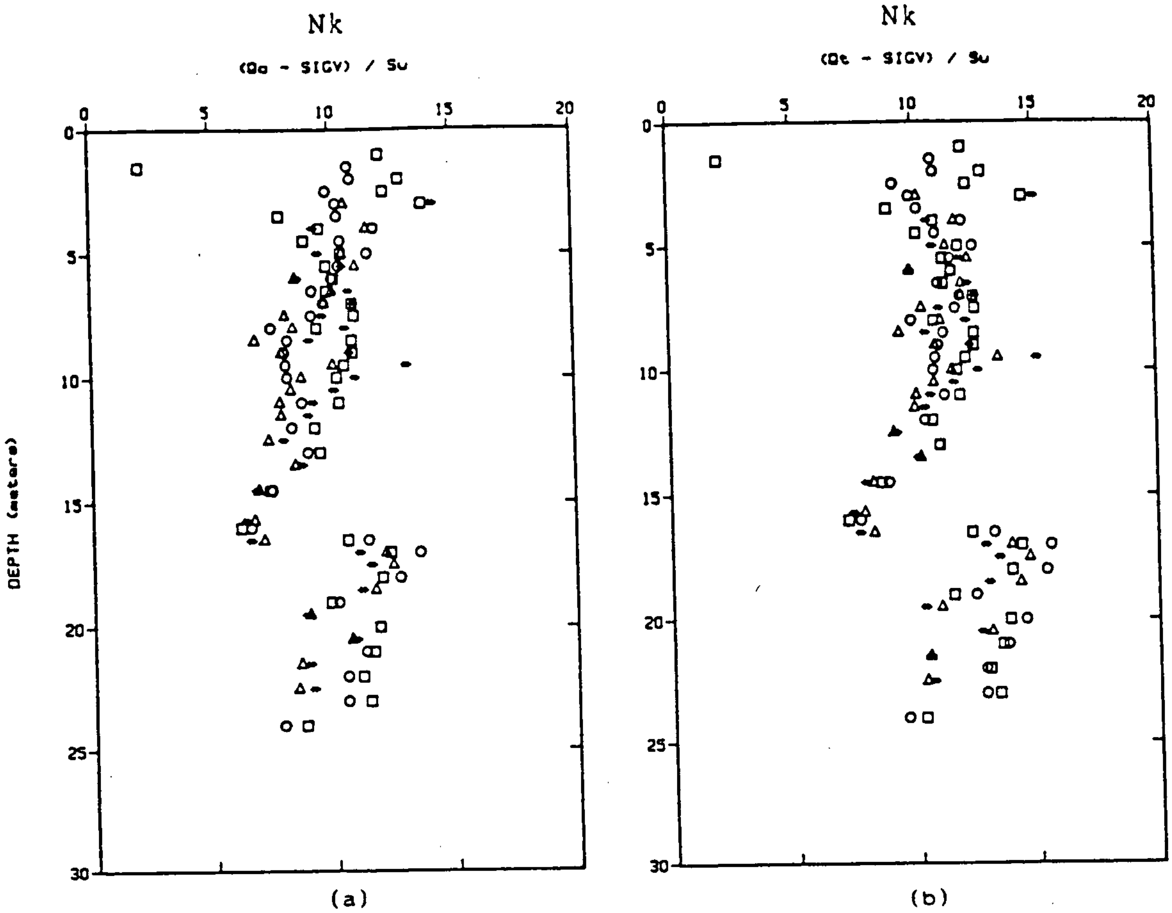

LEGEND

□ CPT 1 - VST 1
△ CPT 1 - VST 3
○ CPT 2 - VST 1
◆ CPT 2 - VST 3

Figure 7.28 $(Q_c-\sigma_{vo})/S_u$ and $(Q_t-\sigma_{vo})/S_u$ vs DEPTH AT LOWER 232nd St. SITE

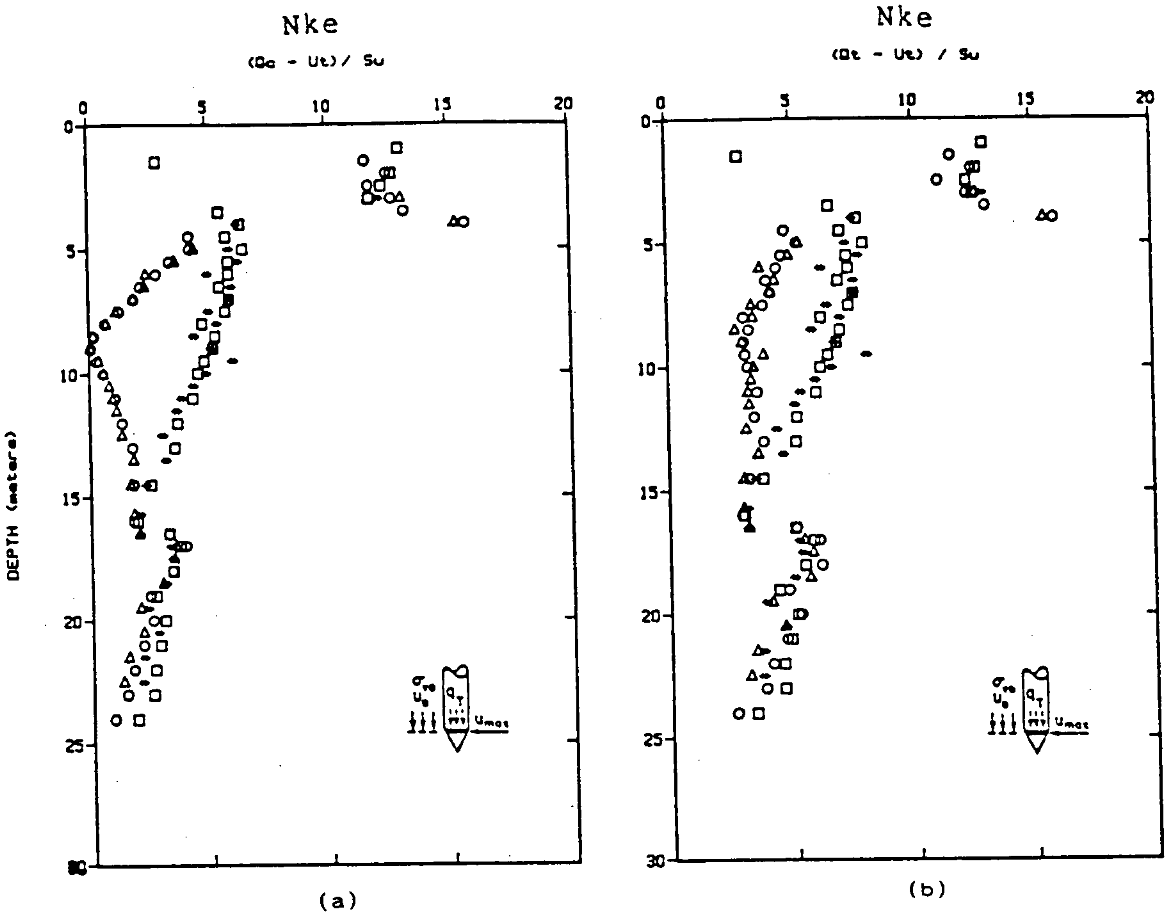

LEGEND

□ CPT 1 - VST 1
△ CPT 1 - VST 3
○ CPT 2 - VST 1
• CPT 2 - VST 3

Figure 7.29 (Qc-Ut)/Su AND (Qt-Ut)/Su vs DEPTH AT LOWER 232nd St. SITE

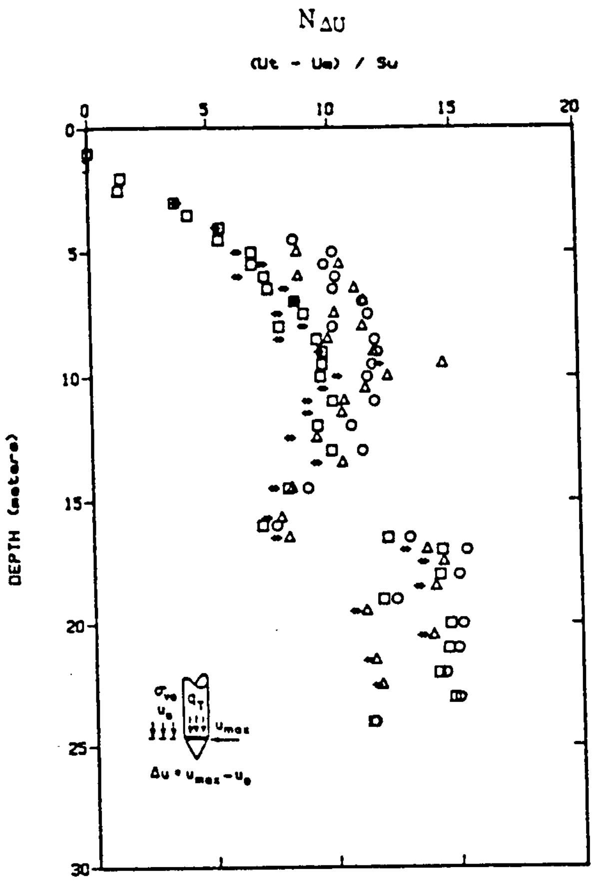

LEGEND

□ CPT 1 - VST 1
△ CPT 1 - VST 3
○ CPT 2 - VST 1
• CPT 2 - VST 3

Figure 7.30 ΔU/Su vs DEPTH AT LOWER 232nd St. SITE

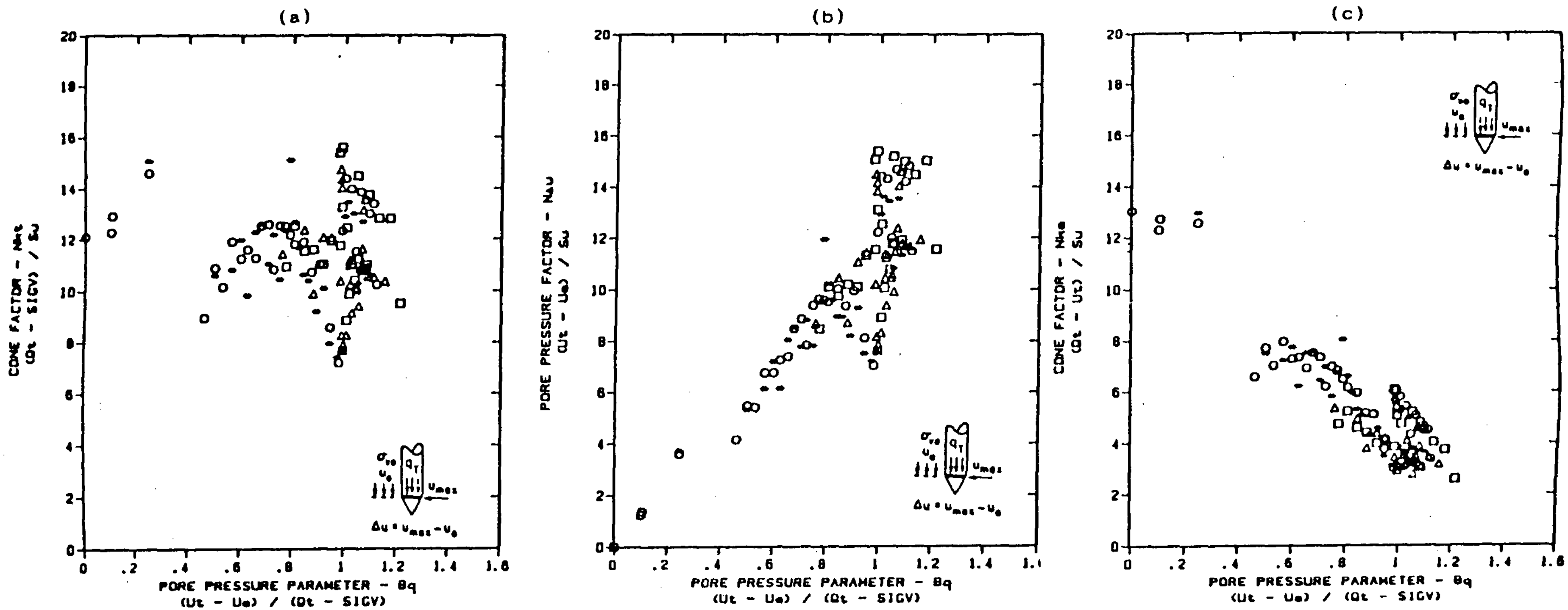

LEGEND

□ CPT 1 - VST 1
△ CPT 1 - VST 3
○ CPT 2 - VST 1
* CPT 2 - VST 3

Figure 7.31 Nkt, NΔU and Nke vs Bq AT LOWER 232nd St. SITE

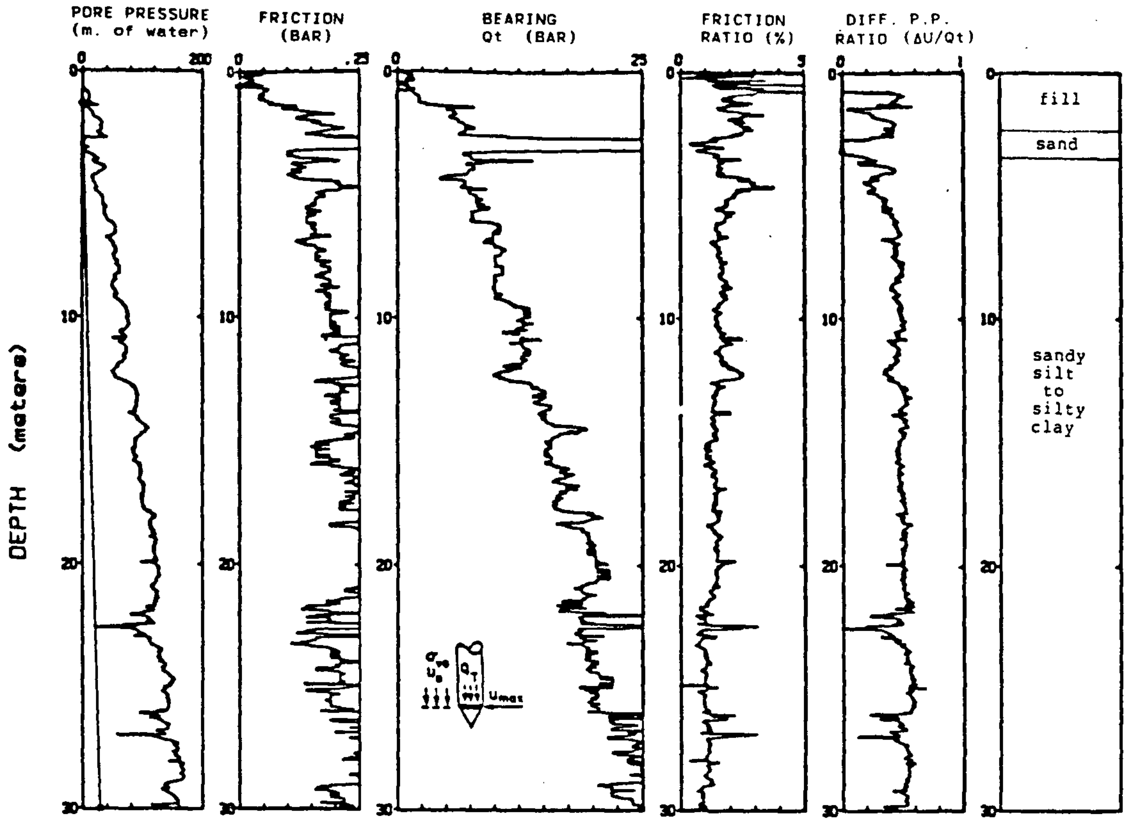

Figure 7.32 TYPICAL CPT PROFILE AT HANEY SLIDE SITE

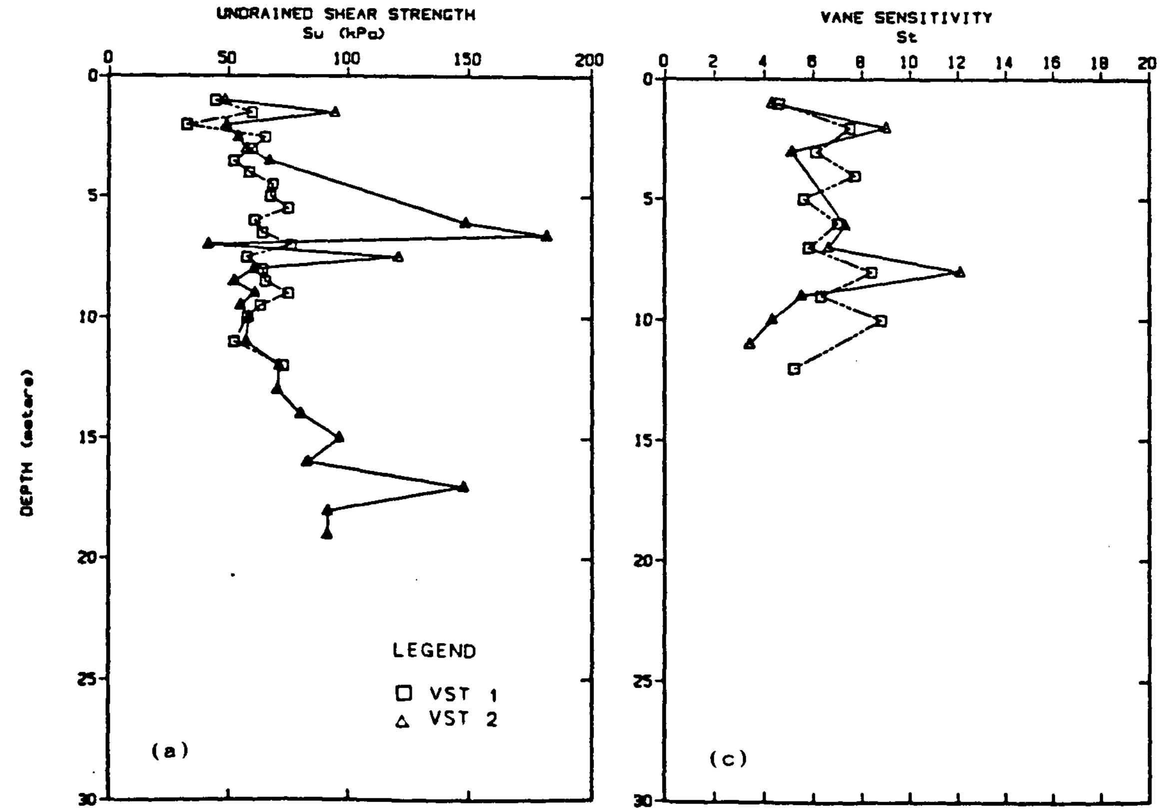

Figure 7.33 FIELD VANE STRENGTH AND SENSITIVITY PROFILES AT HANEY SLIDE SITE

0-2m fill

2-3m sand

3-30 m sandy silt to silty clay with numerous thin fine sand layers

Undrained shear strength and vane sensitivity profiles from the two VST soundings are shown in figure 7.33. The Su profile increases only slightly with depth (disregarding the data obviously influenced by sand lenses) with an average Su/P'=0.6 indicating an overconsolidated material. The OCR ranges from 9 near the surface to approximately 2.5 at a depth of 20m. OCR was calculated using the first method described in section 6.5. Sensitivity does not vary much having an average value of 6.

7.6.2 Correlations Between Su and CPT

The results of the various correlation techniques for the Haney Slide site are shown in figures 7.34 through 7.38. The cone factors Nc and Nk (figures 7.34 and 7.35) tend to increase slightly with depth and be somewhat scattered. On the other hand, the plot of Nke vs depth in figure 7.36b is uniform with depth which is consistent with the sensitivity profile. $N_{\Delta U}$ vs depth (figure 7.37) appears to be scattered, however this is likely due to the influence of the sand layers on the pore pressure response. A consistent trend is observed for $N_{\Delta U}$ vs Bq in figure 7.38b. Although the Nke data is clustered, they do seem to be in line with what has been observed at the other sites.

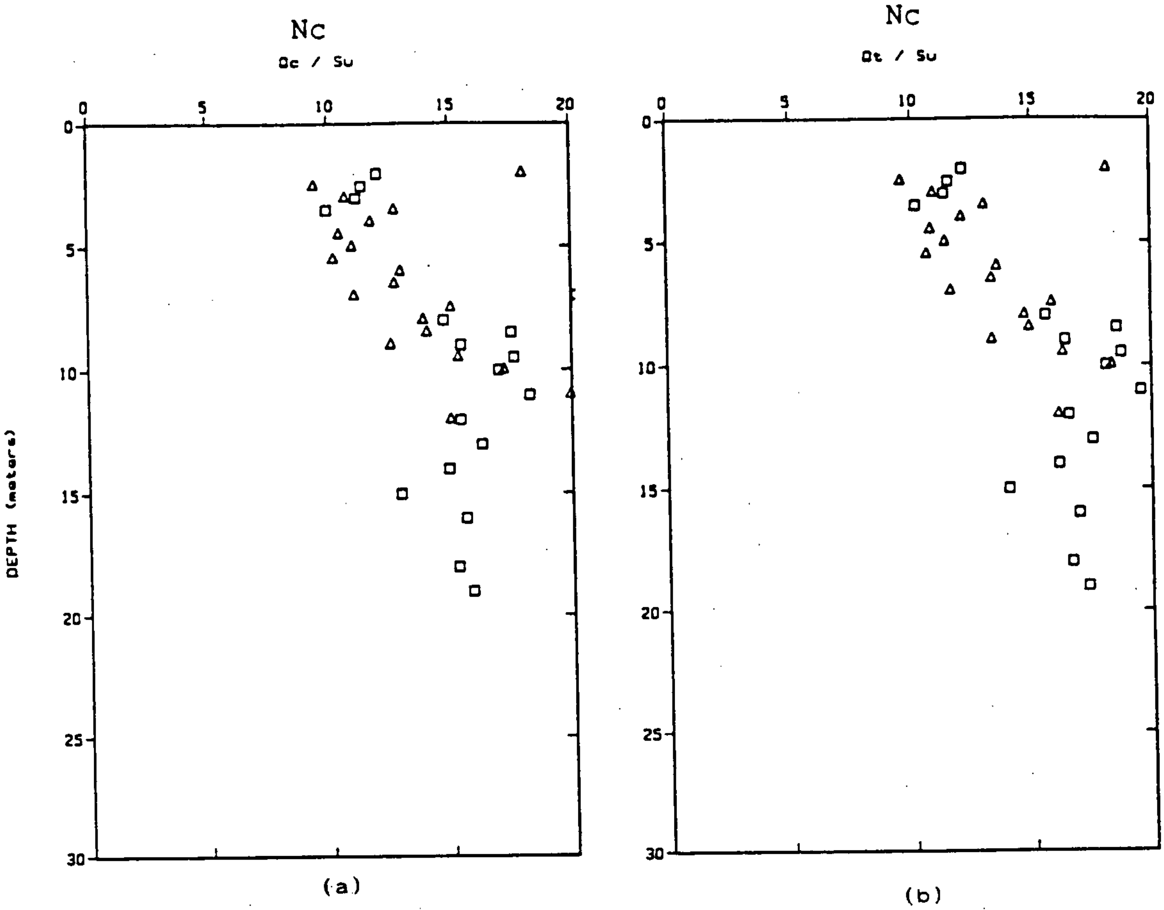

LEGEND

□ VST 1
△ VST 2

Figure 7.34 Qc/Su AND Qt/Su vs DEPTH AT HANEY SLIDE SITE

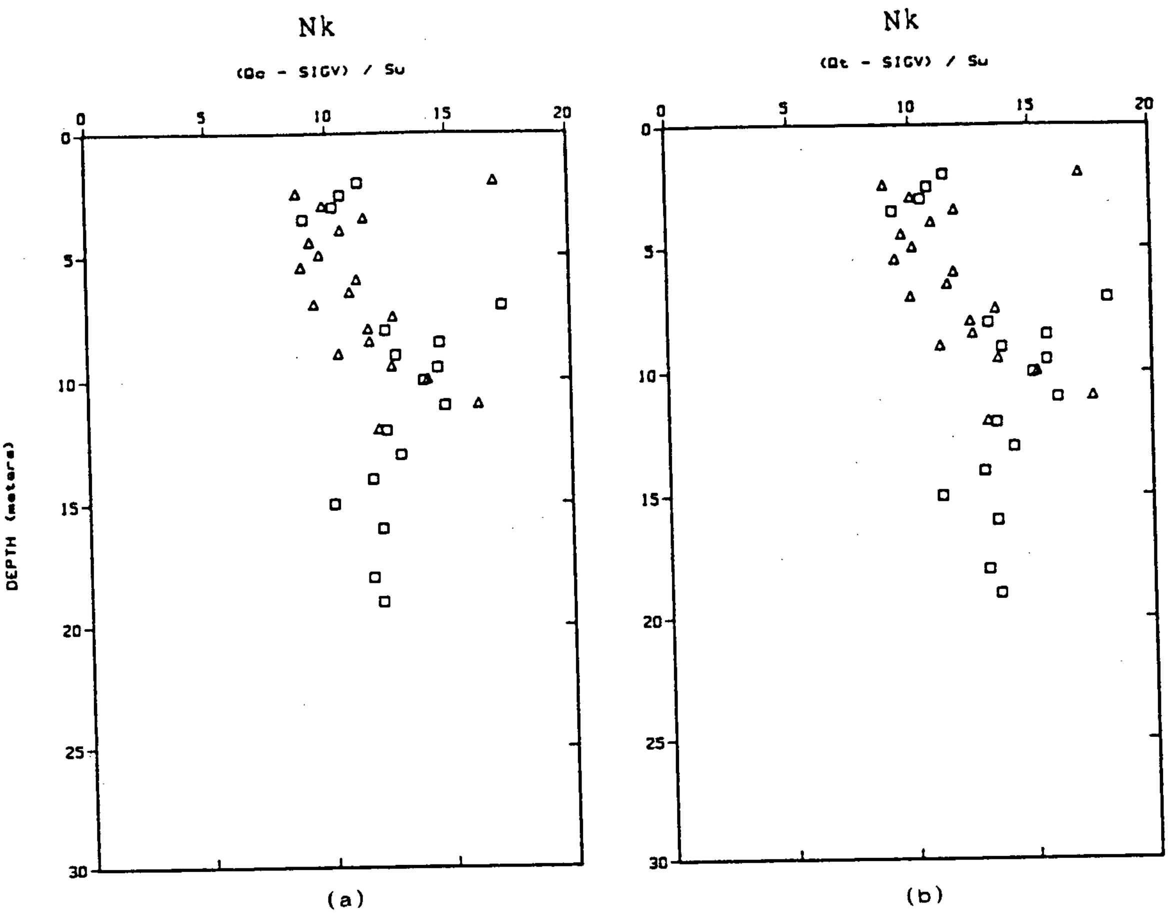

LEGEND

□ VST 1
△ VST 2

Figure 7.35 $(Qc-\sigma_{vo})/Su$ and $(Qt-\sigma_{vo})/Su$ vs DEPTH AT HANEY SLIDE SITE

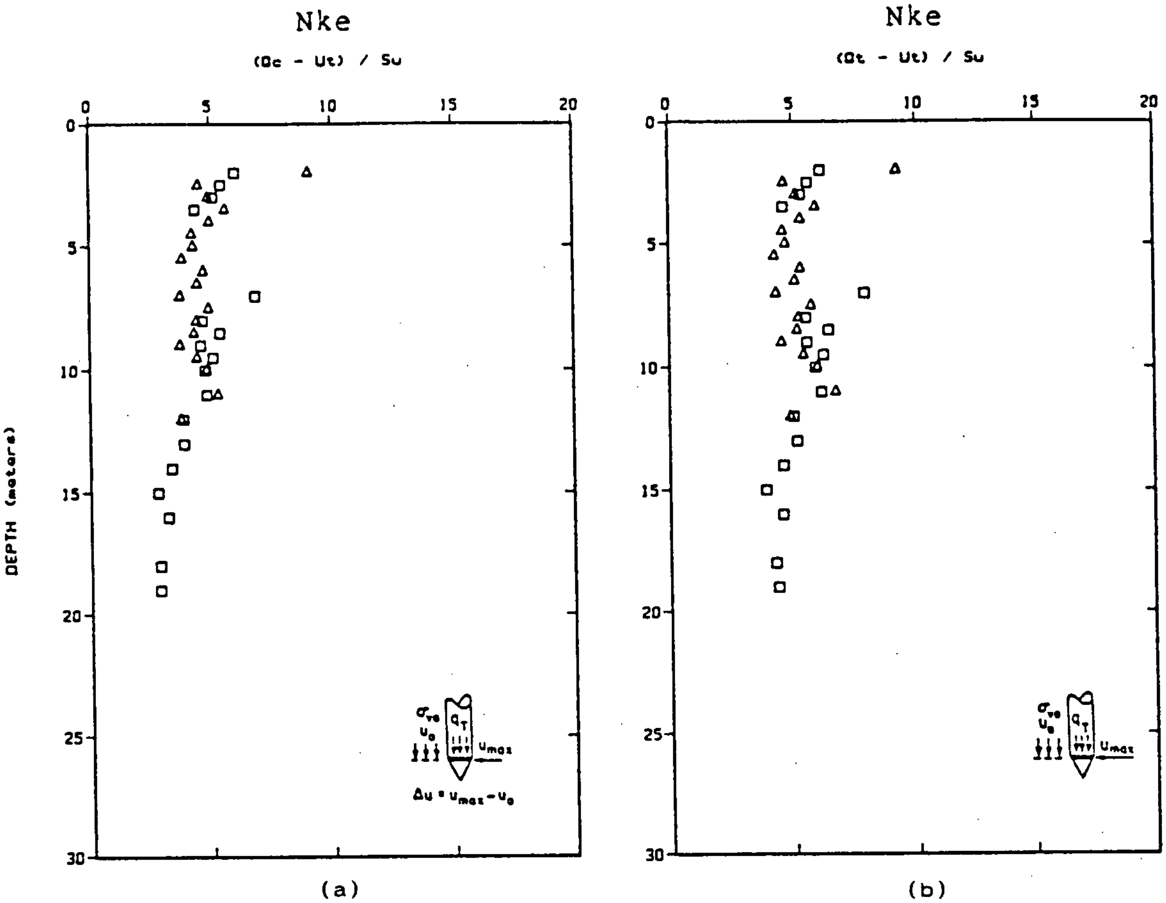

LEGEND

□ VST 1
△ VST 2

Figure 7.36 (Qc-Ut)/Su AND (Qt-Ut)/Su vs DEPTH AT HANEY SLIDE SITE

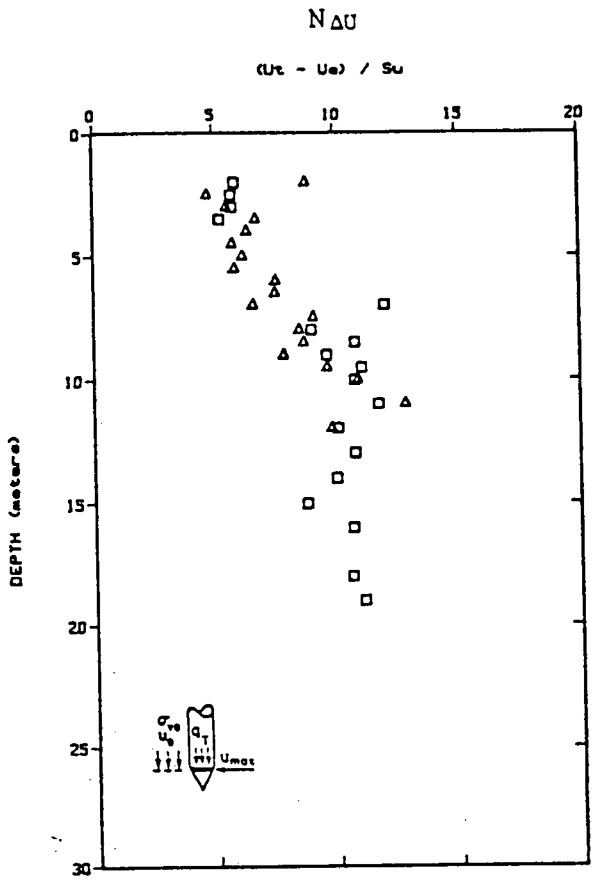

LEGEND

□ VST 1
△ VST 2

Figure 7.37 ΔU/Su vs DEPTH AT HANEY SLIDE SITE

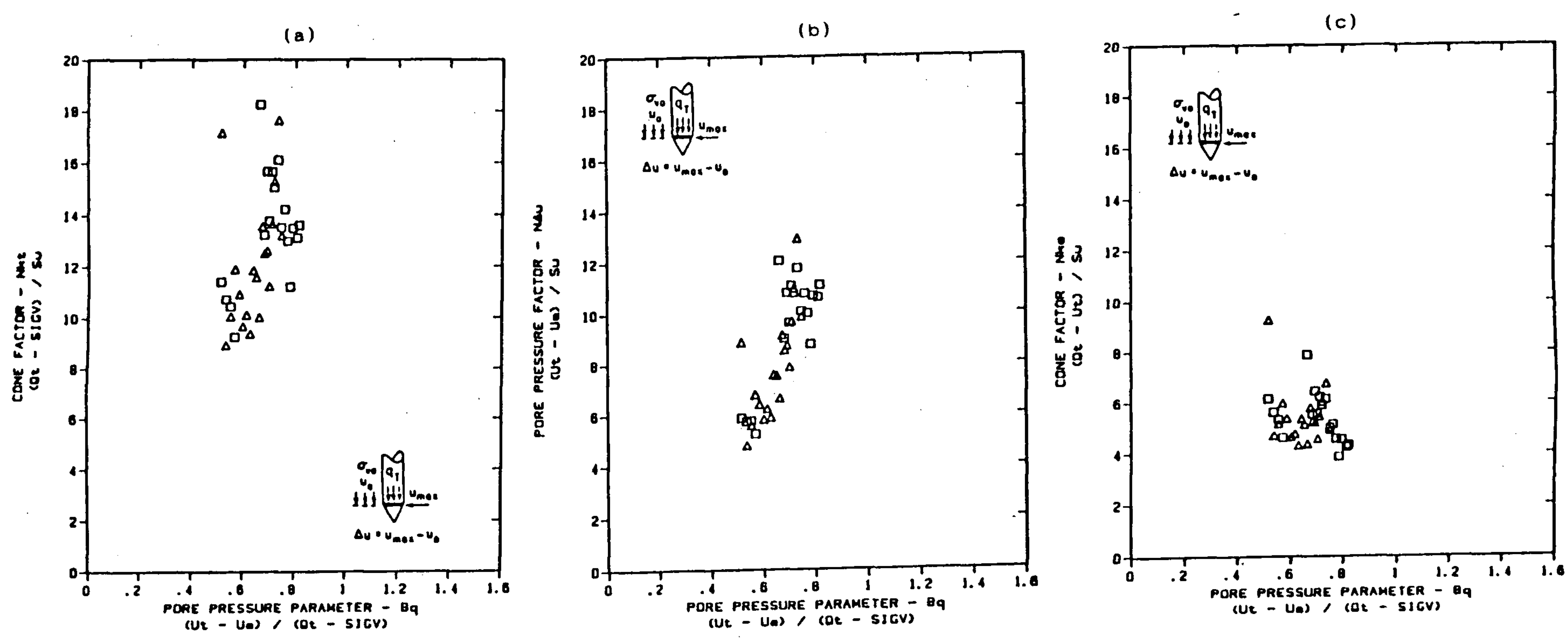

LEGEND

□ VST 1
△ VST 2

Figure 7.38 Nkt, NΔu and Nke vs Bq AT HANEY SLIDE SITE

7.7 A Summary of the Results for the Five Lower Mainland Sites

A summary of the various cone factors for the five lower mainland sites is presented in table 7.3. An average value for all the sites is given for each correlation method. Values for (Qc-Ut)/Su have been purposely left out. The results have shown that there can not be a single cone factor that is applicable to all clays. All the correlation techniques were influenced by the stress history and most notably, the sensitivity of the deposit. The dependance upon soil stiffness was not readily apparent except at the B.C. Hydro railway site, however, this is probably because the range in plasticity for the five sites was not great. The scatter in the correlations using cone bearing was reduced when the bearing was corrected for pore pressures and when overburden stress was accounted for. The scatter in the data was also caused by many other contributing factors; among them were the effects of anisotropy, variations in strain rate, stress paths, progressive failure in the vane tests, disturbance due to insertion of the instruments and the influence of sand lenses on the vane test results and the CPT bearing and pore pressure measurements.

The use of pore pressure data appears to be a promising means of estimating undrained shear strength. Figure 7.39 shows a comparison between predicted and measured Su for the normally consolidated clayey silt at the McDonald Farm site. The predicted Su was based on the method by Campanella et al. 1985, which is described in section 6.3.2. Excellent agreement was found for the predictions from the pore pressures measured

SITE	St[1]	PI[2]	Nc		Nk		Nke	$N_{\Delta U}$	
			$\frac{Qc}{Su}$	$\frac{Qt}{Su}$	$\frac{Qc-\sigma_{vo}}{Su}$	$\frac{Qt-\sigma_{vo}}{Su}$	$\frac{Qt-Ut}{Su}$	$\frac{\Delta U}{Su}$[3]	$\frac{\Delta U}{Su}$[4]
McDONALD FARM	5	15	11.9	13.9	6.1	8.1	3.5	7.4	8.8
B.C. HYDRO RAILWAY	9	24	15.4	18.9	11.6	14.3	6.3	10.3	
UPPER 232nd St.	8	19	11.0	13.3	5.8	8.1	2.5	8.9	
LOWER 232nd St.	14	19	16.7	18.3	9.8	11.3	5.9	8.9	
HANEY SLIDE	6	18	14.2	15.0	16.0	12.7	5.4	8.6	
ALL SITES			14.2	16.0	8.5	10.3	4.7	8.6	

1 - average sensitivity
2 - average plasticity index
3 - pore pressure measured behind the tip
4 - pore pressure measured on the face

Table 7.3 SUMMARY OF CONE FACTORS FOR 5 LOWER MAINLAND SITES

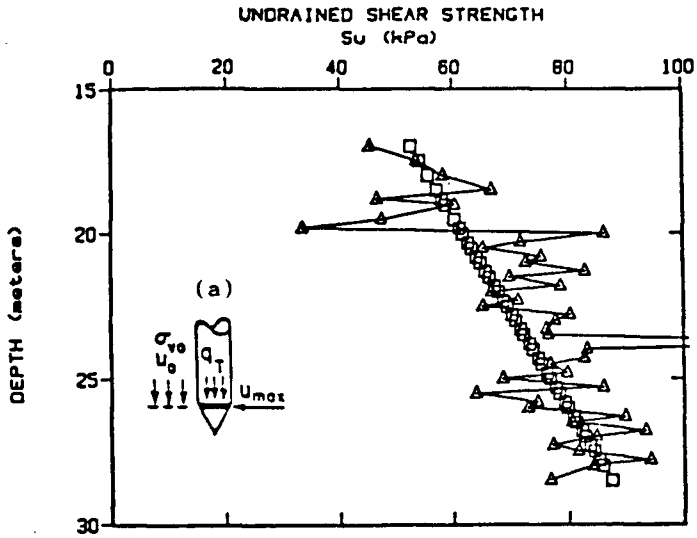

McDONALD FARM

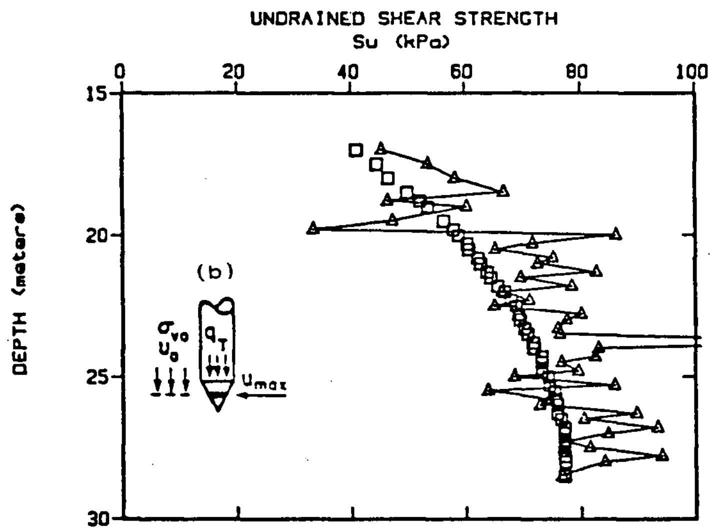

LEGEND

△ Vane Su
□ Predicted Su

Figure 7.39 USE OF EXCESS PORE PRESSURE FOR ESTIMATING UNDRAINED SHEAR STRENGTH behind the tip (cylindrical cavity expansion approach) as well as for those measured on the face (spherical cavity expansion approach).

Figures 7.40 through 7.43 show the approach adopted by Lunne et al. 1985 applied to all five of the lower mainland sites. The variation of Bq with OCR is illustrated in figure 7.40 and shows that the pore pressure parameter decreases with increasing OCR. There is considerable scatter in the data indicating that Bq is not solely affected by stress history. The plot of Nkt vs Bq for all five sites in figure 7.41 indicates that there is no discernible correlation between Nkt and Bq. A more promising correlation is that between $N_{\Delta U}$ and Bq shown in figure 7.42. A regression analysis of the data indicates a correlation coefficient of 0.69. The best correlation was between Nke and Bq as shown is figure 7.43. A correlation coefficient of 0.81 was determined from the data for the five sites. This writer again points out the difficulties one may have in calculating Qn, (Qt-Ut). Bearing and pore pressure values are very similar in soft normally consolidated soils and a loss of accuracy in the bearing can significantly affect the calculation of Nke. This should not present a problem, however, since a prudent engineer is unlikely to rely on a single correlation method, particularly when there are several techniques available.

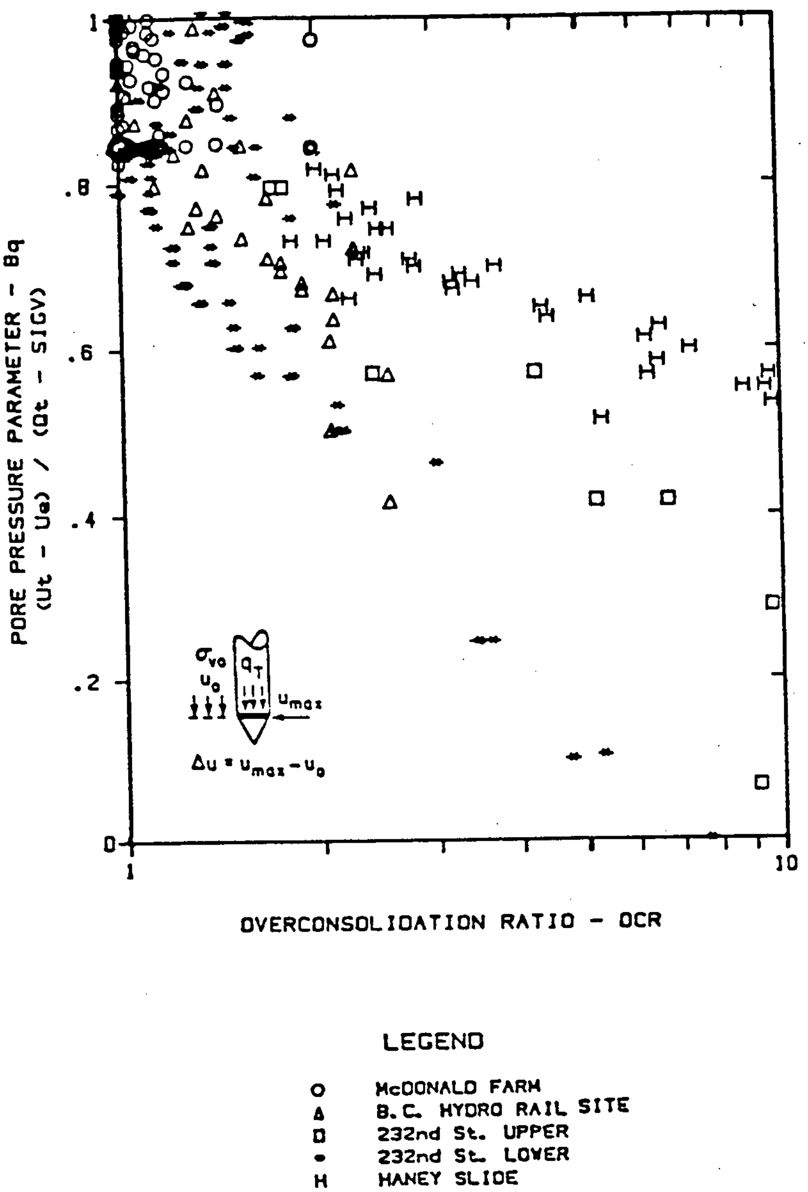

Figure 7.40 Bq vs OCR FOR 5 LOWER MAINLAND SITES

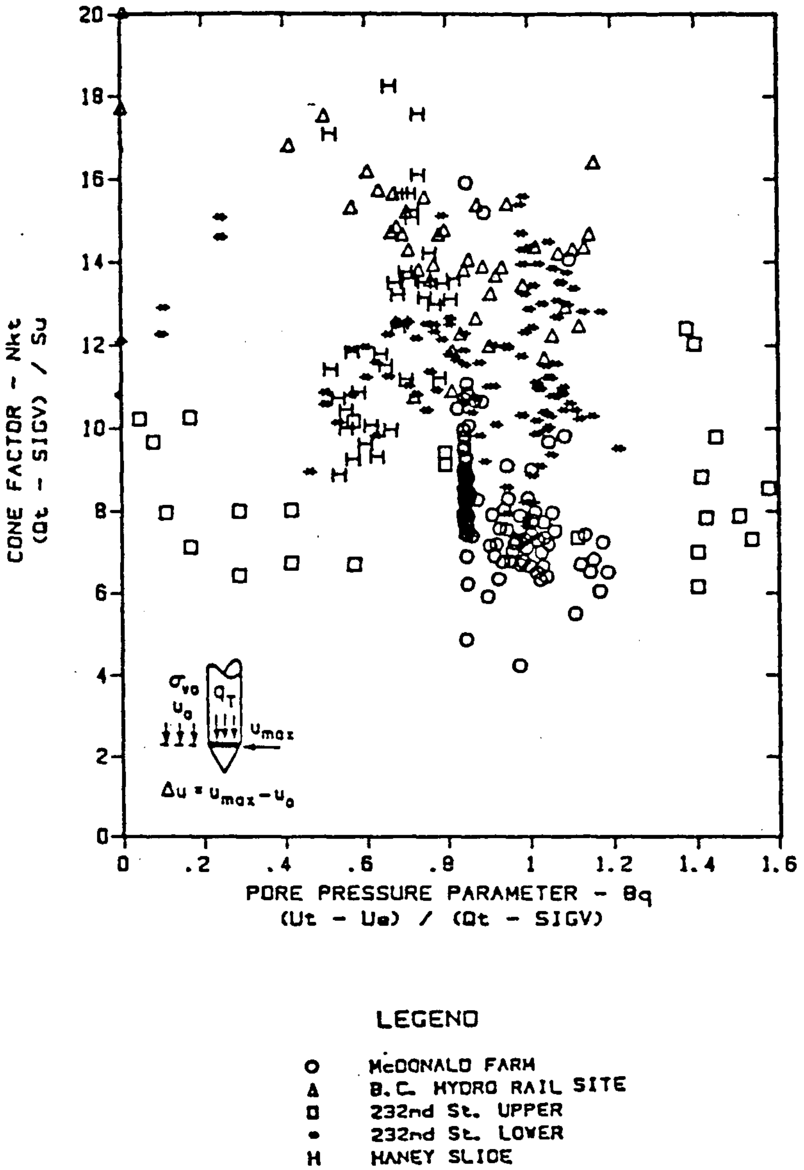

Figure 7.41 Nkt vs Bq FOR 5 LOWER MAINLAND SITES

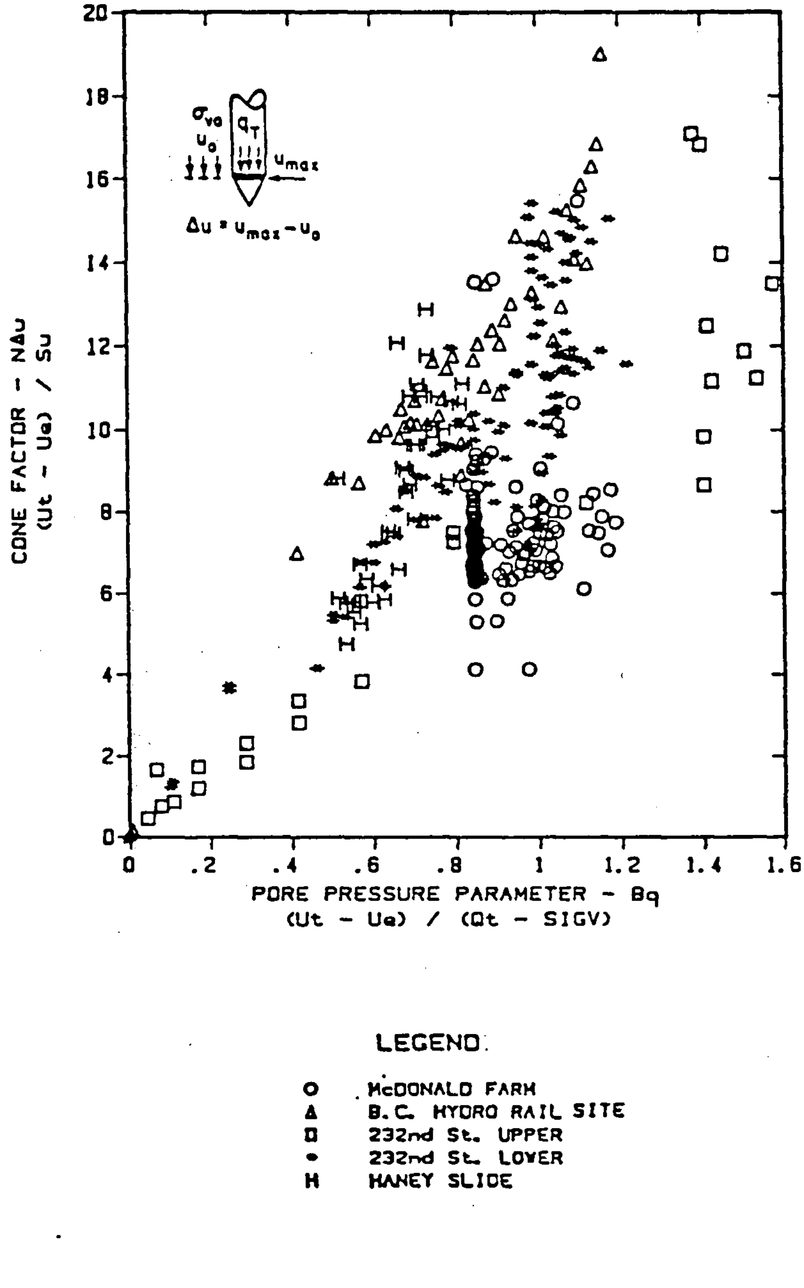

Figure 7.42 $N_{\Delta U}$ vs Bq FOR 5 LOWER MAINLAND SITES

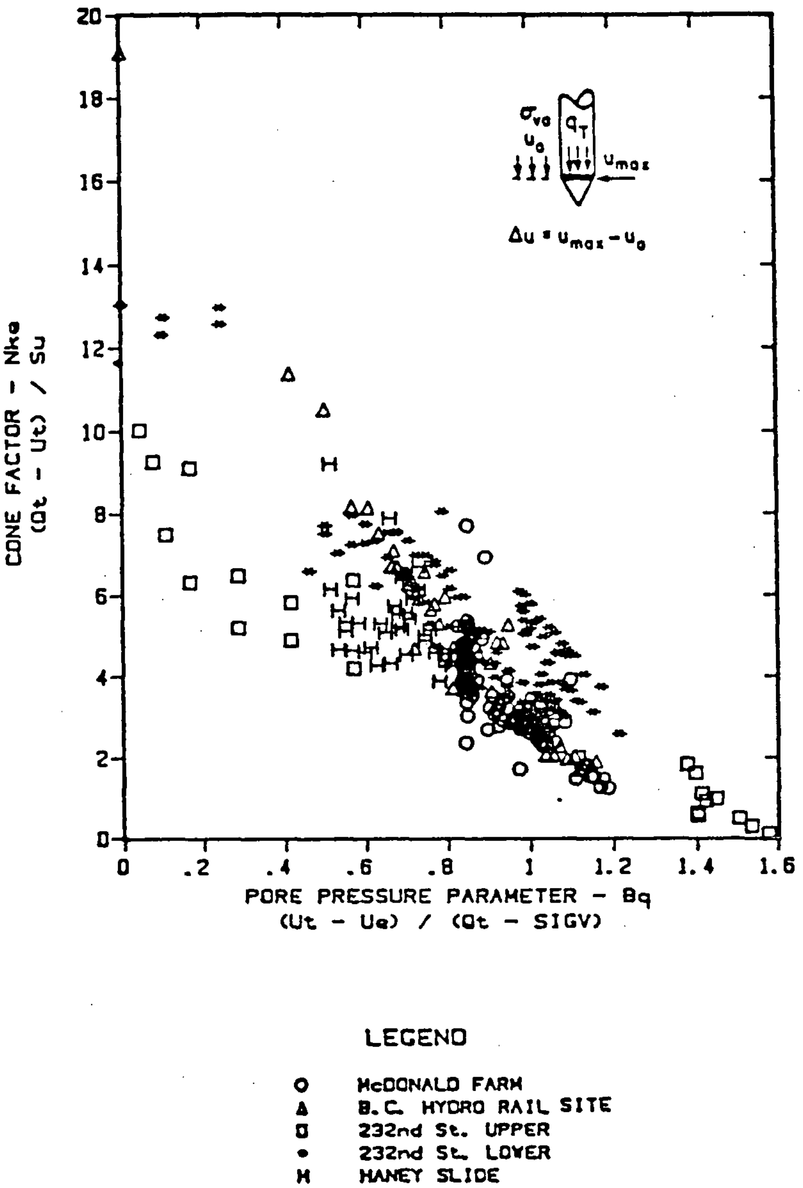

Figure 7.43 Nke vs Bq FOR 5 LOWER MAINLAND SITES

7.8 Correlations Between Su and Sleeve Friction

Figures 7.44 and 7.45 compare friction sleeve measurements to peak vane shear strength, Su. Figures 7.46 and 7.47 compare sleeve friction to remolded shear strength, Sur. Figure 7.44 shows that a reasonable estimate of Su can be made using Su/Fs=5.3, however, there is considerable deviation from this relationship, particularly at shallow depths (figure 7.45). This may be partly due to the low stresses that the friction sleeve experiences. At shallow depths the total force on the sleeve is around 4 kg to 10 kg whereas the capacity of the friction load cell is 1500 kg. Figures 7.46 and 7.47 indicate that the friction measurement is closer to the remolded shear strength of the soil. Neglecting the scatter at shallow depths, the average ratio of Sur to Fs is 1. A summary of Su/Fs and Sur/Fs for the different sites is given in table 7.4.

7.9 Estimating Sensitivity from CPT

It was reported in section 6.6 that a rough estimate of sensitivity could be made from

$$St = \frac{10}{Rf\%} \qquad 6.10$$

Figure 7.48a shows a plot of St·Rft (Rf calculated using corrected bearing Qt) against depth for four of the sites with an average value of 8.1. Again there is some scatter at shallow depths. Neglecting this, the best estimate of St can be made from 6/Rft.

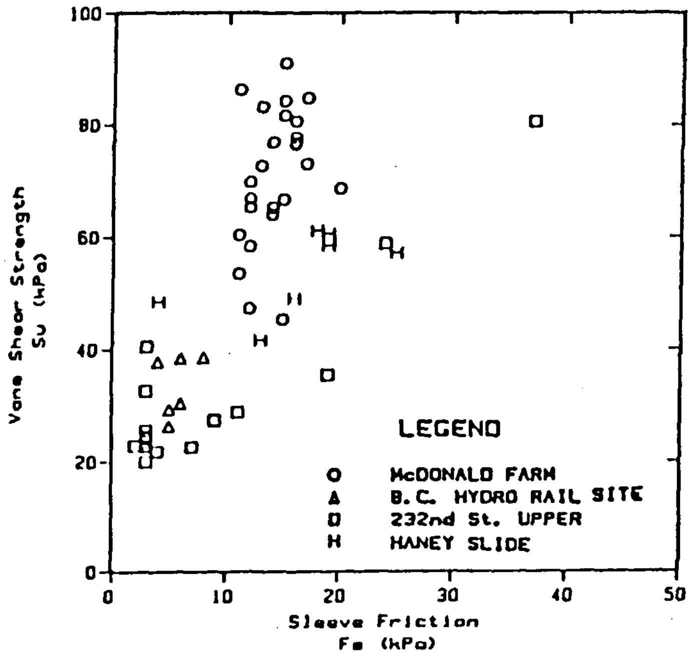

Figure 7.44 VANE SHEAR STRENGTH vs SLEEVE FRICTION FOR 4 LOWER MAINLAND SITES

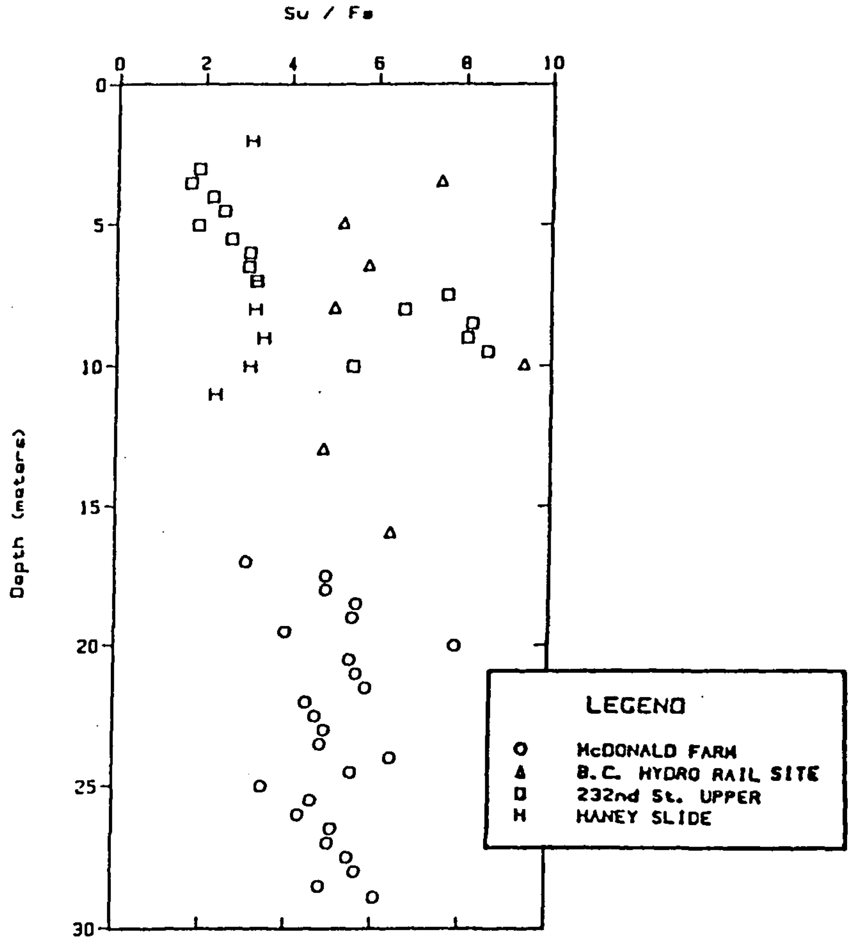

Figure 7.45 Su/Fs vs DEPTH FOR 4 LOWER MAINLAND SITES

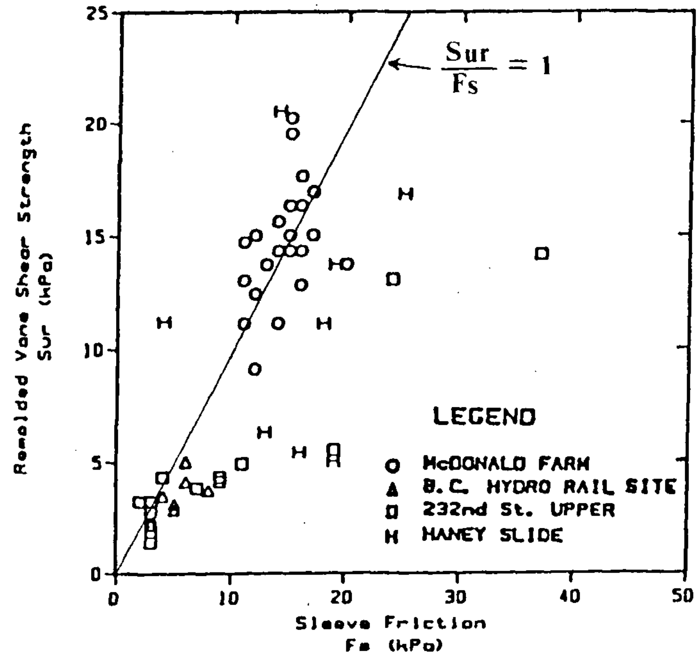

Figure 7.46 REMOLDED SHEAR STRENGTH vs SLEEVE FRICTION FOR 4 LOWER MAINLAND SITES

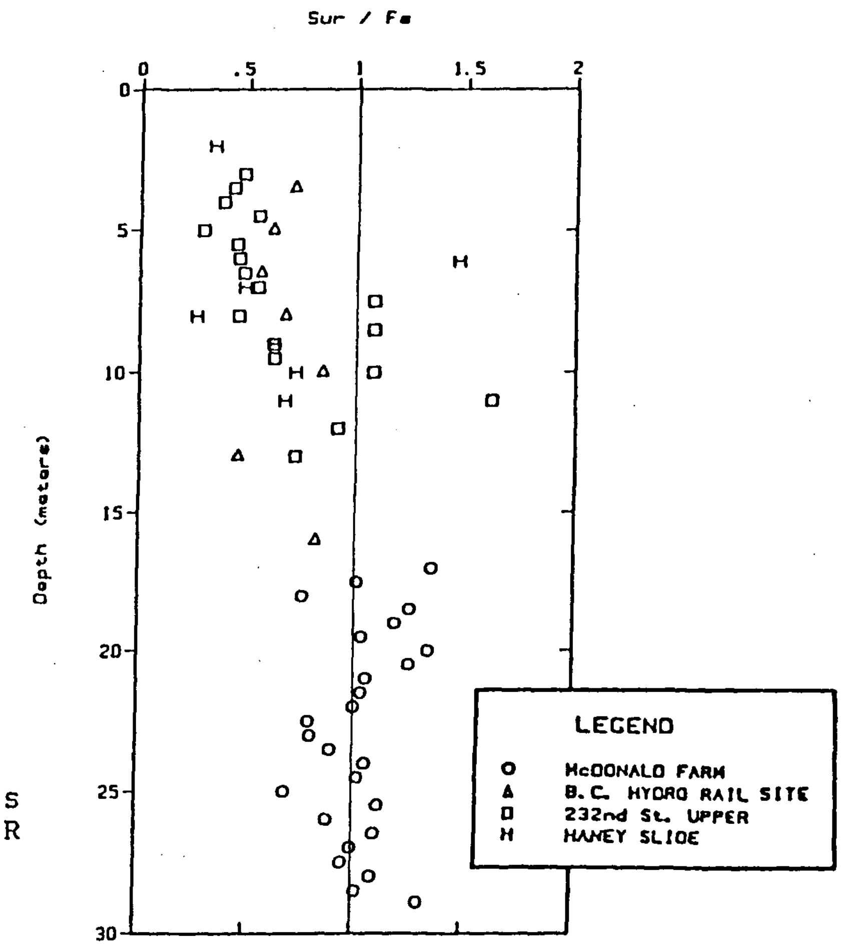

Figure 7.47 Sur/Fs vs DEPTH FOR 4 LOWER MAINLAND SITES

SITE	St[1]	PI[2]	$\frac{Su}{Fs}$	$\frac{Sur}{Fs}$	$\frac{St\ Rft^{3}}{Fs}$	$\frac{Qt-\sigma_{vo}}{Fs \cdot St}$
McDONALD FARM	5	15	5.1	1.0	6.1	10.8
B.C. HYDRO RAILWAY	9	24	5.2	0.67	8.4	9.1
UPPER 232nd St.	8	19	5.7	0.60	9.2	16.5
HANEY SLIDE	6	18	5.1	0.92	12.0	9.0
ALL SITES			5.3	0.84	8.1	12.1

1 - average sensitivity
2 - average plasticity index
3 - friction ratio calculated using corrected cone bearing Qt

Table 7.4 SUMMARY OF CORRELATIONS WITH FRICTION SLEEVE DATA FOR 4 LOWER MAINLAND SITES

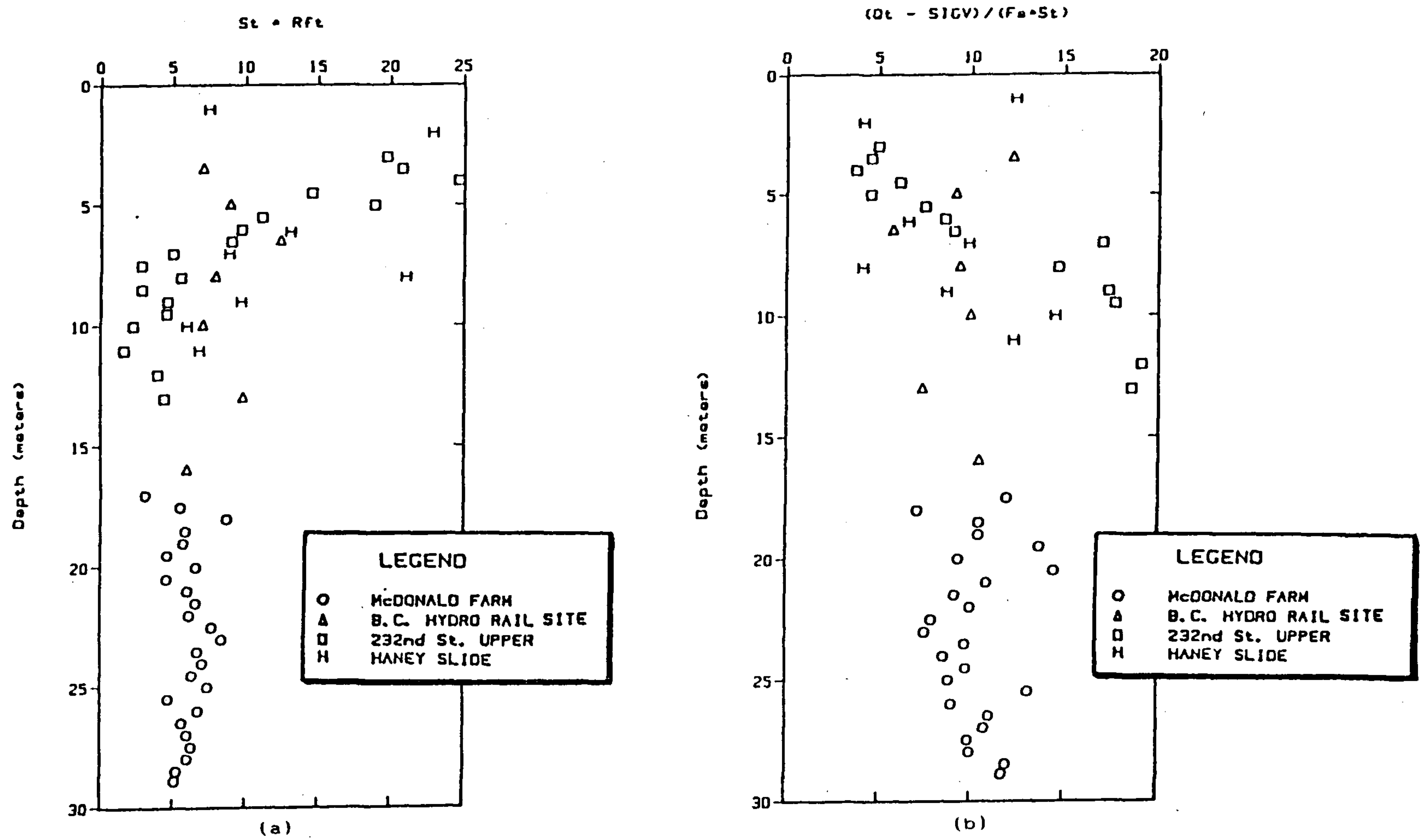

Figure 7.48 ESTIMATING SENSITIVITY FROM CPT

Expression 6.10 neglects the effect of overburden stress. Assuming Fs is close to Sur it may be possible to estimate St from

$$St = \frac{Qn}{Nst \cdot Fs} \qquad 7.1$$

where St - sensitivity
Nst - factor for estimating St
Qn - net bearing; Qt- Ut
Fs - sleeve friction

A plot of Qn/(Fs·St) for four sites is shown in figure 7.48b having an average value of 11 (neglecting scatter). However, there is considerably more scatter using this method than there is using St=6/Rft. A summary of these two methods is given in table 7.4.

CHAPTER 8

SUMMARY AND CONCLUSIONS

8.1 Summary of Factors Influencing the Estimation of Su

This paper has discussed the results of field vane and cone penetration tests from five lower mainland sites in relation to several proposed methods of estimating Su from CPT. The results have shown that there is no unique method for estimating Su from CPT for all clays. Furthermore, the estimation of Su from CPT is heavily influenced by various factors relating to:

1) material type and soil characteristics
2) cone design and CPT test procedures
3) the choice of a reference Su

The choice of a reference Su is significant because Su is not a unique parameter. It depends on the type of test used, the rate of strain and the orientation of the failure planes. The likely variation in Su for various test methods was illustrated in chapter 1 and was the reason for selecting a single test method (field vane) as a reference for this investigation. The use of different reference shear strengths also makes comparisons between results reported in the literature difficult.

The undrained shear strength determined from field vane tests is also influenced by several factors such as strength anisotropy, rate effects, soil disturbance, delays between vane insertion and the start of shearing, the assumed shear stress distribution and the method of analysis. Recent work has shown that the standard analysis is likely incorrect. However, with our present lack of complete understanding of the VST it is best that we continue to use the method for which we have the greatest experience; using a vane of H/D=2 and analysing the data using the standard equation:

Essential to the correlation of Su with CPT is confidence and accuracy in the CPT data. One must understand the limitations of the instrument and their effects on the test results. The cone bearing can suffer accuracy problems in soft normally consolidated clays because the tip load cell is often only stressed from 1% to 3% of its capacity. A further loss of accuracy can occur if pore pressure effects on the cone bearing and sleeve friction are neglected. It is also essential that zero load readings be checked before and after a profile in order to determine whether drifts have occurred in the electronics. Drifts due to temperature have been observed; the effects of which can be substantial as was shown in chapter 3.

Complete and proper saturation of the pore pressure measuring system is required to ensure high quality pore pressure data. Chapter 5 illustrated that pore pressures measured at different locations on the cone can be radically different depending on the type of material in which the test is made. This behaviour must be recognized in order to properly make pore pressure corrections and to compare CPT results. Pore pressure corrections to bearing must be made using pore pressures measured behind the tip.

Despite these problems, the cone penetration test has proved to be unequalled in its ability to identify soil layer boundaries and qualitatively evaluate material types. Layers as thin as 1 cm have been detected by the cone bearing, however, the estimation of layer thickness is complicated by the sampling rate. Significant to the estimation of undrained shear strength is the influence that the surrounding layers have on the tip resistance. A zone of influence extends about 5 to 10 cone diameters ahead and behind the tip depending on the relative stiffness of the layers. This effect can cause a bearing value to be recorded that does not truely represent the material being tested. However, this effect is more pronounced in stiffer soils than in soft layers.

The estimation of Su from CPT appears to be strongly influenced by such soil properties as stress history, sensitivity and stiffness. The results presented in chapter 7 indicated that increases in OCR and sensitivity were reflected by increases in the traditional cone factors Nc and Nk. At the B.C. Hydro railway site the cone factors also increased with decreasing plasticity index (with OCR and sensitivity essentially constant). Considerable scatter was often observed but was minimized when pore pressure effects and overburden stress were accounted for. It is clear that there is no unique value for the traditional cone factor Nk that is applicable to all clays.

The use of pore pressure data appears to be a promising means of estimating Su from CPT. Expressions have been developed that predict the excess pore pressures based on cavity expansion theory. They attempt to include the effects of sensitivity and stress history through the use of Skempton's pore pressure parameter Af. The effects of soil stiffness is included by using the rigidity index G/Su. A spherical cavity expansion approach should be used for pore pressures measured on the face and a cylindrical approach for those measured behind the tip. The method of Campanella et al. 1985 appears to work well, particularly in normally consolidated deposits. Correlations between $N_{\Delta U}$ and Bq and Nke and Bq look promising and should be investigated further with data from other sites.

8.2 Conclusions

This section presents the most important conclusions regarding the factors that affect the estimation of Su from CPT.

8.2.1 Accuracy of CPT Data

Attention to the follwing details in test and data reduction procedures are essential in order to obtain meaningful results.

i) bearing must be corrected for pore pressure and temperature effects

ii) friction measurements must be corrected for the effects of unequal end areas and temperature

iii) pore pressures must be measured behind the tip in order to properly correct the bearing and friction for pore pressure effects

iv) all cone channels should be calibrated for temperature effects

v) complete saturation of the pore pressure measuring system is essential

vi) porous elements should have an average pore size of at least 100 microns to prevent clogging

vii) zero load readings must be checked before and after a profile to detect zero shifts

8.2.2 Influence of Layer Boundaries

i) the cone bearing is influenced by surrounding soil layers, however this effect is more significant in coarse grained materials

ii) the cone bearing will not reach its full resistance in thin (less than from 5 to 10 cone diameters thick) layers of sand

iii) thinner layers of clay are required to record the true bearing

iv) the valleys in the bearing record should be used for estimating the undrained strength in cohesive deposits

8.2.3 Detection of Thin Layers

i) layers of the order 10cm thick are easily detected by the tip resistance

ii) it may be possible to detect layers as thin as 1cm, however, the material properties of this thin layer would have to be considerably different from the surrounding soil to be detected

iii) estimating the thickness of a layer is highly dependent on the sampling rate

iv) the estimation of layer thickness for layers thinner than the sampling rate is highly speculative and can often be in error

v) sampling at discrete intervals can also lead to subdued peaks in the CPT profile

8.2.4 Estimating Su from Cone Bearing

i) the estimation of Su from CPT is strongly influenced by stress history, sensitivity and stiffness

ii) increases in OCR and senstivity resulted in increases in the traditional cone factors Nc and Nk

iii) the cone factors also increased with decreasing plasticity index (i.e. increasing soil stiffness)

iv) scatter in the cone factor was minimized when pore pressure effects and overburden stress were accounted for

v) there is no unique value for the traditional cone factor Nk that is applicable to all clays

8.2.5 Using CPT Pore Pressure Data to Estimate Su

i) the use of pore pressure data appears to be a promising means of estimating Su from CPT

ii) the method of Campanella et al. 1985 (figure 6.5) appears to work well, particularly in normally consolidated deposits

iii) when using a cavity expansion approach, spherical cavity expansion methods should be used for pore pressures measured on the face and cylindrical cavity expansion for those measured behind the tip

iv) the pore pressure parameter Bq decrease with increasing OCR, but there is no unique realtionship between Bq and OCR since Bq is also a function of sensitivity and soil stiffness

v) there is no discernible relation between Nkt and Bq

vi) there appears to be fairly consistent relationships between $N_{\Delta u}$ and Bq and between Nke and Bq

vii) the best correlation is between Nke and Bq, however, unless careful attention is paid to the details discussed in section 8.2.1 considerable error in the calculation of Nke can result

8.2.6 Use of Friction Sleeve Measurements

Comparisons between friction sleeve measurements and Su indicate that the sleeve friction is close to the remolded shear strength Sur, particularly in sensitive soils.

Estimates of sensitivity (field vane) were best made using

$$St = \frac{6}{Rft\%}$$

where the friction ratio Rft has been calculated using bearing and friction corrected for pore pressure effects.

8.3 Recommended Procedures for Estimating Su from CPT

The fact that Su and CPT correlations can be affected by many various parameters indicates that a single method can not work in all clay types. The engineer should not rely on a single method but instead should use a variety of methods to determine the best estimate of Su. Where possible, it is best that local correlations be used.

The following describes recommended procedures for estimating Su from CPT.

8.3.1 Use of CPT Data Without Pore Pressures

It is not recommended that CPT data be used that does not include pore pressures. The variation in Nc and Nk is too great and without pore pressures there is no alternate method for confirming the appropriate cone factor. An estimate of the appropriate cone factor would have to be made from tables 6.1, 6.2, or 7.3 or from figures 6.1, 6.2, or 7.41. An knowledge of PI, sensitivty and OCR would be helpful. Sensitivity can be estimated from the friction ratio and OCR can be estimated from the site geology or the cone bearing.

8.3.2 Use of CPT Data With Pore Pressures

To make use of a combination of the various proposed methods of correlation an iterative approach can be used. This can be done using the following steps:

1) Estimate Sensitivity (St) from Rf (friction ratio)

2) Estimate OCR from Bq (figure 7.40), site geology, or

cone bearing

3) knowing St and OCR estimate Af

4) Estimate G/Su from PI using figure 6.4

5) from figure 6.5 estimate $N_{\Delta u}$

6) Compare this value with $N_{\Delta u}$ obtained from figure 7.42 using Bq

7) Iterate until the $N_{\Delta u}$ values are compatibale

8) Using $N_{\Delta u}$ estimate Su

9) check the estimate of Su against those estimated from Nke (using Bq and figure 7.43) and Nkt (using table 7.3 or figure 7.41)

REFERENCES

Aas, G., 1965. "A Study of the Effect of Vane Shape and Rate of Strain on the Measured Values of In-Situ Shear Strength of Clays", Proceedings of the Sixth International Conference on Soil Mechanics and Foundation Engineering, Vol. 1, pp.141-145.

Aas, G. 1967. "Vane Tests for Investigation of Anisotropy of Undrained Shear Strength of Clays", Proceedings of the Geotechnical Conference at Oslo, Norway, Vol. 1, pp. 3-8.

Arman, A., J.K. Poplin and N. Ahmad, 1975. "Study of the Vane Shear", Proceedings of the ASCE Conference on In-Situ Measurement of Soil Properties, Raleigh, North Carolina, Vol. 1, pp.93-120.

Armstrong, J.E., 1978. "Post Vachon Wisconsin Glaciation, Fraser Lowland, British Columbia", Geological Survey of Canada, Bulletin 332.

Azzouz, A.S., M.M. Baligh and C.C. Ladd, 1983. "Corrected Field Vane Strength for Embankment Design", Journal of the Geotechnical Engineering Division, ASCE, Vol. 109, No. 5,pp. 730-734.

Baligh, M.M., 1975. "Theory of Deep Site Static Cone Penetration Resistance", Report No. R 75 - 56, Department of Civil Engineering, Massachusetts Institute of Technology.

Baligh, M.M., V. Vivatrat, and C.C. Ladd, 1979. "Exploration and Evaluation of Engineering Properties for Foundation Design of Offshore Structures", M.I.T. Sea Grant College Program Report Mo. MITS 79 - 8, M.I.T.

Begemann, H.K., 1965. "The Friction Jacket Cone as an Aide in Determining the Soil Profile", Proceedings of the Sixth International Conference on Soil Mechanics and Foundation Engineering, Vol. 1, pp. 17-20.

Berre, T. and L. Bjerrum, 1973. "Shear Strength of Normally Consolidated Clays", Proceedings of the Eighth International Conference on Soil Mechanics and Foundation Engineering, Moscow, U.S.S.R., Vol. 1.1, pp. 39-49.

Bjerrum, L., 1972. "Embankments on Soft Grounds", ASCE Proceedings of the Specialty Conference on Performance of Earth and Earth-Supported Structures, Vol. 2, pp. 1-54.

Bjerrum, L., 1973. "Problems of Soil Mechanics and Construction on Soft Clays and Structurally Unstable Soils (Collapsible, Expansive and Others)", Proceedings of the Eighth International Conference on Soil Mechanics and Foundation Engineering, Moscow, U.S.S.R., Vol. 3, pp. 111-159.

Bjerrum, L. and N. Flodin, 1960. "Development of Soil Mechanics in Sweden, 1900-1925", Geotechnique 10, No. 1, pp. 1-18.

Blight, G.E., 1968. "A Note on Field Vane Testing of Silty Soils", Canadian Geotechnical Journal, Vol. 3, No. 3, pp. 142-149.

Brand, E.W., Z.C. Moh and P. Wironjanagud, 1974. "Interpretation of Dutch Cone Tests in Bangkok Clay", Proceedings of the European Symposium on Penetration Testing, Stockholm, Sweden, Vol. 2, pp. 51-58.

Cadling, L. and S. Odenstad, 1950. "The Vane Borer. An Apparatus for Determining the Shear Strength of Clay Soils Directly in the Ground", R. Swedish Geotechnical Institute Proceedings No. 2, Stockholm, Sweden.

Campanella, R.G. and P.K. Robertson, 1981. "Applied Cone Research", Symposium on Cone Penetration Testing and Experience, Geotechnical Engineering Division, ASCE, October, pp. 343-362.

Campanella, R.G. and P.K. Robertson, 1982. "State of the Art in In-Situ Testing of Soils: Developments Since 1978", Engineering Foundation Conference on Updating Subsurface Sampling of Soils and Rocks and Their In-Situ Testing, Santa Barbara, California.

Campanella, R.G. and P.K. Robertson, 1984. "A Seismic Cone Penetrometer to Measure Engineering Properties of Soil", Submitted to Society of Exploration Geophysics Meeting, Atlanta Georgia.

Campanella, R.G., P.K. Robertson, D.G. Gillespie, and J. Greig, 1985. "Recent Developments in In-Situ Testing of Soils", Proceedings of the Eleventh International Conference on Soil Mechanics and Foundation Engineering, San Francisco, California.

Cleveland, E.P., 1971. "Use of the Dutch Cone Penetration Test for Soil Exploration in Kentucky", M.Sc. Thesis, University of Kentucky, Kentucky.

Davies, P.M., 1985. "Application of the Piezometer Cone Penetration Test to Slope Stability Evaluation Focus: Haney Slide", B.A.Sc. Thesis, University of British Columbia, Vancouver, Canada.

Donald, I.B., D.O. Jordan, R.J. Parker, and C.T. Toh, 1977. "The Vane Test-A Critical Appraisal", Proceedings of the Ninth International Conference on Soil Mechanics and Foundation Engineering, Tokyo, Japan, Vol. 1, pp. 81-88.

Douglas, B.J. and R.S. Olsen, 1981. "Soil Classification Using Electric Cone Penetrometer", Symposium on Cone Penetration Testing and Experience, Geotechnical Engineering Division, ASCE, St. Louis, U.S.A.

Drnevich, V.P., C.T. Gorman, and T.C. Hopkins, 1974. "Shear Strength of Cohesive Soils and Friction Sleeve Resistance", Proceedings of the European Symposium on Penetration Testing, Stockholm, Sweden, Vol. 2:2, pp. 129 - 132.

Eide, O., 1968. "Geotechnical Problems with Soft Bangkok Clay on the Nakhon Sawan Highway Project", Publication No. 78, Norwegian Geotechnical Institute, Oslo, Norway.

Flaate, K., 1966. "Factors Influencing the Results of Vane Tests", Canadian Geotechnical Journal, Vol. 3, No. 1, pp. 18-31.

Ghionna, V., M. Jamolkowski, S. Lacasse, R. Lancellota, and T. Lunne, 1983. "Evaluation of Self Boring Pressuremeter", Proceedings of the International Symposium on In-Situ Testing, Paris, France, Vol. 2, pp. 294-301.

Gibson R.E. and W.F. Anderson, 1961. "In-Situ Measurements of Soil Properties with the Pressuremeter", Civil Engineering and Public Works Review, Vol. 56, No. 658, pp. 615-618.

Gillespie, D.G., 1981. "The Piezometer Cone Penetration Test", M.A.Sc. Thesis, University of British Columbia, Vancouver, Canada.

Helenelund, K.V., 1977. "Methods for Reducing Undrained Shear Strength of Soft Clay", Swedish Geotechnical Repot, No. 3.

Jamiolkowsky, M., C.C. Ladd, J.J. Germaine, and R. Lancellotta, 1985. "New Developments in Field and Laboratory Testing of Soils", State of the Art paper for the Eleventh International Conference on Soil Mechanics and Foundation Engineering, San Francisco, California.

Jamiolkowsky, M., R. Lancellotta, L. Tordella, and M. Battaglio, 1982. "Undrained Strength from CPT", Proceedings of the Second European Symposium on Penetration Testing", Amsterdam, Vol. 2, pp. 599 - 606.

Jones, G.A. and E. Rust, 1982. "Piezometer Penetration Testing", Proceedings of the Second European Symposium on Penetration Testing, Amsterdam, Vol. 2, pp. 607-613.

Jones, G.A., D. Van Zyl and E. Rust, 1981. "Mine Tailings Characterization by Piezometer Cone", Symposium on Cone Penetration Testing and Experience, Geotechnical Engineering Division, ASCE, St. Louis, Missouri, pp. 303 - 324.

Kenney, T.C. and D.J. Folkes, 1979. "Mechanical Properties of Soft Soils", State of the Art Report to the 32nd Canadian Geotechnical Conference, Vol. 2.

Kimura, T. and K. Saitoh, 1983. "Effect of Disturbance Due to Insertion on Vane Shear Strength of Normally Consolidated Cohesive Soils", Soils and Foundations, Vol. 23, No. 2, pp. 113-124.

Koutsoftas, D. and J. Fischer, 1976. "In-Situ Drained Shear Strength of Two Marine Clays", Journal of the Geotechnical Engineering Division, ASCE, Vol. 102, No. GT9, pp. 989-1005.

Ladanyi, B., 1972. "In-situ Determination of Undrained Stress-Strain Behaviour of Sensitive Clays with the Pressuremeter", Canadian Geotechnical Journal, Vol. 9, No. 3.

Ladd, C.C. and R. Foott, 1974. "New Design Procedure for Stability of Soft Calys", Journal of the Geotechnical Engineering Division, ASCE, Vol. 100, No. GT7, pp. 763-786.

Ladd, C.C., R. Foott, K. Ishihara, F. Schlosser and H.G. Poulos, 1977. "Stress Deformation and Strength Characteristics", Proceedings of the Ninth International Conference on Soil Mechanics and Foundation Engineering, Tokyo, Japan, Vol. 2, pp. 421-494.

La Rochelle, P., M. Roy and F. Tavenas, 1973. "Field Measurements of Cohesion in Champlain Clays", Proceedings of the Eighth International Conference on Soil Mechanics and Foundation Engineering, Moscow, U.S.S.R., Vol. 1.1, pp. 229-236.

Lunne, T.,O. Eide and J. De Ruiter, 1976. "Correlation Between Cone Resistance and Vane Strength in Some Scandanavian Soft to Medium Stiff Clays: Reply", Canadian Geotechnical Journal, Vol. 13, pp. 430 - 441.

Lunne, T. and A. Klevin, 1981. "Role of CPT in North Sea Foundation Engineering", Symposium on Cone Penetration Testing and Experience, Geotechnical Engineering Division, ASCE, pp. 49-75.

Lunne, T., H.P. Christofferson, and T.I. Tjelta, 1985. "Engineering Use of the Piezocone Data in the North Sea Clays", Proceedings of the Eleventh International Conference on Soil Mechanics and Foundation Engineering, San Francisco, California.

Massarch, K.R., and B.B. Broms, 1981. "Pipe Driving in Clay Slopes", Proceedings of the Tenth International Conference on Soil Mechanics and Foundation Engineering, Stockolm, Sweden, pp. 24 - 29.

Menzies, B.K. and C.M. Merrifield, 1980. "Measurement of Shear Stress Distribution on the Edges of a Shear Vane Blade", Geotechnique, Vol. 30 pp. 314-318.

Poplin, N.K., A. Arman and N. Ahmad, 1978. "Evaluation of the Vane Shear Test in Louisiana", Engineering Research Bulletin No. 118, Louisiana State University, Louisiana.

Rice, A.H., 1984. "The Seismic Cone Penetrometer",M.A.Sc. Thesis, University of British Columbia, Vancouver, Canada.

Richardson, A.M., E.W. Brand and A. Memon, 1975 "In-Situ Determination of Anisotropy of a Soft Clay", Proceedings of the Specialty Conference on In-Situ Measurement of Soil Properties, ASCE, Raleigh, North Carolina, Vol. 1, pp. 336-349.

Robertson, P.K., 1985. "In Situ Testing and its Application to Foundation Engineering", Colloqium delivered to the Canadian Geotechnical Conference, Edmonton, Canada.

Robertson, P.K. and R.G. Campanella, 1983. "Interpretation of Cone Penetration Tests: Parts 1 and 2", Canadian Geotechnical Journal, Vol. 20, No. 4, pp. 718 - 745.

Robertson, P.K. and R.G. Campanella, 1984. "Guidelines For Use and Interpretation of the Electronic Cone Penetration Test", Soil Mechanics Series No. 69, Department of Civil Engineering, University of British Columbia, Vancouver, Canada.

Schmertmann, J.H., 1975. "Measurement of In-Situ Shear Strength", Proceedings of the Specialty Conference on In-Situ Measurement of Soil Properties, ASCE, Raleigh, North Carolina, Vol. 2, pp. 57-138.

Schmertman, J.H., 1978. "Guidelines for Cone Penetration Test Performance and Design", Federal Highways Administration, Report FHWA-TS-78-209, Washington, D.C.

Senneset, K., N. Janbu and G. Svano, 1982. "Strength and Deformation Parameters from Cone Penetration Tests", Proceedings of the Second European Symposium on Penetration Testing, Amsterdam, pp. 863 - 870.

Senneset, K. and N. Jambu, 1984. "Shear Strength Parameters Obtained from Static Cone Penetration Tests", A-84-1, Institute of Geotechnics and Foundation Engineering, The Norweigian Institute of Technology, Trondheim, Norway.

Torstenson, B.A., 1973. "Time-Dependent Effects in the Field Vane Test", Proceedings of the International Symposium on Soft Clay, Bangkok, pp. 387-397.

Treadwell, D.D., 1976. "The Influence of Gravity, Prestress, Compressibility and Layering on Soil Resistance to Static Penetration", Ph.D. Thesis, University of California, Berkeley.

Vesic, A.S., 1972. "Expansion of Cavities in Infinite Soil Masses", Journal of the Soil Mechanics and Foundation Engineering Division, ASCE, Vol. 98, SM3, pp. 265-290.

Wesley, L.D., 1967. "The Dutch Penetrometer and Its Use in Indonesia", Proceedings, Southeast Asian Regional Conference on Soil Engineering, Bangkok, pp. 223-230.

Wiesel, C.E.R., 1973. "Some Factors Influencing In-Situ Vane Test Results", Proceedings of the Eighth International Conference on Soil Mechanics and Foundation Engineering, Vol. 2., pp. 475-479.

Wroth, C.P., 1984. "The Interpretation of In-Situ Soil Tests", Written Version of the 1984 Rankine Lecture.

APPENDIX A

COMPARISON BETWEEN A CPT BEARING PROFILE AND A CONTINUOUS SAMPLE LOG

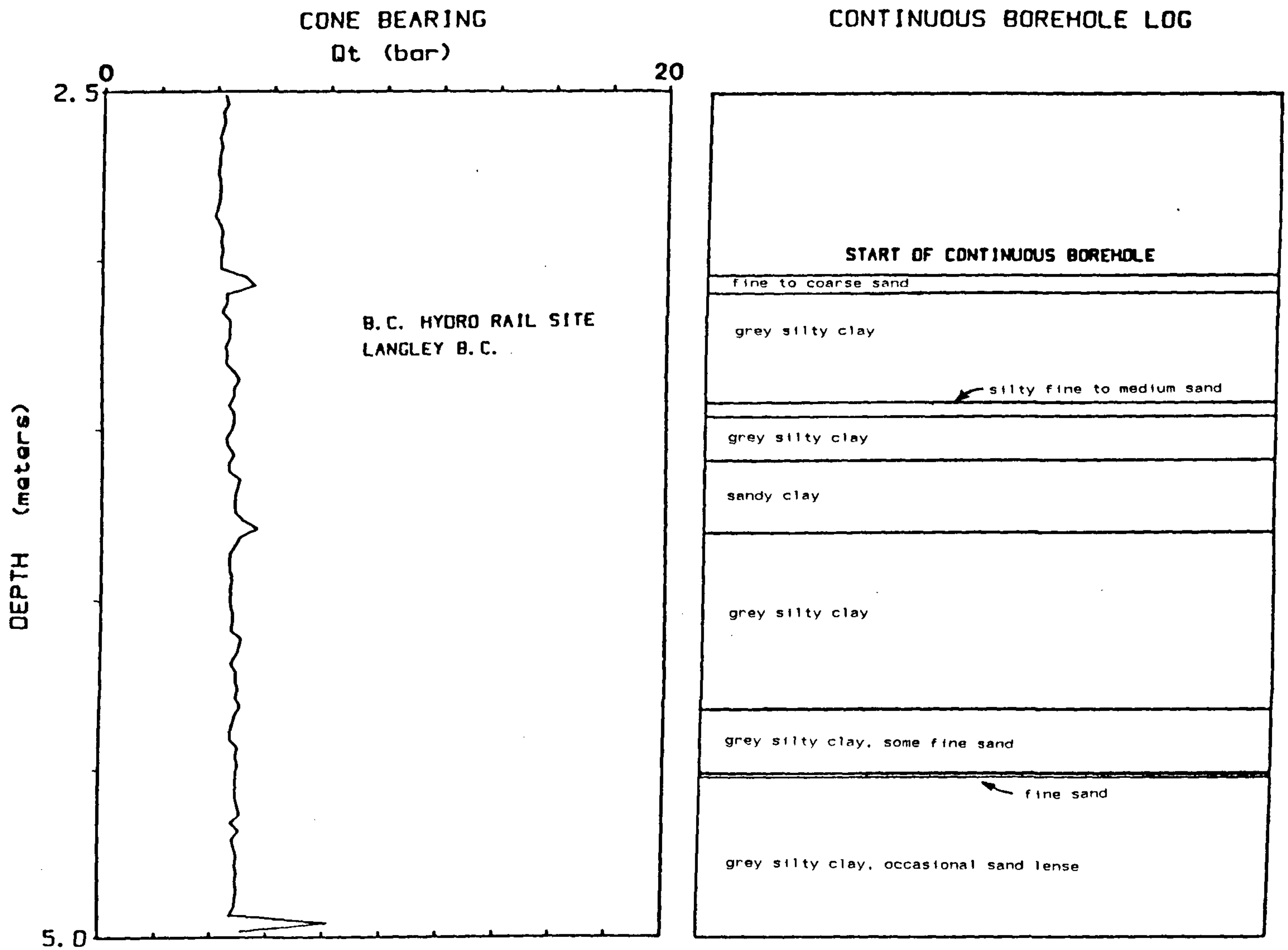

Figure A.1a COMPARISON BETWEEN A CPT BEARING PROFILE AND A CONTINUOUS SAMPLE LOG

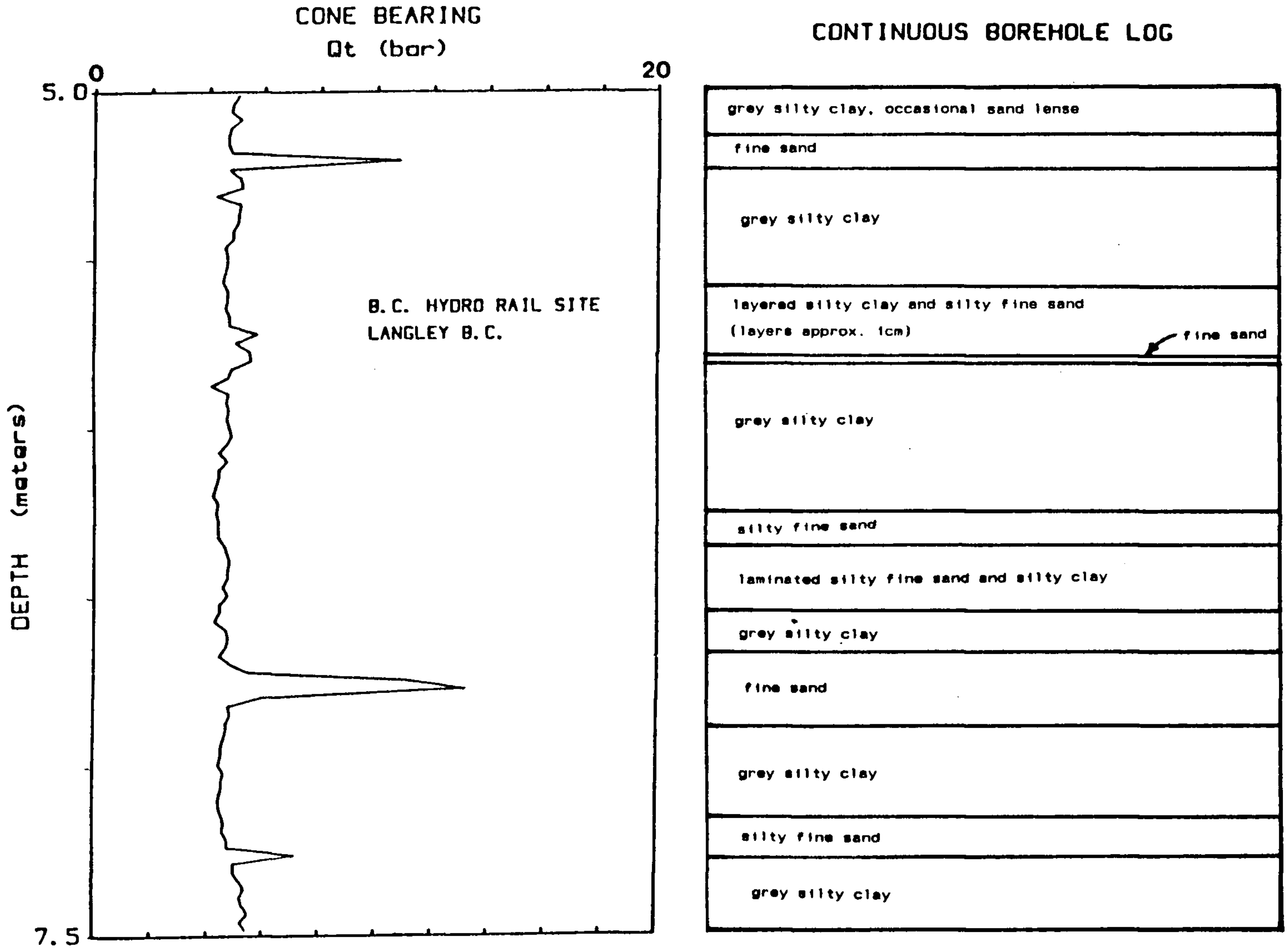

Figure A.1b COMPARISON BETWEEN A CPT BEARING PROFILE AND A CONTINUOUS SAMPLE LOG

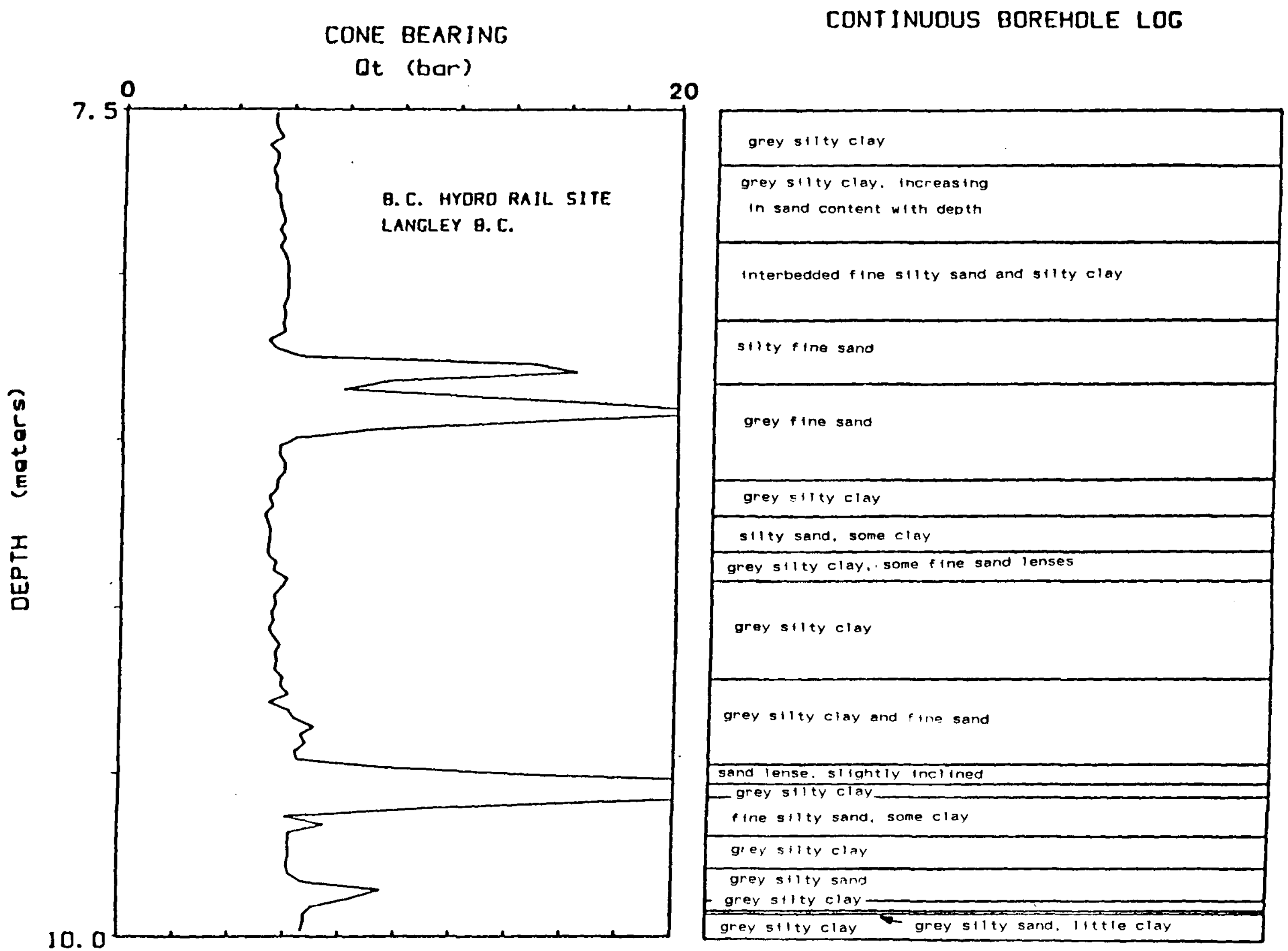

Figure A.1c COMPARISON BETWEEN A CPT BEARING PROFILE AND A CONTINUOUS SAMPLE LOG

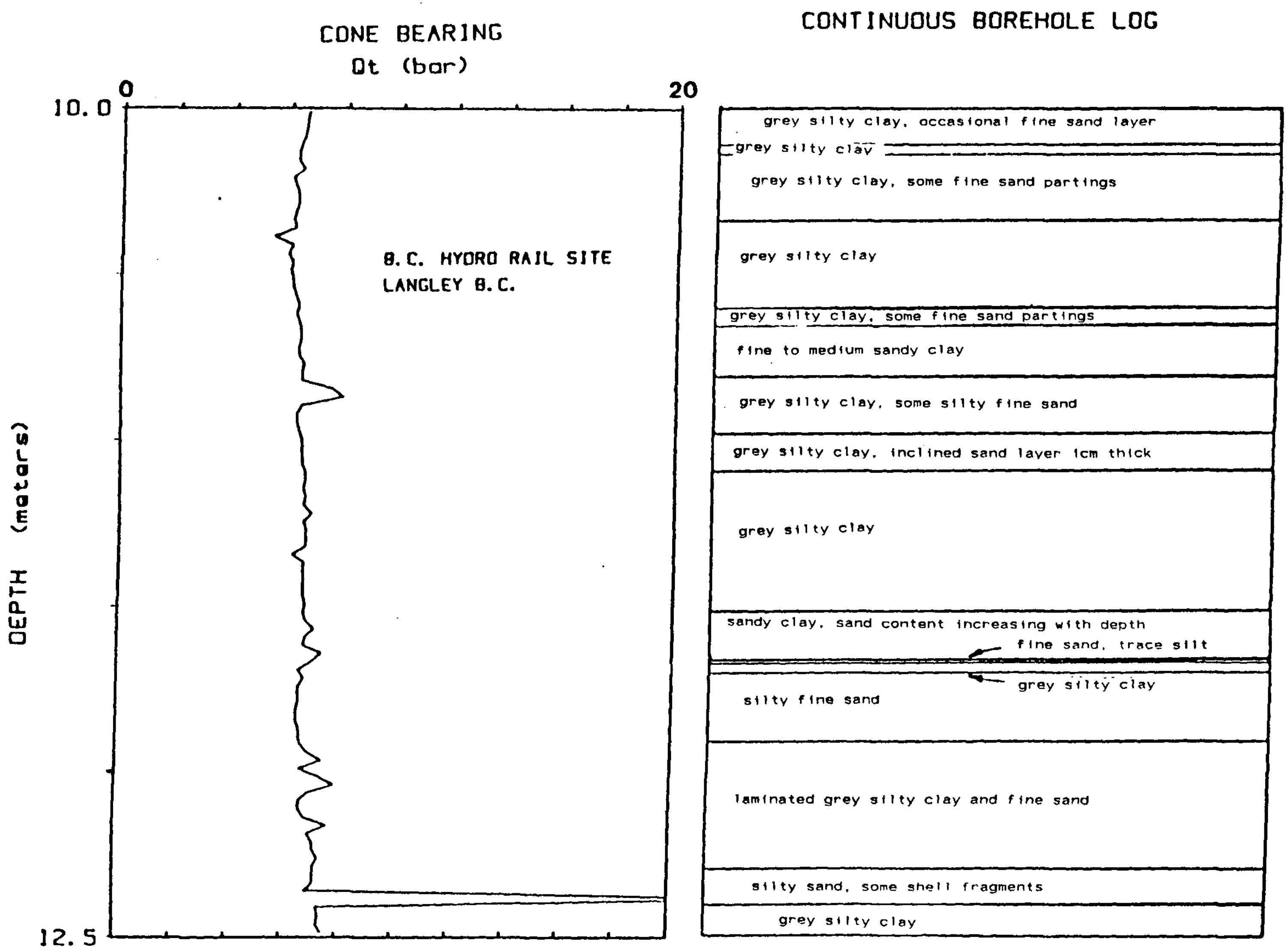

Figure A.1d COMPARISON BETWEEN A CPT BEARING PROFILE AND A CONTINUOUS SAMPLE LOG

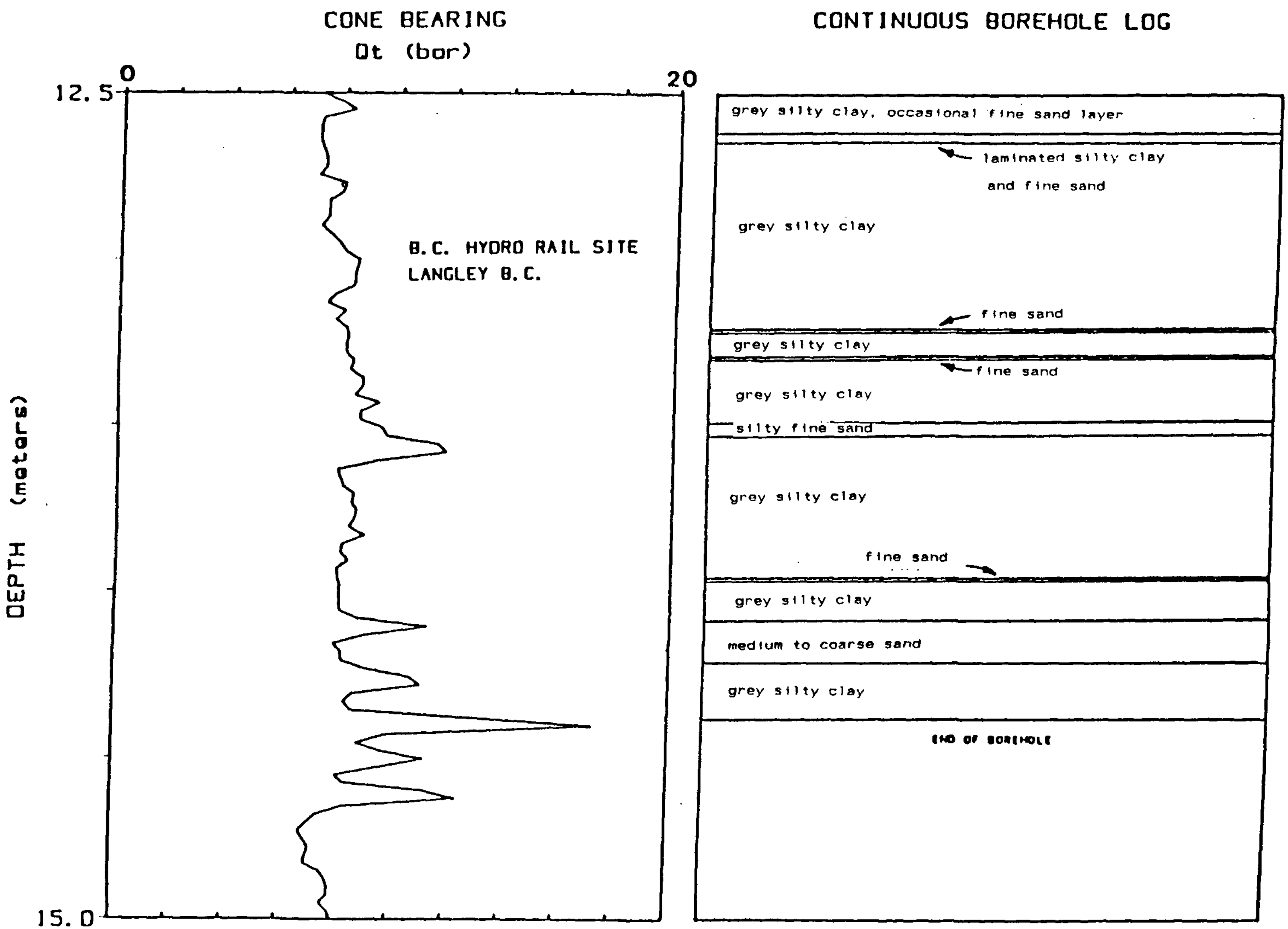

Figure A.1e COMPARISON BETWEEN A CPT BEARING PROFILE AND A CONTINUOUS SAMPLE LOG